

Kinetics and Modeling of Batch Bioethanol Production Using Suspended Co-Cultures of *Saccharomyces cerevisiae* and *Pichia stipitis* in Glucose-Xylose Media

by

Fernando José Mérida Figueróa

A thesis submitted in partial fulfillment of the requirements for the degree of

MASTER OF SCIENCE
in
CHEMICAL ENGINEERING

UNIVERSITY OF PUERTO RICO
MAYAGÜEZ CAMPUS
MAY 2010

Approved by:

José Colucci, Ph.D.
Member, Graduate Committee

Date

Govind Nadathur, Ph.D.
Member, Graduate Committee

Date

Juan Carlos Sáez, Ph.D.
Member, Graduate Committee

Date

Lorenzo Saliceti Piazza, Ph.D.
President, Graduate Committee

Date

Miguel A. Pando, Ph.D.
Representative of Graduate Studies

Date

David Suleiman, Ph.D.
Chair, Department of Chemical Engineering

Date

ABSTRACT

A mathematical structured model was developed to predict the behavior of glucose-xylose mixtures using the suspended co-culture of the wild-type yeast strains *Saccharomyces cerevisiae* Montrachet and *Pichia stipitis* NRRL Y-11545 for ethanol production. Kinetic characterization was estimated in single substrate and single strain batch fermentations in order to construct the model for the mixture systems. The simple Monod model was used to describe the behavior of single substrate fermentations with a high degree of accuracy ($R^2 > 0.96$) and residual standard deviations, ($RSD < 7.5\%$). The agreement between the simulated and experimental data was superior for the fermentation system glucose – *S. cerevisiae*, and the system xylose – *P. stipitis* promoted the best balance between cell growth and ethanol production with a yield coefficient of 0.35 g of ethanol/g xylose.

A non-linear ordinary differential equation system comprising of nine equations was constructed under the cybernetic framework to model the behavior of glucose-xylose mixtures with the specified yeast co-culture. The results obtained from the simulations suggest that the proposed model fits accurately the experimental data. The sensitivity of the model was slightly higher for the mixture having the same proportion of glucose and xylose (50% glucose – 50% xylose), with average values of $R^2 = 0.99$ and $RSD = 2.21\%$. The accurate prediction of the experimental concentrations confirms that the model utilized provides reliable kinetic information. Small deviations were observed but they are commonly found in one simulation system which has not been object of further error minimizations. In the future, the model can be utilized for other process configurations such as fed-batch and continuous culture, either with the same co-culture scheme or using immobilization techniques to evaluate both fermentation efficiency and model accuracy.

RESUMEN

Un modelo matemático estructurado fue desarrollado para predecir el comportamiento de mezclas de glucosa y xilosa usando el co-cultivo suspendido de las levaduras *Saccharomyces cerevisiae* Montrachet y *Pichia stipitis* NRRL Y-11545 en su estado natural, para la producción de etanol. La caracterización cinética fue estimada en experimentos por tandas, con un solo sustrato y una sola levadura, a fin de construir el modelo para los sistemas de mezcla. El modelo simple de Monod fue usado para describir el comportamiento de los sistemas fermentativos de un solo sustrato con un alto grado de precisión ($R^2 > 0.96$) y desviaciones estándar residuales ($RSD > 7.5\%$). La concordancia entre los datos simulados y los experimentales fue mejor para el sistema de fermentación glucosa – *S. cerevisiae*, y el sistema xilosa – *P. stipitis* promovió el mejor balance entre crecimiento celular y producción de etanol con un coeficiente de rendimiento de 0.35 g de etanol/g de xilosa.

Un sistema de ecuaciones diferenciales ordinarias no lineales comprendido de nueve ecuaciones fue construido bajo la perspectiva cibernética para modelar el comportamiento de las mezclas de glucosa y xilosa con el co-cultivo de levaduras ya especificado. Los resultados obtenidos de las simulaciones sugieren que el modelo propuesto se ajusta en forma precisa a los datos experimentales. La sensibilidad del modelo fue ligeramente mayor para las mezclas que contienen 50% glucosa y 50% xilosa, con valores promedio de $R^2 = 0.99$ Y $RSD = 2.21\%$. La precisa predicción de las concentraciones experimentales confirma que el modelo utilizado provee información cinética confiable. Pequeñas desviaciones fueron observadas, pero son encontradas comúnmente en un sistema de simulación que no ha sido objeto de futuras minimizaciones de error. En el futuro, el modelo puede ser utilizado para otras configuraciones de proceso tales como semi-tandas y cultivo continuo, ya sea con el mismo esquema de co-cultivo o usando técnicas de inmovilización para evaluar tanto la eficiencia de la fermentación como la precisión del modelo.

Copyright © 2010 by Fernando José Mérida Figueróa, MS Thesis, UPRM. All Rights reserved. Printed in the United States of America. Except as permitted under the United States Copyright Act of 1976, no part of this publication may be reproduced or distributed in any form or by any means, or stored in database or retrieval system, without the prior written permission of the publisher.

Dedicated to:

My parents

JUAN DOMINGO and AURA LEONOR,

my brothers

JOSÉ JUAN and MARÍA JOSÉ.

You are and will always be the most important thing in my life. I love you.

The town of Chiantla,

*“La niña bonita de Los Cuchumatanes”... that little and beautiful town in the threshold of
the sky, where I was born and from where I always keep the best memories.*

My beautiful GUATEMALA,

“The country of the eternal spring” and “The soul of the earth”...

Hopefully my work will contribute to boost its scientific development.

GOD,

*For being that entity that science will never be able to explain, but Who always has an
explanation to everything.*

*My family, my friends and every person from whom I have received and shared support,
advice and apprenticeship.*

“Quien tiene un ideal, posee una razón para vivir”....

- Leonor Figueróa

ACKNOWLEDGEMENTS

This work has been possible thanks to the opportune intervention of many people, whose support was pivotal to crowning with triumph the ending of my research work, and therefore my Master of Science program in Chemical Engineering.

I want to thank infinitely my family, for their unconditional support which has been the mainstay for the achievement of every goal I have reached throughout my life. The word “thanks” is not enough to express my never-ending gratefulness.

To all of those friends I have met since my childhood until the present day, because no matter the distance or the time, they are always there to celebrate with me my joys, to provide me a shoulder to cry my sorrows, and to remind me that I always have a hand to reach out anywhere I need it.

To Professor Lorenzo Saliceti, for all of his academic, moral and personal support, which has made possible the culmination of this project. To the Department of Chemical Engineering, the Industrial Biotechnology Program, Sustainable Agro Biotechnology Industry (SABI) and the BioSEI funds from the UPRM Research and Development Center.

I also want to thank Jorge Sánchez, Jesús Rodríguez, Orlando Mezquita and Misael Díaz for all of their support in the areas of programming, optimization and statistics. To my undergraduate students and all of the people who made easier those entire days, dawn and weekends in the laboratory.

Finally thanks to Puerto Rico and all of the “boricua” people who are now my second family. Today I can also say that I have my second home in this beautiful island and with the passage of time I will evoke with my heart plenty of happiness and memories, the name of Puerto Rico, “la isla del encanto”.

TABLE OF CONTENTS

1. INTRODUCTION.....	1
1.1. Objectives.....	7
1.1.1. General objective.....	7
1.1.2. Specific objectives.....	8
1.2. References cited	8
2. LITERATURE REVIEW.....	11
2.1. Bioethanol as a transportation fuel.....	11
2.1.1. Historical development	11
2.1.2. Ethanol fuel specifications	16
2.1.3. Economic and environmental issues for bioethanol.....	18
2.2. Biomass-to-ethanol technology.....	21
2.2.1. Classic feedstocks for ethanol production.....	21
2.2.2. Components of lignocellulose.....	24
2.2.3. Processing of lignocellulosics to bioethanol	29
2.2.3.1. Pre-treatment of biomass.....	29
2.2.3.2. Hydrolysis	30
2.2.3.3. Fermentation of biomass hydrolysates.....	31
2.2.3.4. Product recovery	32
2.3. Biocatalysts for ethanol fermentation	34
2.3.1. Hexose-fermenting microbes	35
2.3.2. Pentose-fermenting microbes	36
2.3.3. Genetically engineered microbial strains	37
2.4. Fermentation of mixtures of glucose and xylose	40
2.5. Mathematical modeling of fermentation processes.....	42
2.5.1. Kinetics and modeling of single substrate fermentations.....	44
2.5.1.1. Mass balances for batch fermentation.....	49
2.5.2. Kinetics and modeling of multiple substrate fermentations.....	52
2.6. References cited	58
3. MATERIALS AND METHODS.....	65
3.1. Microorganisms.....	65
3.2. Inoculum preparation	65

3.2.1.	Inocula for single substrate fermentations	65
3.2.2.	Inocula for mixed substrate and mixed strains fermentations.....	66
3.3.	Batch fermentations.....	67
3.4.	Cell growth and cell mass concentration.....	69
3.5.	Sugar, ethanol and by-product concentrations	73
3.6.	Profile concentrations model development and simulation	74
3.6.1.	Single substrate fermentations	74
3.6.2.	Co-fermentations of glucose/xylose mixtures.....	79
3.7.	Literature cited	81
4.	SINGLE SUBSTRATE FERMENTATIONS.....	84
4.1.	Fermentation kinetics and experimental profiles	85
4.2.	Fermentation yields	97
4.2.1.	Yield of biomass on substrate	97
4.2.2.	Yield of ethanol on substrate.....	100
4.2.3.	Yield of ethanol on biomass.....	103
4.3.	Unstructured kinetic modeling	108
4.4.	Literature cited	115
5.	MIXED SUBSTRATE FERMENTATIONS.....	118
5.1.	Construction of the structured cybernetic model	118
5.2.	Simulation of glucose-xylose mixtures using one single yeast strain.....	124
5.3.	Experimental profiles and fermentation yields	135
5.4.	Structured modeling glucose-xylose mixtures using	143
5.5.	Literature cited	154
6.	CONCLUSIONS AND RECOMMENDATIONS.....	157
6.1.	Single substrate fermentations	157
6.1.1.	Conclusions	157
6.1.2.	Recommendations	159
6.2.	Mixed substrate fermentations	160
6.2.1.	Conclusions	161
6.2.2.	Recommendations	162
	APPENDIX A: CONSISTENCY OF THE PROPOSED MODELS.....	166
A.1	Single substrate fermentations.....	166
A.2	Mixed substrate – mixed strain fermentations.....	168
	APPENDIX B: ANALYSIS OF RESIDUALS.....	170

LIST OF TABLES

Table 2.1 – Gasoline and ethanol properties [5].....	18
Table 2.2 – Estimated production costs for bioethanol in 2003 [19].	19
Table 2.3 – Approximate composition of selected lignocellulosic materials for ethanol production [38].	28
Table 2.4 – Unstructured models to quantify fermentation kinetics. Adapted from Sáez and Saliceti [38].	44
Table 4.1 – Summary of the apparent yield coefficients and specific rates.	107
Table 4.2 – Maximum yield coefficients.	107
Table 4.3 – Optimized kinetic parameters used in Monod model.	112
Table 4.4 – Statistical analysis for kinetic modeling with the simple Monod model. Units: MSE [(g/L) ²]; LCC [%]; RSD [%].....	114
Table 5.1 – Substrate and ethanol volumetric rates from each sugar in the fermentation mixtures with the yeast co-culture.	140
Table 5.2 – Summary of yield coefficients for glucose-xylose fermentations with the yeast co-culture.....	142
Table 5.3 – Statistical analysis for kinetic modeling using cybernetic model. Units: MSE [(g/L) ²]; LCC [%]; RSD [%].....	150

LIST OF FIGURES

Figure 2.1 – Ford Model Car (1896), which used pure ethanol [5].	12
Figure 2.2 – Historical oil price. Data from BP Statistical Review of World Energy, British Petroleum, London, 2007 [9].	13
Figure 2.3 – Worldwide ethanol production after 1975 in million of liters. Data from RISE [11].	14
Figure 2.4 – MTBE production in USA. Data from the U.S. Department of Energy [12]. ...	15
Figure 2.5 – Ethanol production in USA (billions of gallons). Data from the Renewable Fuels Association [11].	16
Figure 2.6 – Total fuel cycle carbon dioxide emissions [2].	20
Figure 2.7 – Percentage of reduction of greenhouse gas emissions in fuel ethanol [21].	21
Figure 2.8 – Technological routes for ethanol production [5].	24
Figure 2.9 – Lignocellulose microscopic structure and distribution [32].	25
Figure 2.10 – Structure of a short segment of cellulose [35].	26
Figure 2.11 – Structure of xylan a short segment of hemicellulose [36].	27
Figure 2.12 – Structure of segment of lignin [37].	27
Figure 2.13 – Generic block diagram of fuel ethanol production from lignocellulosic biomass, from Cardona and Sánchez [50].	34
Figure 2.14 – Metabolic pathways to produce ethanol from glucose and xylose. (Adapted from Nelson and Cox [59]).	39
Figure 2.15 – Schematic diagram of the cybernetic model (Adapted from Venkatesh and co-workers [80]).	53
Figure 3.1 - Inoculum preparation for single substrate fermentations in Innova 4000 incubator shaker.	66
Figure 3.2 - Inoculum preparation for co-fermentations in an Innova 4000 incubator shaker.	67
Figure 3.3 - Batch fermentation in an Innova 4000 incubator shaker.	69
Figure 3.4 - Aseptic sampling throughout the course of fermentation.	69
Figure 3.5 - Manifold filtration unit used for cell filtration.	70
Figure 3.6 – Linear correlation between DCM concentration (g/L) and OD at 600 nm for glucose with <i>Saccharomyces cerevisiae</i>	71

Figure 3.7 – Linear correlation between DCM concentration (g/L) and OD at 600 nm for glucose with <i>Pichia stipitis</i>	71
Figure 3.8 – Linear correlation between DCM concentration (g/L) and OD at 600 nm for xylose with <i>Saccharomyces cerevisiae</i>	72
Figure 3.9 – Linear correlation between DCM concentration (g/L) and OD at 600 nm for xylose with <i>Pichia stipitis</i>	72
Figure 3.10 - High performance liquid chromatography device (Shimadzu LC-10ATVP) for analysis of sugars, ethanol and byproduct concentrations.	73
Figure 3.11 – Biochemistry Analyzer device (YSI 2700) for sugar monitoring.....	74
Figure 3.12 – Growth curve and maximum specific growth rate determination for one run of glucose fermentation with <i>S. cerevisiae</i>	75
Figure 3.13 – Linear regression between ethanol and cell mass concentrations for yield coefficient $Y_{P/X}$. The slope of the regression equation represents the value of the yield coefficient, $Y_{P/X}$	76
Figure 3.14 – Matlab Editor Window with proposed ordinary differential system.	77
Figure 3.15 – MATLAB Editor Window with the ode45 Runge-Kutta solver method and simultaneous optimization for μ_{\max} and K_s value based in minimization of Equation 3.1.	78
Figure 3.16 - Polymath Editor Window with the RK45 solver method for the system Glucose – <i>S. cerevisiae</i>	79
Figure 3.17 - MATLAB Editor Window with a set of non-linear ordinary differential equations for a mixture of glucose and xylose with <i>P. stipitis</i> , including a rate maximization subroutine in the calculation of the cybernetic variables.	81
Figure 4.1 – Determination of μ_{\max} for glucose fermentation with <i>S. cerevisiae</i> . Error bars are ± 1 standard deviation of 3 replicates.....	87
Figure 4.2 – Determination of μ_{\max} for glucose fermentation with <i>P. stipitis</i> . Error bars are ± 1 standard deviation of 3 replicates.....	87
Figure 4.3 – Determination of μ_{\max} for xylose fermentation with <i>P. stipitis</i> . Error bars are ± 1 standard deviation of 3 replicates.....	88
Figure 4.4 – Apparent exponential phase for xylose culture medium with <i>S. cerevisiae</i> . Error bars are ± 1 standard deviation of 3 replicates.	89
Figure 4.5 – Experimental profile concentration for xylose fermentation with <i>S. cerevisiae</i> . Error bars are ± 1 standard deviation of 3 replicates.....	90
Figure 4.6 – Experimental profile concentration for xylose fermentation with <i>P. stipitis</i> . Error bars are ± 1 standard deviation of 3 replicates.	91

Figure 4.7 – Experimental profile concentration for glucose fermentation with <i>P. stipitis</i> . Error bars are ± 1 standard deviation of 3 replicates.....	93
Figure 4.8 – Experimental profile concentration for glucose fermentation with <i>S. cerevisiae</i> . Error bars are ± 1 standard deviation of 3 replicates.....	95
Figure 4.9 – Total substrate consumption rates for single substrate fermentations, Q_S . Xyl - <i>P. stipitis</i> : 0.19 g/L-h; Glu – <i>P. stipitis</i> : 0.63 g/L-h; Glu – <i>S. cerevisiae</i> : 3.93 g/L-h. ...	96
Figure 4.10 – Total ethanol production rates for single substrate fermentations, Q_P . Xyl - <i>P. stipitis</i> : 0.07 g/L-h; Glu – <i>P. stipitis</i> : 0.20 g/L-h; Glu – <i>S. cerevisiae</i> : 1.19 g/L-h.	96
Figure 4.11 – Determination of biomass yield on substrate, $Y_{X/S}$	99
Figure 4.12 – Determination of ethanol yield on substrate, $Y_{P/S}$	102
Figure 4.13 – Determination of ethanol yield on biomass, $Y_{P/X}$	105
Figure 4.14 – Comparison of the experimental data and predicted kinetics using the simple Monod model in xylose fermentation with <i>P. stipitis</i>	110
Figure 4.15 – Comparison of the experimental data and predicted kinetics using the simple Monod model in glucose fermentation with <i>P. stipitis</i>	111
Figure 4.16 – Comparison of the experimental data and predicted kinetics using the simple Monod model in glucose fermentation with <i>S. cerevisiae</i>	111
Figure 5.1 – Comparison of the Monod model to the cybernetic perspective for single substrate fermentations. A: Glucose – <i>S. cerevisiae</i> ; B: Glucose – <i>P. stipitis</i> ; C: Xylose – <i>P.</i> <i>stipitis</i>	126
Figure 5.2 – Simulations of glucose-xylose fermentation mixtures with <i>S. cerevisiae</i> . A: 75% Glu – 25% Xyl; B: 50% Glu – 50% Xyl; C: 25% Glu – 75% Xyl.	128
Figure 5.3 – Simulation of enzyme levels in glucose-xylose fermentation with <i>S. cerevisiae</i> . A: 75% Glu – 25% Xyl; B: 50% Glu – 50% Xyl; C: 25% Glu – 75% Xyl.	130
Figure 5.4 – Simulations of glucose-xylose fermentation mixtures with <i>P. stipitis</i> . A: 75% Glu – 25% Xyl; B: 50% Glu – 50% Xyl; C: 25% Glu – 75% Xyl.	132
Figure 5.5 – Simulation of enzyme levels in glucose-xylose fermentation with <i>P. stipitis</i> . A: 75% Glu – 25% Xyl; B: 50% Glu – 50% Xyl; C: 25% Glu – 75% Xyl.	134
Figure 5.6 – Cell growth curves for glucose-xylose mixtures with yeast co-culture. A: 75% Glu – 25% Xyl; B: 50% Glu – 50% Xyl; C: 25% Glu – 75% Xyl. Error bars are ± 1 standard deviation of 3 replicates.	136

Figure 5.7 – Experimental profiles for glucose-xylose fermentations using suspended co-culture of <i>S. cerevisiae</i> and <i>P. stipitis</i> . A: 75% Glu – 25% Xyl; B: 50% Glu – 50% Xyl; C: 25% Glu – 75% Xyl. Error bars are ± 1 standard deviation of 3 replicates.	139
Figure 5.8 – Comparison of the experimental data and predicted kinetics of the mixture A, with 75% of glucose and 25% of xylose using a suspended co-culture of <i>S. cerevisiae</i> and <i>P. stipitis</i>	145
Figure 5.9 – Comparison of the experimental data and predicted kinetics of the mixture B, with 50% of glucose and 50% of xylose using a suspended co-culture of <i>S. cerevisiae</i> and <i>P. stipitis</i>	146
Figure 5.10 – Comparison of the experimental data and predicted kinetics of the mixture C, with 25% of glucose and 75% of xylose using a suspended co-culture of <i>S. cerevisiae</i> and <i>P. stipitis</i>	148
Figure 5.11 – Simulation of enzyme levels in glucose-xylose fermentation with <i>S. cerevisiae</i> : e_1 and e_2 , and <i>P. stipitis</i> : e_3 and e_4 A: 75% Glu – 25% Xyl; B: 50% Glu – 50% Xyl; C: 25% Glu – 75% Xyl.	152
Figure A.1 – Comparison of the consistency between predicted and experimental cell concentrations	166
Figure A.2 – Comparison of the consistency between predicted and experimental substrate concentrations	167
Figure A.3 – Comparison of the consistency between predicted and experimental ethanol concentrations	167
Figure A.4 – Comparison of the consistency between predicted and experimental total cell concentrations	168
Figure A.5 – Comparison of the consistency between predicted and experimental glucose concentrations	168
Figure A.6 – Comparison of the consistency between predicted and experimental xylose concentrations	169
Figure A.7 – Comparison of the consistency between predicted and experimental ethanol concentrations	169
Figure B.1 – Residual probability plots for the system xylose – <i>P. stipitis</i>	170
Figure B.2 – Residual probability plots for the system glucose – <i>P. stipitis</i>	171
Figure B.3 – Residual probability plots for the system xylose – <i>S. cerevisiae</i>	172
Figure B.4 – Residual probability plots for the mixture of 75% glucose and 25% xylose.	173
Figure B.5 – Residual probability plots for the mixture of 50% glucose and 50% xylose.	174

Figure B.6 – Residual probability plots for the mixture of 25% glucose and 75% xylose....175

LIST OF SYMBOLS

B	Biomass concentration (g/L)
C	Concentration of any of the components in a fermentation process (g/L)
e	Specific level of a key enzyme
E	Key enzyme concentration (g/L)
$E(\theta)$	Objective error function of the sensitivity of predicted models
K_s	Monod saturation constant (g/L)
n	Stoichiometric coefficient of hydrolysis reaction of cellulose (moles)
P	Ethanol concentration (g/L)
q_P	Specific ethanol production (g P/g X – h)
q_S	Specific substrate consumption (g S/g X – h)
Q_P	Total ethanol production rate (g P/L-h)
Q_S	Total substrate consumption rate (g S/L-h)
r	Rate of production or consumption of any of the components in a fermentation process (h^{-1})
S	Substrate concentration (g/L)
t	Time (h)
u	Cybernetic variable controlling the regulatory mechanisms of catabolite repression and induction
v	Cybernetic variable controlling the regulatory actions of inhibition and activation of key enzymes
X	Dry cell mass concentration (g/L)
$Y_{P/S}$	Ethanol yield coefficient on substrate (g P/g S)
$Y_{P/X}$	Ethanol yield coefficient on cells (g P/g X)
$Y_{X/S}$	Cell mass yield coefficient on substrate (g X/g S)
α	Maximum specific level of the key enzyme (h^{-1})
β	Protein decay constant (h^{-1})
μ	Specific cell growth rate (h^{-1})
μ_{max}	Maximum specific cell growth rate (h^{-1})

1. INTRODUCTION

Ethanol is one of the most important renewable and versatile transportation fuels contributing to the reduction of negative environmental impacts generated by the worldwide utilization of fossil fuels. The outstanding advantages of fuel ethanol include its use as an additive (high octane), high heat of vaporization, and other characteristics that allow achieving higher efficiency use than gasoline in optimized engines. Internal combustion engines that burn ethanol as a fuel have a big advantage when compared with engines that burn the typical hydrocarbon components of refined oils. This is because ethanol is more oxygenated, and its combustion in oxygen generates less energy in comparison with either a pure hydrocarbon or a typical gasoline [1-2]. Likewise, ethanol is a good substitute for methyl tert-butyl ether (MTBE) which was the first approved oxygenated candidate for gasoline, but due to environmental pollution incidents caused by MTBE spillage, several states in USA switched from MTBE to ethanol and ethanol demand began to expand considerably [3]. However, the production of bioethanol -ethanol produced from biomass- is complicated and lately has been constituted as a controversy by the fact that some of the sources or raw materials for this biofuel have been used historically as food for humans and as feed for animals [4]. Therefore, according to the current energy requirements there are three fundamental benefits to further develop ethanol as a renewable alternative transportation fuel: (i) to reduce world dependence on petroleum-based fuels (biofuels can be produced locally in sustainable systems), (ii) to improve the environment by decreasing net greenhouse gas emissions (renewable fuels contribute to recycle carbon dioxide, which is extracted from the atmosphere to regenerate biomass), and (iii) to provide new employment (e.g., agriculture & agro industries).

Ethanol can be produced from a considerable large list of feedstock containing fermentable sugars that are metabolized by different microorganisms. The majority of this

feedstock has not been widely studied yet, and presents some difficulties to release the fermentable sugars. Two classes of this feedstock have been the most utilized globally in the last decades: sugar cane and corn starch, particularly in regions like Brazil and United States, respectively. However, the use of these two feedstock has been currently extended to several countries worldwide, such as China, India, France, Germany and many others [5] and global ethanol production reached 51 GL/year in 2006, of which about 39 GL were used as fuel and the rest for beverage and other industrial applications [6]. As mentioned before, to minimize controversy generated by using these food/feed grade-feedstocks to produce ethanol, attention and priority have been assigned to the study of lignocellulosic biomass as raw material for ethanol production. In Chapter 2, a complete literature review will be discussed covering the areas of bioethanol production, modeling and yeast fermentation. A general classification proposed by Cardona and Sánchez [5] separates biomass sources for bioethanol production as follows: (i) sucrose-containing feedstock, (ii) starchy materials, and (iii) lignocellulosic biomass. This thesis is focused on the last category, which deserves special attention because of the availability of lignocellulosic materials that can be utilized for ethanol production and other useful applications. Furthermore, because of current technologies for bioethanol production are crop-based using substrates such as sugar cane juice and cornstarch, a lot of efforts have to be made to make use of less expensive lignocellulosic materials to reduce the cost of raw materials, the ones that can be as high as 40% of the total production cost [7]. Typically, lignocellulose is composed about 35% to 50% cellulose, which is a long chain of single glucose sugar molecules bonded together in a crystalline structure [8]. Another 20% to 35% is made up of hemicellulose, a long, branched chain of heterogeneous sugar molecules, including xylose as one abundant component and other different proportions of five and six carbon sugars (pentoses and hexoses). The remaining fraction comprises lignin, an insoluble phenylpropane polymer which is often attached to the cellulose fibers to form a

lignocellulosic complex. This complex and the lignin alone are usually quite resistant to conversion by microbial systems and many chemical agents [9].

Globally, production of ethanol from lignocellulosic biomass comprises five main steps: (i) biomass pretreatment, (ii) hydrolysis of polysaccharides, (iii) fermentation of sugars, (iv) separation of final products, and (v) effluent treatment [10]. The present work is focused in the fermentation step using the co-culture of the wild-type yeast strains to chemically represent the fermentation media after the hydrolysis of cellulose and hemicellulose. Then, because of the premise is to work with mixtures of glucose and xylose from cellulose and hemicellulose respectively, using efficient microbial strains, it is necessary to find those strains, and they must consume both glucose and xylose to increase and improve ethanol yield. Several microorganisms can efficiently ferment the glucose component in cellulose to ethanol but conversion of pentose sugars in the hemicellulose fraction, and particularly xylose, remained a bottleneck in biomass-to-ethanol conversion until some years ago. Besides, the microorganisms should exhibit some essential traits to achieve high ethanol yields and tolerance, and the priority must be to ferment the variety of sugars found in lignocellulosic biomass to ethanol as the sole fermentation product and to resist the high ethanol concentrations necessary for economical product recovery.

Saccharomyces cerevisiae is a well known yeast strain in the alcoholic beverages industry since ancient times and has been generally regarded as safe (GRAS); currently it is seemingly the best “platform” for lignocellulosic biomass because of its relative tolerance to the growth inhibitors found in the acid hydrolysates of lignocellulosic biomass [11]. It is able to ferment glucose to ethanol with high yields achieving up to 90 g/L of ethanol with an initial glucose concentration basis of approximately 200 g/L [12]. The main disadvantage in *S. cerevisiae* is the limited range of monosaccharides and disaccharides that can be converted into ethanol; xylose can not be fermented by *S. cerevisiae* because it lacks both a xylose-

assimilation pathway and adequate levels of key pentose phosphate pathway enzymes, although it is capable to ferment xylulose but not as quickly or efficiently as glucose [13-14]. Therefore, several studies have been made to identify and test efficient xylose-fermenting yeast strains to produce ethanol, being the best strains so far: *Brettanomyces naardenensis*, *Pichia stipitis*, *Pichia segobiensis*, *Pachysolen tannophilus*, *Kluyveromyces marxianus*, *Candida shehatae*, and *Candida tenuis* [16]. Usually, the naturally xylose-fermenting yeasts have been shown to produce ethanol at 78% to 84% of theoretical yield (0.51 g ethanol/g sugar) and at concentrations of up to 5%. Intensive studies have been developed to test the efficiency of strains before mentioned, in both single-sugar and mixture fermentations, and the results have been high ethanol concentrations achieved with respect to the initial sugar concentrations, and high ethanol yields as well. When working with mixtures of glucose and xylose, *P. stipitis* best results have been achieved for the transformation of substrates into ethanol [16] and besides have shown that when xylose is the sole carbon source, the final ethanol concentration at the end of fermentation along with ethanol yield is slightly higher if compared with 100% glucose media [17]. Therefore, *Pichia stipitis* appears to provide the best overall performance in terms of complete sugar utilization, minimal co-product formation, and insensitivity to temperature and substrate concentrations [18] having the highest native capacity for xylose fermentation of any known microbe and most of its strains are among the best xylose-fermenting yeasts in type culture collections [19].

Once efficient yeast strains have been identified the purpose is to use them in a co-culture scheme along with glucose and xylose mixtures, setting different initial sugar ratios and based in the optimal culture conditions with the main objective to develop mathematical models to predict the behavior of cell, substrates and products concentrations as a function of fermentation time. Modeling a fermentation process presents some advantages such as process knowledge improvement, decreasing the cost of expensive industrial experimentation,

mathematical optimization and process control. The ability to predict the behavior of fermentation systems enhances the possibility of optimizing their performance. Mathematical equations of model systems represent a tool for this and the most recent advances in computer hardware and software have made the approach more effective than previous simplistic attempts [20-21].

An adequate model which describes accurately the experimental concentration profile in a fermentation process requires determination and optimization of kinetic parameters such as maximum specific growth rate and saturation constants. Besides, it is necessary to choose the model that best fits experimental conditions, also taking into account all relevant aspects regarding the chemical, physical, biochemical and technical areas of the process. Therefore in this research work, based upon operational conditions and methods described in Chapter 3, the model chosen is the unstructured and non-segregated model developed by Monod [22], which has been used widely and successfully since several years ago to describe cellular growth and fermentation kinetics of a broad collection of substrates and microbes. This model is one of the simplest models including the effect of nutrient concentration, assuming that only one substrate (the growth limiting substrate) is important in determining the rate of cell proliferation. As will be discussed in Chapter 4, this model fits accurately the set of experimental data obtained in a series of single substrate fermentations, using one substrate-one yeast strain, with no inhibition effects, neither substrate nor product, present in the performed fermentations. Kinetic information such as maximum specific growth rate and saturation constant, and yield coefficients were collected after processing experimental data and then were used to construct the model that quantifies growth kinetics, substrate consumption and ethanol production. This chapter also presents an analysis of the efficiency of each yeast strain in the fermentation process, comparisons between biomass yields and ethanol yields and the complete set of mass balance equations utilized to describe

the rates of consumption and production of substrates and products, respectively. However, the efforts to model fermentations with more than two substrates with a simple Monod model are not adequate because simple unstructured models are developed to explain a particular set of experimental data and do not take into consideration the optimal nature of microbial growth on multiple substrates. In a multiple substrate co-culture environment the cells show to have mechanisms to grow first on the preferable substrate available and proliferate much faster than the cells that respond differently. In this environment microorganisms have to be viewed as optimal strategists, which means that under adequate conditions they display the ability to “think” and “decide” how to best utilize the resources so as to maximize a particular objective. Therefore as discussed in Chapter 5, a structured model has been used to simulate the concentration profiles in co-fermentations of glucose and xylose, but this model has a basic premise which represents the most important attribute of modeling efforts: information obtained from growth on single substrate experiments on each of the substrates will yield all of the information required for predicting growth in mixed substrates [23-24]. The model is based in the same mass balances made for single substrate fermentations but it also takes into account other important considerations and conditions that the model demands, specially regarding to the enzyme balances and allocation resources policies. The first structured model developed was made to analyze the profile concentrations of glucose and xylose for each one of the strains used. This is, one model was developed for *S. cerevisiae* and the other one was developed for *P. stipitis*. After these models matched successfully single substrate fermentations, the complete structured model was constructed on the basis of additive kinetics for both yeast strains utilized. Hence all the numeric subscripts belong to sugar identification and the alphanumeric subscripts belong to yeast strains differentiation. Final fermentation runs were carried out to validate the structured model and the fitting was quantified by means of experimental statistical tools such as determination of mean square errors, linear

correlation coefficients and residual standard deviations between experimental and predicted data. The conclusions of this research project are displayed in Chapter 6, which also includes a list of recommendations to complement the scope of this work and to extend it to other process configurations in bioprocess engineering.

It is imperative to recognize the value and relevance of this work, because as shown in the next chapter, there is a large compilation of previous studies concerning research projects made with mixtures of glucose and xylose to produce fuel ethanol and modeling of fermentation processes, nevertheless at the moment of this document's writing there are no apparent publications in which the objective is to model co-fermentations of glucose and xylose using co-cultures of the yeast strains above mentioned. Therefore the efforts made in this research project are vanguardist in the development of the lignocellulosic ethanol framework, mainly in areas such as optimization and process design. Likewise, the area of yeast dynamics is also promoted when evaluating the performance of two different types of strains in an environment governed by sequential consumption of two substrates, the ones that have to be completely metabolized to achieve the highest ethanol yields in the bioprocess.

1.1. Objectives

1.1.1. General objective

- To experimentally determine kinetics and yield coefficients to further develop a structured model to mathematically predict the ethanol production using the wild-type yeast strains *Saccharomyces cerevisiae* and *Pichia stipitis* and media containing mixtures of glucose and xylose.

1.1.2. Specific objectives

- To determine kinetic parameters such as the maximum growth rates, Monod's saturation constant, and product yield coefficients in single glucose and xylose batch fermentations and to analyze experimental data as a function of fermentation time.
- To use the above experimental parameters in order to model the growth of cells, substrate consumption and ethanol production in multiple substrate fermentations - glucose and xylose- using an appropriate structured model or based on the sequential utilization of two carbon carbohydrate sources (glucose and xylose).
- To validate the developed mathematical modeling, for both single and multiple substrates, with experimental fermentation runs.

1.2. References cited

- [1] Cheremisinoff, N.P. (1979). Gasohol for Energy Production. Ann Arbor Science Publishers, Ann Arbor, MI. **Chap. 6**.
- [2] Bailey, B.K. (1996). Performance of ethanol as a transportation fuel, in Wyman, C.E. (Ed), Handbook on Bioethanol: Production and Utilization, Taylor & Francis, Washington, DC, **Chap. 3**.
- [3] Ethanol Industry Outlook (2006). Renewable Fuels Association, Washington, DC. <http://www.ethanolrfa.org/> Access date: Oct. 2009.
- [4] Mitchel, D. (2008). A Note on Rising Food Prices. Policy research working paper. The World Bank.
- [5] Sánchez, O.; Cardona, C.A. (2007). Trends in biotechnological production of fuel ethanol from different feedstocks. *Bioresource Technology*. **99**:5270-5292.
- [6] Walter, A.; Rosillo-Calle, F.; Dolzan, P.; Piacencte, E.; Borges da Cunha, K. (2008). Perspectives on fuel ethanol consumption and trade. *Biomass and Bioenergy*. **32**:730-748.
- [7] Zaldivar, J.; Nielsen, J.; Olson, L. (2001). Fuel ethanol production from lignocellulose: a challenger for metabolic engineering and process integration. *Appl. Microbiol. Biotechnol.* **56**:17-34.

- [8] Zhang, Y-HP; Lynd, L.R. (2004). Toward an aggregated understanding of enzymatic hydrolysis of cellulose: noncomplexed cellulose systems. *Biotechnol. Bioeng.* **88**(7):797-824.
- [9] Balat, M.; Balat, H.; Öz, C. (2007). Progress in bioethanol processing. *Progress in Energy and Combustion Science.* **34**:551-573.
- [10] Cardona, C.; Sánchez, O. (2007). Fuel ethanol production: Process design trends and integration opportunities. *Bioresource Technology.* **98**:2415-2457.
- [11] Hahn-Hägerdal, B. (2001) Metabolic engineering of *Saccharomyces cerevisiae* for xylose utilization. *Adv. Biochem. Eng./Biotechnol.* **75**:53.
- [12] Vallet, C. (1996). Natural abundance isotopic fractionation in the fermentation reaction: influence of the nature of the yeast. *Bioorg. Chem.* **24**:319.
- [13] Van Dijken, J.P. (1986). Alcoholic fermentation by non-fermenting yeasts. *Yeast.* **2**:123.
- [14] Lagunas, R. (1986). Misconceptions about the energy metabolism of *Saccharomyces cerevisiae*. *Yeast.* **2**:221.
- [15] Toivola, A.; Yarrow, D.; van den Bosch, E.; van Dijken, J.; Scheffers, W.A. (1984). Alcoholic fermentation of D-xylose by yeasts. *App. and Environ. Microb.* **47**(6):1221-1223.
- [16] Sánchez, S.; Bravo, V.; Castro, E.; Moya, A.J.; Camacho, F. (2002). The fermentation of mixtures of D-glucose and D-xylose by *Candida shehatae*, *Pichia stipitis* or *Pachysolen tannophilus* to produce ethanol. *Journal of Chem. Technol. and Biotechnol.* **77**:641-648.
- [17] Agbogbo, F.K; Coward-Kelly, G.; Torry-Smith, M.; Wenger, K.S. (2006). Fermentation of glucose/xylose mixtures using *Pichia stipitis*. *Process Biochemistry.* **41**:2333-2336.
- [18] McMillan, J.D. (1993). Xylose fermentation to ethanol: A review. *National Renewable Energy Laboratory, Golden CO.* TP-421-4944
- [19] Jeffries, T.W. *et al.* (2007). Genome sequence of the lignocellulose-bioconverting and xylose-fermenting yeast *Pichia stipitis*. *Nature Biotechnology.* **25**(3):319-326
- [20] Arellano-Plaza, M.; Herrera-López, E.; Díaz-Montaño, D.M.; Moran, A.; Ramírez-Córdova, J.J. (2007). Unstructured kinetic model for tequila batch fermentation. *International Journal of Mathematics and Computers in Simulation.* **1**(1):1-6
- [21] Volesky, B.; Votruba, H. (1992). Modeling and Optimization of Fermentation Processes. *Elsevier, Amsterdam.*
- [22] Monod, J. (1942). Recherches sur la croissance des cultures bacteriennes. *Hermann and Cie, Paris*

- [23] Kompala, D.; Ramkrishna, D.; Tsao, G. (1984). Cybernetic modeling of microbial growth on multiple substrates. *Biotechnol. Bioeng.* **26**:1272-1281.
- [24] Kompala, D.; Ramkrishna, D. (1986). Investigation of bacterial growth on mixed substrates: Experimental evaluation of cybernetic models. *Biotechnol. Bioeng.* **28**:1044-1055.

2. LITERATURE REVIEW

2.1. Bioethanol as a transportation fuel

2.1.1. Historical development

Ethanol has been known and produced by human beings since ancient times. Modern techniques and development of molecular archaeology have proven that ethanol was present in wine making, as early as 5400-5000 BC in Western Asia, and further spread around the world, to Egypt and Mediterranean Europe. In fact, partial DNA sequence data identified a yeast similar to the modern *Saccharomyces cerevisiae* as the biological agent used for the production of wine, beer and bread in Ancient Egypt. [1]. Whisky, brandy and other distilled spirits from grape and other fruits emerged worldwide and their production techniques were refined and further modernized. Distillation was introduced in 1310 and a comprehensive text on the subject was published in Germany by 1556 [1]. Grain spirits production arose for the first time in North America in 1640, and operations conducted in stills were extended all over Ireland and Scotland until the twin-column distillation apparatus devised by the Irishman Aeneas Coffey was implemented in 1830, which continues to yield high-proof ethanol (94-96% by volume) [2].

The above references are regarding to historical development of for alcoholic beverages. However, the use of ethanol as a fuel additive is believed to have begun by the end of the nineteenth century, when emerged as a fuel of choice for automobiles among engineers and motorists [2]. For example, the Automobile Club of America sponsored a competition for alcohol-powered vehicles in 1906, which steered the attention towards ethanol as an important resource by fear about oil scarcity, rising gasoline prices, and the monopolistic practices of Standard Oil [3]. Figure 2.1 shows the first automobile designed to use pure ethanol as a fuel in 1896. The first companies that attempted use of alternative fuels to replace gasoline were Ford and Diesel, and these alternatives were ethanol and powdered coal

respectively, but soon they opted for the less expensive option of gasoline and other crude oil fractions like kerosene [4].



Figure 2.1 – Ford Model Car (1896), which used pure ethanol [5].

Nevertheless, Henry Ford continued his interest in alternative fuels, and he sponsored conferences concerning with the industrial uses of agricultural mass products. He created model A in 1935 - 1937, an automobile that was often equipped with an adjustable carburator designed to allow the use of gasoline, alcohol, or a mixture of two fuels. Several countries (Argentina, Australia, Cuba, Japan, New Zealand and other) in the 1920s and 1930s used ethanol blends in gasoline and Germany became pioneer in alcohol-fueled vehicles during World War II. By 1944, the U.S. Army had developed a nascent biomass-derived alcohol industry [6]. However, these efforts were mostly of a contingency or emergency nature and were abandoned once oil began to flow in increasingly large amounts after World War II ended in 1945.

From the 1970s onwards considerable rising oil prices have occurred similar to those of the 1860's motivating energy conservation as a priority, encouraging every country to use alternative fuels like alcohol and liquefied gas. By 1980, Brazil was the pioneer country to

establish a national alcohol program (PROÁLCOOL) and this boosted the production of ethanol-based automobiles, reaching 96% of the total sales in 1980 in that country [7]. Nevertheless these sales diminished as a consequence of the reduction in prices of the crude oil barrel and it was until 2003 when the Brazilian automobile producers introduced truly flexible-fuel vehicles (FFVs), with engines capable of being powered by pure gasoline, 93% aqueous ethanol, or by a blend of gasoline and anhydrous ethanol [8]. But ten years before, in 1993 a law was enacted, stating that all gasoline sold should have at least a 20% of ethanol by volume. Figure 2.2 shows the changes in oil price from 1860 until 2007 and the main worldwide events that have promoted those changes, comparing the value of the money in 2007 (green line) with respect to the value in each year that is being analyzed (black line).

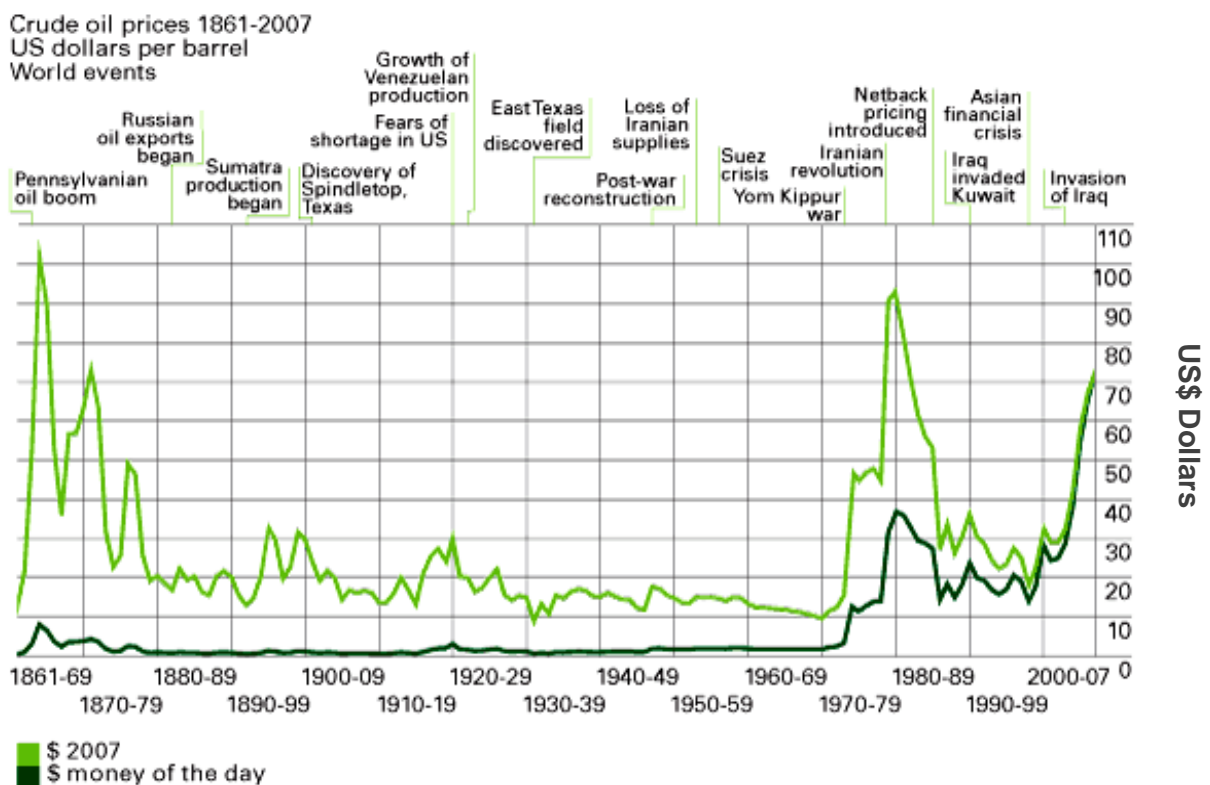


Figure 2.2 – Historical oil price. Data from BP Statistical Review of World Energy, British Petroleum, London, 2007 [9].

Finally in 2006, the tax rate for gasoline was set to be 58% higher than that for hydrated ethanol (93% ethanol and 7% water), and also tax rates were made advantageous for gasoline/ethanol blends higher than 13% [10]. In 2004-2005, Brazil was the world's largest producer of ethanol and Figure 2.3 shows world's fuel-ethanol production in the last 32 years.

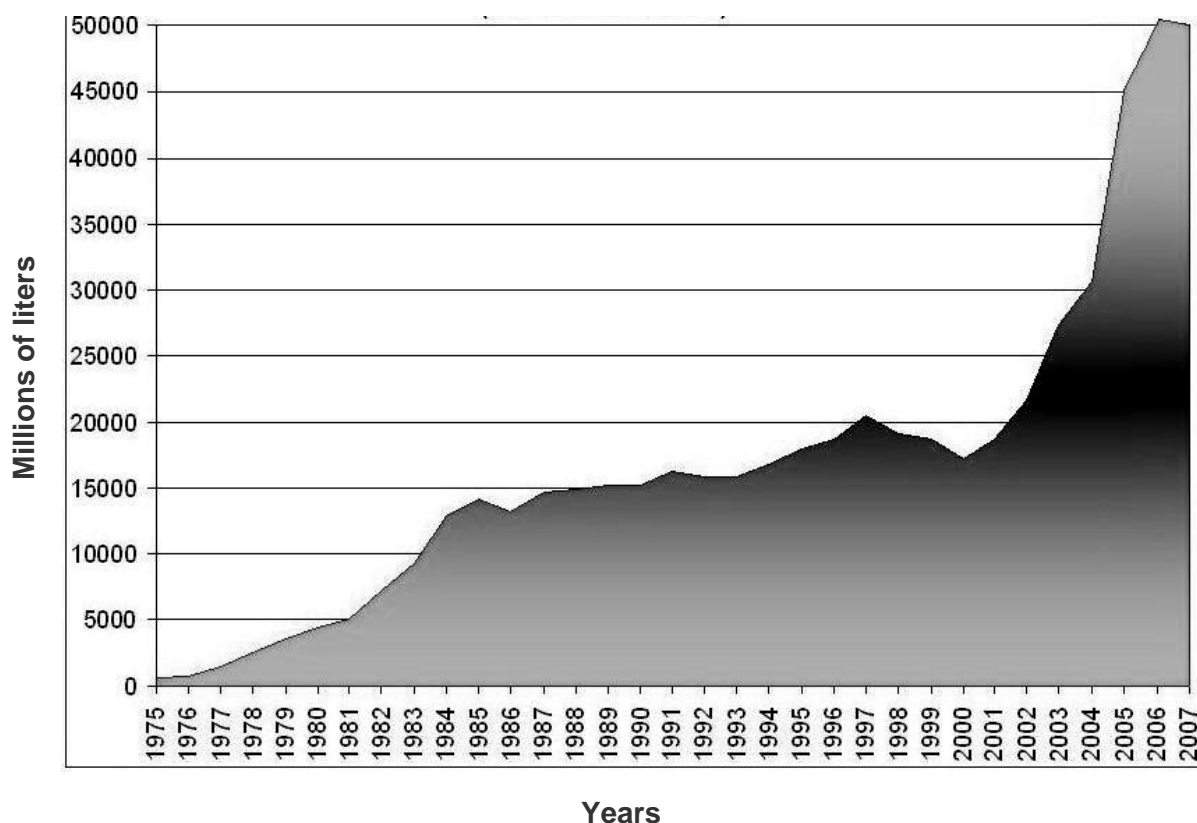


Figure 2.3 – Worldwide ethanol production after 1975 in million of liters. Data from RISE [11].

Besides Brazil, the second major contributing country in the development of fuel ethanol production is the United States [2]. Throughout the twentieth century, ethanol production in USA was intended for the manufacture of a large number of chemical intermediates and fine chemicals, using synthetic routes with ethylene from the petrochemical industry as a raw material, but the oil price shock of the early 1970s, coupled with the

requirements for cleaner burning gasoline and the mandatory inclusion of oxygen-rich additives in gasoline, certainly focused attention on ethanol as an “extender” for gasoline. The compound mainly used was methyl tert-butyl ether (MTBE), another petrochemical industry product, but after 1999 its use stopped because of its toxic and polluting effects [11]. Since then, MTBE’s consumption in the United States decreased considerably as shown in Figure 2.4, ethanol consumption has exceeded that of MTBE from 2003 onwards. In that moment, the perfect candidate to replace MTBE was ethanol, and therefore its production increased rapidly after showing little sustained growth for most of the 1990s, having an exponential growth after 2002 (Figure 2.5).

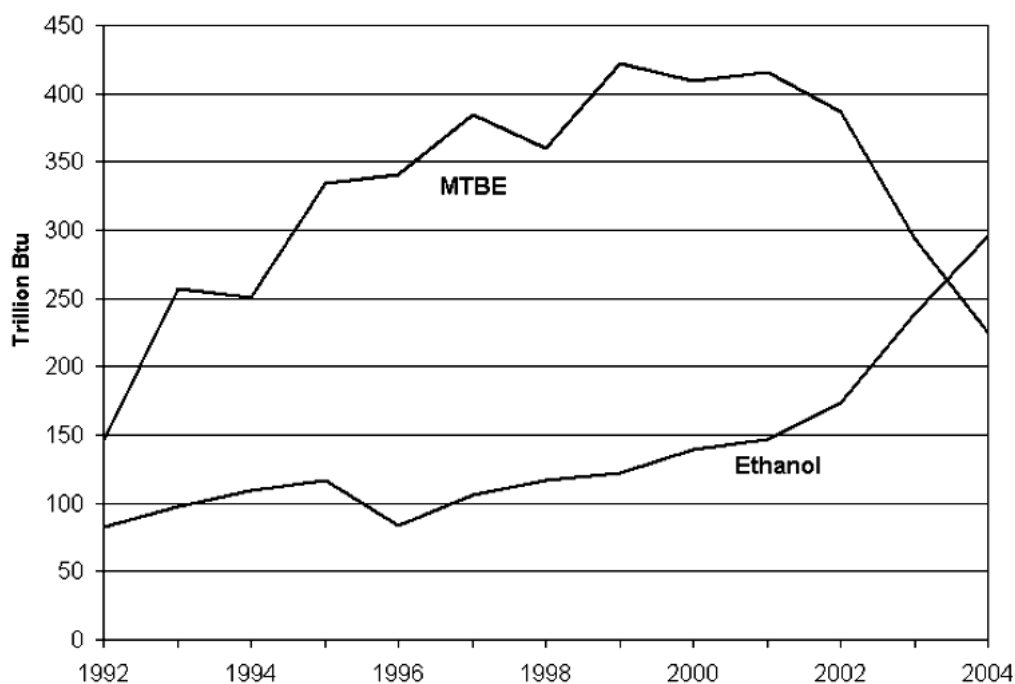


Figure 2.4 – MTBE production in USA. Data from the U.S. Department of Energy [12].

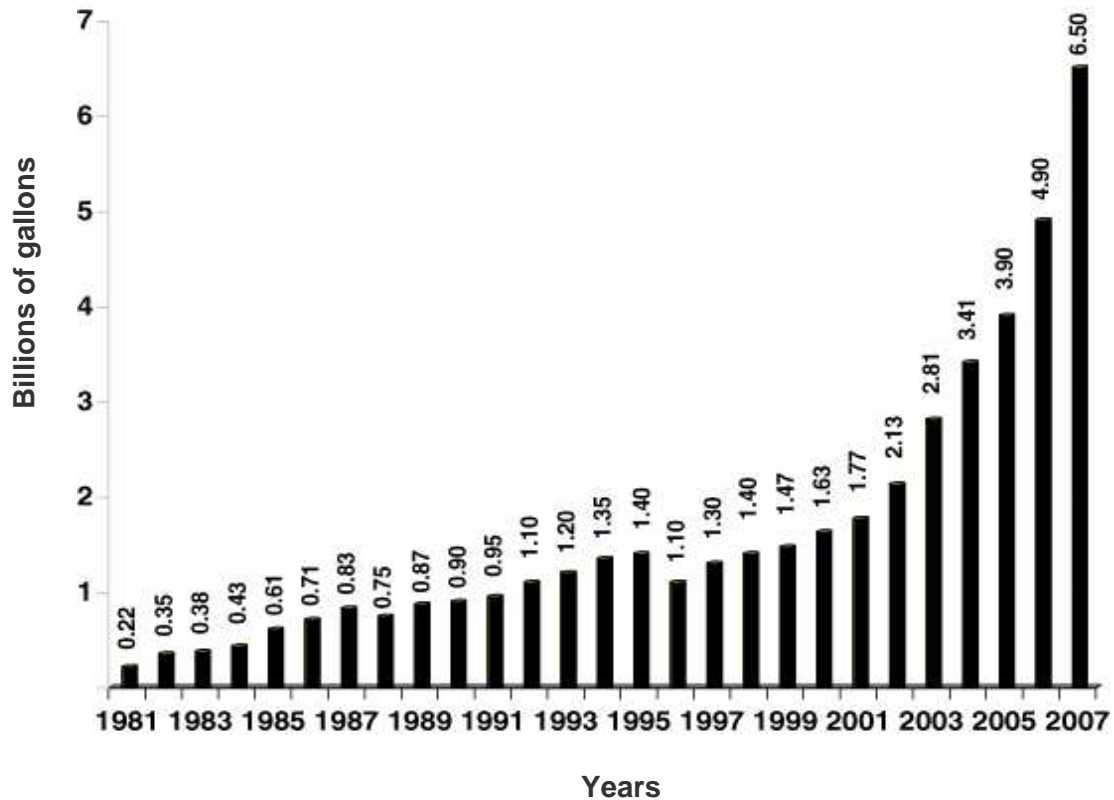


Figure 2.5 – Ethanol production in USA (billions of gallons). Data from the Renewable Fuels Association [11].

In 2005, the United States became the largest ethanol producer nation, followed by Brazil, China, India, France and Russia. The ethanol blend most commonly used is E85 (85% ethanol, 15% gasoline), which is well suited for most flexible-fuel vehicles, although blend E10 is also popular [13]. Greater quantities of ethanol are expected to be used as a motor fuel in the future because of two federal policies included in the 2005 Energy Policy Act (EPACT 2005) [13]: a \$0.51 tax credit per gallon of ethanol used as a motor fuel and a new mandate for up to 7.5 billion gallons of renewable fuel to be used in gasoline by 2012.

2.1.2. Ethanol fuel specifications

The use of ethanol as a fuel in the transportation area is supported by a compilation of chemical and physical properties that make this liquid fuel an excellent alternative to enable cleaner combustion and better engine performance, reducing the dependence on fossil fuels

(mainly oil), and avoiding the release of excessive environmental contaminants that promote and aggravate global warming issues. It is important to clarify that use of ethanol can be analyzed from three points of view: (i) as an oxygenated additive (substituting MTBE from 2002 to date), (ii) as an anhydrous blender for fuel in low-level and high-level gasoline and ethanol mixtures, and (iii) as a pure fuel. Also, recent advances in lignocellulosic feedstock processing technology may give ethanol a stronger cost position relative to other alternative fuels [14].

The outstanding ethanol properties compared with gasoline are discussed below, and Table 2.1 summarizes this comparison. Ethanol has a higher octane number, which is a measure of a fuel's resistance to self-ignition and detonation, and this means higher compression ratios resulting in greater engine efficiencies and higher power from a given engine size. Regarding flammability limits, once ignited, ethanol burns faster than gasoline, thus allowing more efficient torque development [15]. Also ethanol has a much higher heat of vaporization (about 390 BTU/lb) than gasoline (about 170 BTU/lb), which increases the power produced from a given engine size, and decreases the maximum combustion temperature and the thermal load on the engine. Ethanol's stoichiometric flame temperature of 1930°C (compared to 1977°C for gasoline and 2054°C for diesel fuel) contributes to higher efficiencies for an optimized ethanol engine. Finally, solubility could be an obstacle to a greater acceptance of ethanol as a fuel because of the possibility of water phase separation from a gasoline-ethanol blend. However, the more ethanol added to gasoline, the less this problem tends to occur, because gasoline-ethanol blends have a capacity to dissolve water that is directly proportional to the ethanol content [5].

Table 2.1 – Gasoline and ethanol properties [5].

Parameter	Unit	Gasoline	Ethanol
Lower caloric value	kJ/kg	43500	28225
	kJ/L	32180	22350
Density	kJ/L	0.72 – 0.78	0.792
Research Octane Number (RON)	-	90 - 100	102 - 130
Motor Octane Number (MON)	-	80 - 92	89 – 96
Vaporization latent heat	kJ/kg	330 - 400	842 - 930
Stoichiometric relation air/fuel		14.5	9.0
Steam pressure	kPa	40 - 65	15 – 17
Ignition temperature	°C	220	420
Solubility in water	% in volume	~0	100

2.1.3. Economic and environmental issues for bioethanol

To be competitive, and to win economic acceptance, the cost for bioconversion of biomass to liquid fuel must be lower than the current gasoline production costs. Regarding bioethanol production, the cost of feedstock and cellulolytic enzymes are two important parameters for a low cost ethanol production. Biomass feedstock cost represents around 40% of the ethanol production cost [16]. An important factor for reducing the cost of bioethanol production is to use larger industrial facilities rather than smaller ones. Wilke and co-workers [17] have made the first effort to analyze the cost of the conversion of biomass to ethanol process based on a Simultaneous Hydrolysis and Fermentation (SHF) operation and concluded that neat ethanol could compete with gasoline at the oil prices in the range of \$20 to \$30 per barrel. They also suggested an integrated approach, that is, process engineering, fermentation and enzyme and metabolic engineering, all together [17]. Estimates and economic analyses from primary scientific journals, data from a range of sources (including reports prepared for governments and conference proceedings) show productions costs for

bioethanol on the basis of 2003, as described in Table 2.2. Ethanol produced from sugar, starch (grain), and lignocellulosic sources covered production cost estimates from less than \$1/gallon to more than \$4/gallon. Even with the lower production costs for lignocellulosic ethanol in the United States, taking into account financial outlays and risks, an ethanol price of \$2.75/gallon would be more realistic, according to Bohlman's review [18].

Table 2.2 – Estimated production costs for bioethanol in 2003 [19].

Source of Ethanol	Production cost (€/GJ)	Production cost (\$/liter)	Production cost (\$/gallon)
Sugarcane (Brazil)	10 – 12	0.24 – 0.29	0.91 – 1.10
Starch and sugar (U.S. and Europe)	16.2 – 23	0.39 – 0.55	1.48 – 2.08
Lignocellulosic (U.S.)	15 – 19	0.36 – 0.46	1.36 – 1.74
Lignocellulosic (Europe)	34 – 45	0.82 – 1.08	3.10 – 4.09

Regarding environmental issues, ethanol represents a closed carbon dioxide cycle because after burning of ethanol, the released CO₂ is recycled back into plant materials by the photosynthesis effect to synthesize cellulose, which means no net addition of CO₂ to the atmosphere, making ethanol an environmentally beneficial energy source. However, the main feature of ethanol as a renewable fuel and its promise to the environment is a tiny contribution to the green house gas effect. Direct comparisons of gas emissions resulting from the combustion of anhydrous ethanol, ethanol-gasoline blends, and gasoline are straightforward to perform but are poor indicators of the overall consequences of substituting ethanol for gasoline. Therefore, one effective methodology to study the environmental impact of ethanol is to compare CO₂ emissions among various fuels as shown in Figure 2.6. Noncarbon-based fuels (i.e., electric vehicles powered using electricity generated by nuclear and solar options)

along with ethanol from biomass are the best options because of their low CO₂ emissions. Ethanol from corn showed no net advantage, despite more recent estimates that place its production as giving modest reductions in greenhouse gas emissions, 12-14% [12,20].

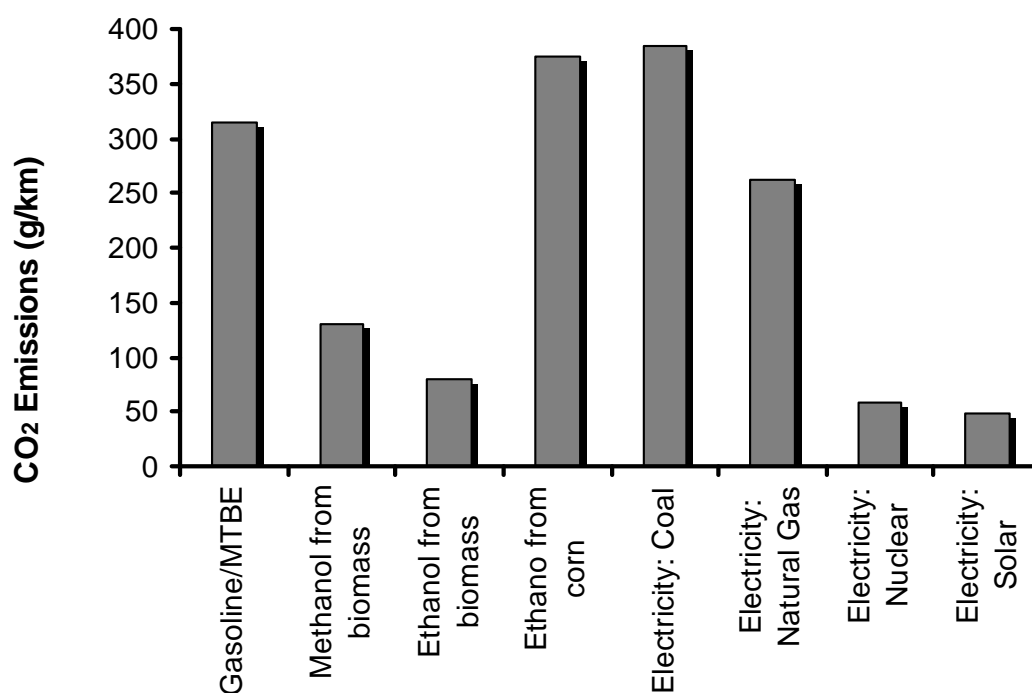


Figure 2.6 – Total fuel cycle carbon dioxide emissions [2].

Figure 2.7 shows how cellulosic ethanol has the major contribution to the reduction of greenhouse gas emissions when compared to gasoline, and also to corn and sugarcane based ethanol. Filled bars represent the percentage of greenhouse gas emissions where gasoline contributes to 100% of emissions and cellulosic ethanol has a contribution of 14%, approximately [21].

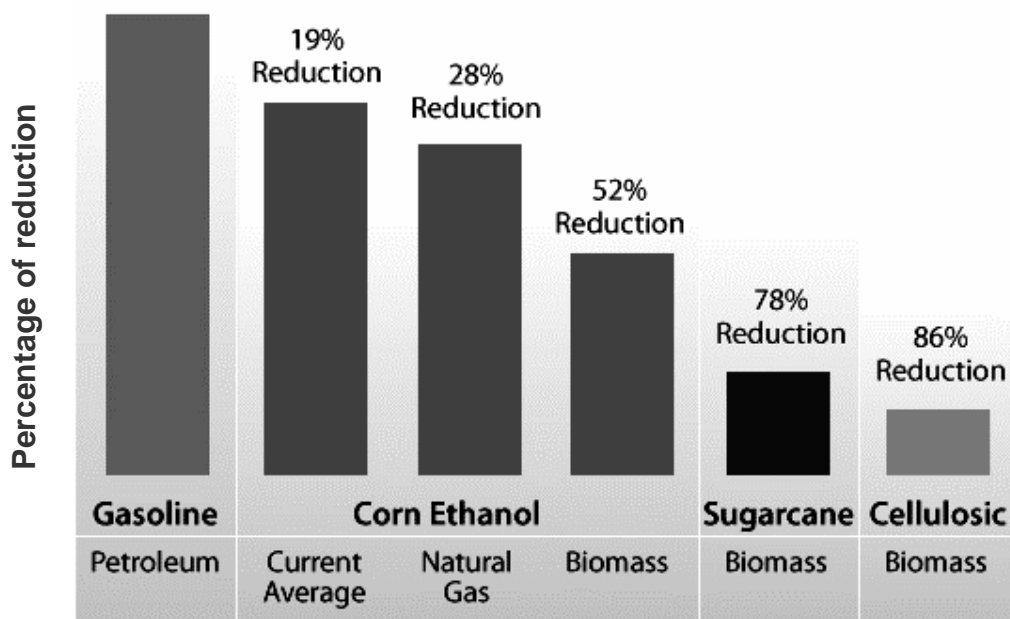


Figure 2.7 – Percentage of reduction of greenhouse gas emissions in fuel ethanol [21].

2.2. Biomass-to-ethanol technology

2.2.1. Classic feedstocks for ethanol production

As mentioned in section 2.1, historical development of bioethanol motivated the use of different feedstocks for its production, depending on the policies established in each country encouraging to reduce the use of petroleum-derived fuels and toxic oxygenate additives. In general, bioethanol feedstocks can be conveniently classified into three types, as described briefly in chapter 1: (i) sucrose-containing feedstock (e.g. sugar cane, sugar beet and sweet sorghum), (ii) starchy materials (e.g. corn, wheat and barley), and (iii) lignocellulosic biomass (e.g. wood, agricultural wastes, straw and grasses) [22]. A brief introduction concerning types (i) and (ii) will be made now, although emphasis will be made on the third type because of the scope and purpose of this research work.

The first type of feedstocks comprises ethanol produced from sugars, which involves either sugar cane juice or molasses (by-product of sugar mills), and the leading country using

these feedstocks is Brazil with about 27% of global production. The Brazilian bioethanol industry was poised for a major jump during 2006-2008 as a part of new national plan to increase sugar cane production by 40% by 2009 [23]. The main advantage in sugar-based bioethanol production lies on the reduction of one step if compared with starch-bioethanol, since sugars are already present in the feedstock. The process is based on extraction of sugars (by means of milling or diffusion), which may be then fed straight to fermentation [5]. The most employed microorganism is *Saccharomyces cerevisiae* due to its capability to hydrolyze cane sucrose into glucose and fructose, two easily assimilable hexoses. Ethanol yields achieved using sugar cane molasses and *S. cerevisiae* range 85-90% in batch processes [24] and 94.5% in continuous processes carried on in continuous-stirred tank reactors (CSTR) using residence times of 3-6 hours and achieving productivities of 5-20 g/L-h [25]. Production cost of ethanol from sugar cane was estimated in ~\$160/m³ being the lowest cost so far of all different feedstocks for bioethanol production [26]. Sugar beet is also very utilized, especially in European countries, and one of the main advantages is a lower cycle of crop production, higher yield, and high tolerance of a wide range of climatic variations.

The second type comprises ethanol from starchy materials, being corn the most utilized, almost exclusively in countries like United States. Starch is a high yield feedstock, a homopolymer consisting of only D-glucose monomers but acid or enzymatic hydrolysis to break down the chains of this polymer is required to obtain glucose syrup and then produce ethanol by yeast fermentation. USA has a large corn-based bioethanol industry with a capacity of over 15 billion of liters per year and its production capacity is anticipated to continue to rise to about 28 billion of liters per year by 2012, as dictated by the Energy Policy Act of 2005 [26]. Ethanol produced from corn has the higher conversion rate, with 410 liters/ton, although ethanol yield is so much lower if compared to sugar cane, and the production cost reaches values ranging from \$250-420/m³ [26]. This is due mainly by two

reasons: yeasts such as *S. cerevisiae* cannot utilize starchy materials and therefore enzymes such as glucoamylases and α -amylases need to be added, and the other one is that starchy materials need to be cooked at high temperatures to obtain a high bioethanol yield [28]. The starch-based bioethanol industry has been commercially viable for about 30 years; in that time, tremendous improvements have been made in enzyme efficiency, reducing process costs and time, and increasing bioethanol yields [27].

The third type of feedstock involves lignocellulosic biomass, and it is currently considered as the best option when compared to sugar and starchy materials because of the so called “food versus fuel” controversy generated by using these food/feed grade-feedstocks to produce ethanol and thus increasing the costs for general food market, which have reached alarming bounds. Therefore, attention and priority have been assigned to the study of lignocellulosic biomass as a raw material for ethanol production. As mentioned in Chapter 1, production of ethanol from biomass is one way to reduce both consumption of crude oil and environmental pollution. Bioethanol can be produced from cellulosic feedstocks, but one major problem related to production processes is the availability of raw materials; the availability can vary considerably from season to season and depends on the geographic locations. Lignocellulosic biomass is the most promising feedstock considering its great availability and low cost, but the large-scale commercial production of fuel bioethanol from lignocellulosic materials has still not been implemented widely [22]. The lignocellulosic complex is the most abundant biopolymer in the Earth, reaching about 50% of world biomass and its annual production was estimated in 10-50 billion ton [24] and could produce up to 442 billion liters per year of bioethanol [29]. Figure 2.8 shows the summarized technological routes for ethanol production from the three feedstocks described above.

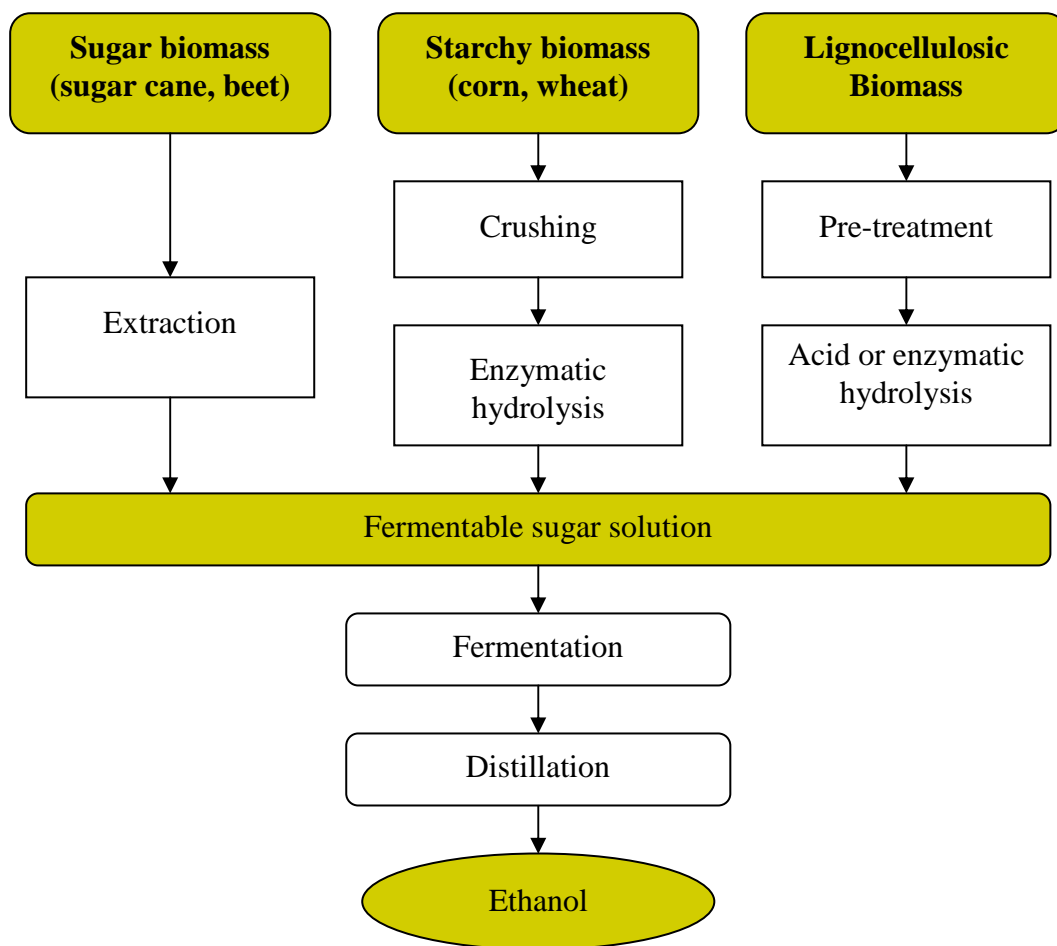


Figure 2.8 – Technological routes for ethanol production [5].

2.2.2. Components of lignocellulose

Lignocellulose is one component of the cell wall in higher plants, which provides the structural rigidity necessary for growth. Three polymers comprise the entire microscopic structure of lignocellulose: cellulose $(C_6H_{10}O_5)_x$, hemicellulose such as xylan $(C_5H_8O_4)_m$, and lignin $[C_9H_{10}O_3.(OCH_3)_{0.9-1.7}]_n$ in trunk, foliage, and bark [30,31]. Figure 2.9 shows a schematic representation of these three components in a microfibril array of any given plant cell.

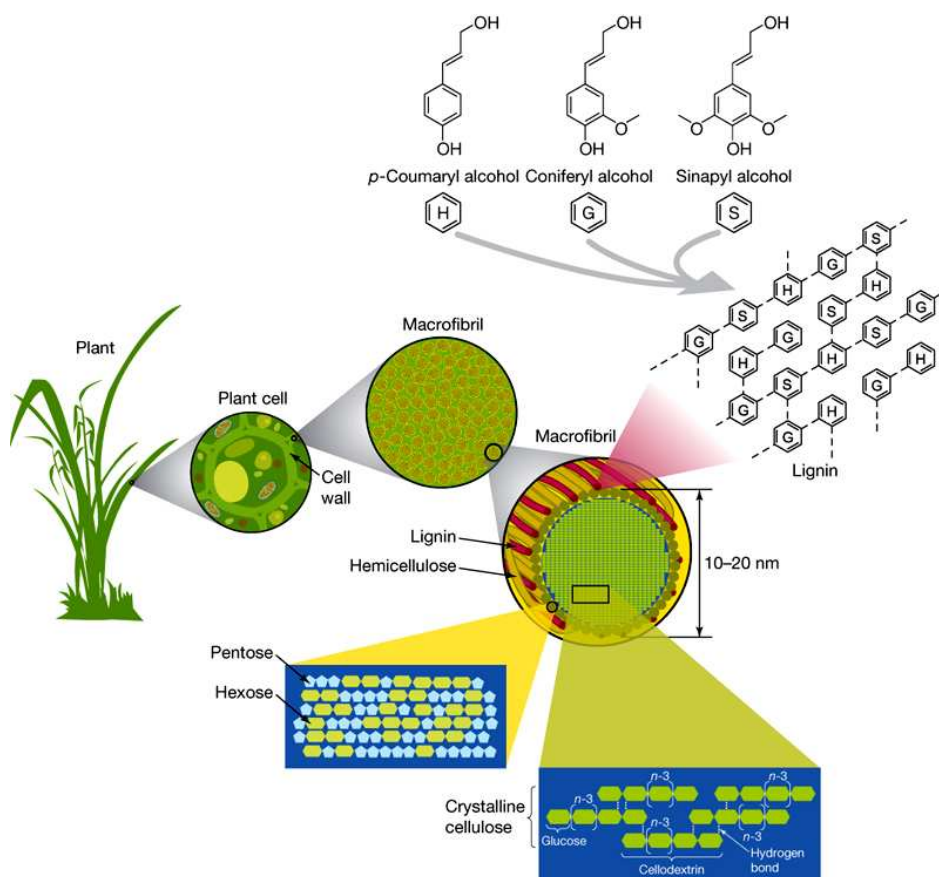


Figure 2.9 – Lignocellulose microscopic structure and distribution [32].

Cellulose is a homopolysaccharide comprising approximately the 35-50% of lignocellulose materials. It is composed of β -D-glucopyranose units (glucose chair conformation) linked together by $\beta(1\rightarrow4)$ -glycosidic bonds. The cellulose molecules are linear; the β -D-glucopyranose chain units are in a chair conformation and the substituents HO-2, HO-3, and CH₂-OH are oriented equatorially. Glucose anhydride, which is formed via the removal of water from each glucose unit, is polymerized into long cellulose chains that contain 5000-10000 glucose units. The basic repeating unit of the cellulose polymer consists of two glucose anhydride units, called a cellobiose unit [33]. The second major chemical constituent in lignocellulose biomass is hemicellulose (~20-35%), which is a mixture of various polymerized monosaccharides such as glucose, mannose, galactose, xylose, arabinose,

4-*O*-methyl glucuronic acid and galacturonic acid residues, but xylose and arabinose are the predominant pentose sugars derived from the hemicellulose of most hardwood feedstocks, agricultural residues and other herbaceous crops, such as switchgrass. Lignocellulose's remaining fraction are the lignins, highly branched, substituted, mononuclear aromatic polymers in the cell walls of certain biomasses, especially woody species. Lignin cannot be readily converted to ethanol but can be used as a fuel or precursor for specific chemical syntheses. Likewise, there is no microorganism currently available that can utilize lignin monomers for ethanol production [34]. Lignins and hemicelluloses may form chemically linked complexes that bind water-soluble hemicelluloses into a three-dimensional array, cemented together by lignin, that sheaths the cellulose microfibrils and protects them from enzymatic and chemical degradation [2]. Figures 2.10 to 2.12 show the basic chemical structure of these three polymers.

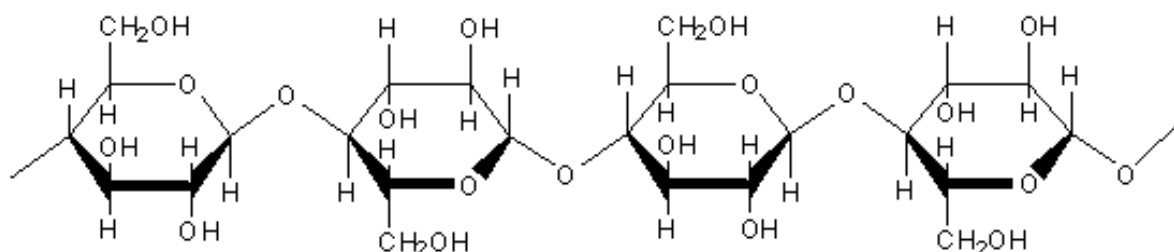


Figure 2.10 – Structure of a short segment of cellulose [35].

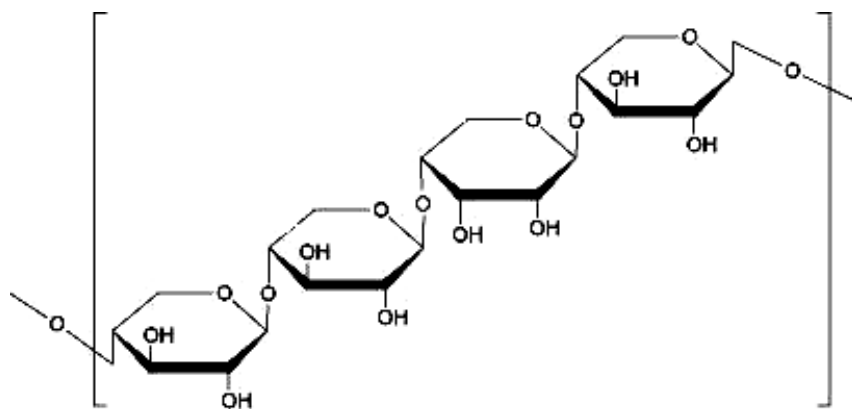


Figure 2.11 – Structure of xylan a short segment of hemicellulose [36].

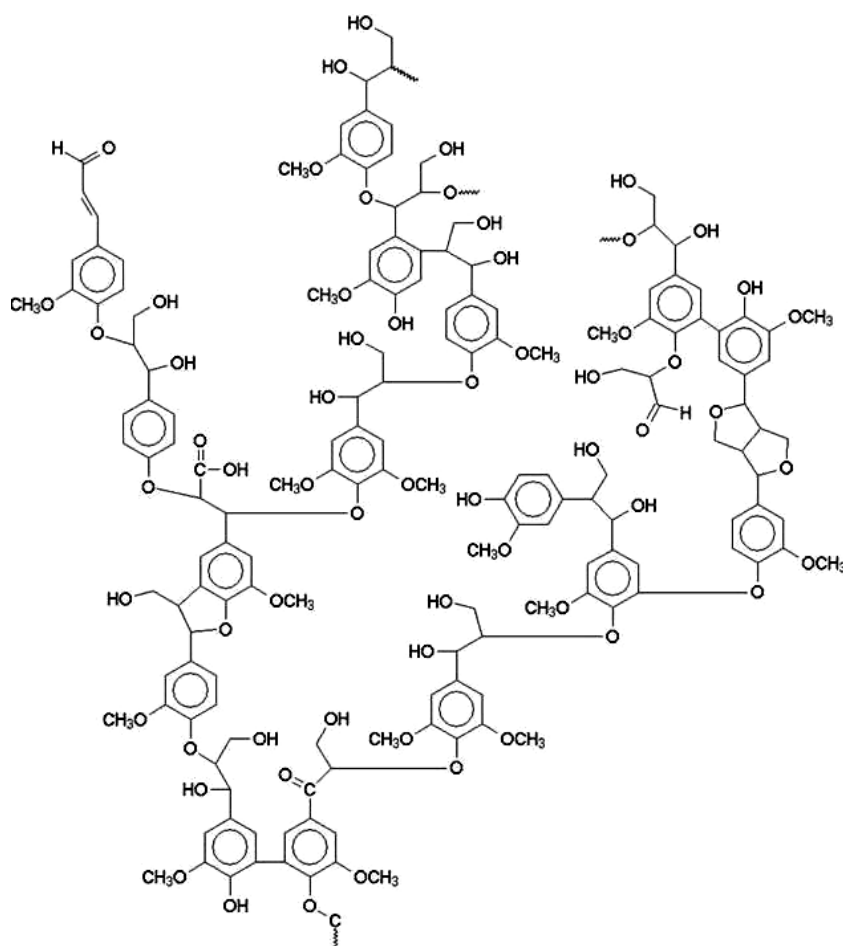


Figure 2.12 – Structure of segment of lignin [37].

The contents of these three fractions in lignocellulosic materials may vary depending on the type of material and the geographic area. According to Sáez's review [38] lignocellulosic materials can be divided in five main groups: herbaceous, crop residues, hardwood, softwood and cellulose wastes. Table 2.3 shows some examples of each one of these five main categories and the abundance of each one of the three fractions described above.

Table 2.3 – Approximate composition of selected lignocellulosic materials for ethanol production [38].

Material	Cellulose (%)	Hemicellulose (%)	Lignin (%)
Herbaceous			
Alfalfa hay	38	9	14
Switchgrass	45	31	12
Leaves	15 – 20	80 - 85	0
Crop residues			
Corn cobs	45	35	15
Corn stover	41	21 - 28	17 – 22
Sugarcane bagasse	40	22.5	25
Wheat straw	36	28	29
Nut shells	25 – 30	25 - 30	30 – 40
Hardwood			
Aspen	46	26	18
Hybrid poplar	43	21	26
Softwood			
Spruce	43	26	29
Pine	44	26	29
Cellulose wastes			
Newsprint	61	16	21
Newspaper	40 – 55	25 - 40	18 – 30
Recycled paper sludge	50	10	0
Sorted refuse	60	20	20

2.2.3. Processing of lignocellulosics to bioethanol

There are several options for a lignocellulose-to-bioethanol process, but regardless of which is chosen, some features must be assessed in comparison with established sugar- or starch-based bioethanol production. These features include efficient de-polymerization of cellulose and hemicellulose to soluble sugars, efficient fermentation of a mixed-sugar hydrolysate containing hexoses and pentoses, advanced process integration to minimize process energy demand and reduction of lignin content of the feedstock to decrease the cost of bioethanol [22]. Processing of lignocellulosics to bioethanol consists of four major unit operations: pre-treatment, hydrolysis, fermentation and product recovery. Each one is described below.

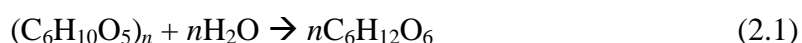
2.2.3.1. Pre-treatment of biomass

Pre-treatment of biomass is necessary because the matrix of cellulose and lignin bound by hemicellulose chains should be broken in order to reduce the crystallinity degree of the cellulose and to increase the fraction of amorphous cellulose, with the objective of making more accessible to the enzymes that convert the carbohydrate polymers into fermentable sugars and to ethanol producing microorganisms. Additionally, the hemicellulose fraction should be hydrolyzed and lignin should be released or removed. Several methods and/or combination of methods already exist to carry out pre-treatment. The physical-chemical method known as steam explosion is the most studied and applied, since it is recognized as one of the most cost-effective for hardwood and agricultural residues, but it is less efficient for softwood. [39]. One very promising method is the pre-treatment with Liquid Hot Water (LHW) or thermohydrolysis, which presents elevated recovery rates of pentoses and does not generate inhibitors [40]. Chemical methods such as dilute acid hydrolysis are also available, but the costs are higher than the ones corresponding to steam explosion. Finally, there are

biological methods, the ones that have low energy requirements and mild environmental conditions. However, most of the biological processes are too slow, limiting their application at the industrial level. The fungus *Phanerochaete chrysosporium* has been proposed in the patent of Zhang [41] for degrading the lignin in a biomass-to-ethanol process scheme involving the separate fermentation of pentoses and hexoses. No matter which of the methods described before is used, one of the main problems in pre-treatment and hydrolysis of biomass is the variability in the composition of both lignin and hemicellulose, and this depends on several factors such as the type of plant, crop age, method of harvesting, etc. [42]. After the pre-treatment step and even after the hydrolysis step, detoxification should be carried out to remove inhibitors produced by the addition of chemicals and from the degradation products of soluble sugars and lignin. Therefore, detoxification of the streams that will undergo fermentation is required. Among the various physical, chemical and biological existent methods, the best candidates are alkali treatment and addition of calcium hydroxide (overliming) or ammonia, this last one has shown better results than treatment with sodium or potassium hydroxide [42].

2.2.3.2. Hydrolysis

The hydrolysis step is next to the pre-treatment, and here takes place the cleavage of the cellulose polymer to glucose units with the addition of one molecule of water, according to the chemical reaction:



Hydrolysis of lignocellulosic biomass is more complicated than that of pure cellulose due to the presence of nonglucan components such as lignin and hemicellulose [41]. A

number of processes for hydrolyzing cellulose into glucose have been developed over the years, and the majority of these processing schemes utilize either cellulolytic enzymes or sulfuric acid of various concentrations. Nowadays, enzymatic hydrolysis has demonstrated better results for the subsequent fermentation because no degradation components of glucose are formed although the process is slower. Several other chemical methods are also available, such as dilute acid processes with fast rates of reaction but with the disadvantage of low sugar yield. Even novel physical methods such as gamma-ray or electron-beam irradiation, or microwave irradiation are currently being tested in pilot plants [43]. Most of the commercial cellulases are obtained aerobically from microorganisms such as *Trichoderma reesei* and *Aspergillus niger*; they release a mixture of cellulases, among which at least two cellobiohydrolases, five endoglucanases, and β -glucosidases and hemicellulases have been found [41].

2.2.3.3. Fermentation of biomass hydrolysates

When carbohydrates coming from cellulose and hemicellulose are released free in solution, after any of the hydrolysis methods mentioned above, the next step is the fermentation of these carbohydrates to produce ethanol, using microorganisms such as yeast or bacteria. Because such lignocellulose hydrolysates contain more than one type of carbohydrate, including oligosaccharides, microorganisms should be required to efficiently ferment these sugars for the successful industrial production of bioethanol [44]. The general reactions involved in the production of ethanol, considering glucose and xylose as the main free sugars in solution after hydrolysis step are respectively:



The classic configuration employed for fermenting biomass hydrolysates involves a sequential process where the hydrolysis and fermentation are carried out in different units, this is known as separate hydrolysis and fermentation (SHF). In the alternative variant, the simultaneous saccharification and fermentation (SSF), the hydrolysis and fermentation are performed in a single processing unit. This last configuration has been improved through the use of genetically engineered microorganisms capable of fermenting simultaneously hexoses and pentoses from cellulose and hemicellulose respectively, or through the use of two or more different strains of microorganisms with the ability to ferment their corresponding sugars. This new variant of SSF is known as simultaneous saccharification and co-fermentation (SSCF). The main feature of SHF process is that each step can be performed at its individual optimal operation conditions but one disadvantage is that cellulolytic enzymes are end-product inhibited, so that the rate of hydrolysis is progressively reduced when glucose and cellobiose accumulate [45]. The SSF shows more attractive profiles than the SHF as higher ethanol yields and less energy consumption are possible; but this process operates at non-optimal conditions for hydrolysis and requires a higher enzyme dosage, which positively influences on substrate conversion, but negatively on process costs [42]. In the SSCF technology, the enzymatic hydrolysis continuously releases hexose sugars, which increase the rate of glycolysis such that the pentose sugars are fermented faster and with higher yields. SSF and SSCF are preferred technologies since both can be performed in the same bioreaction tank, resulting in lower capital costs [46].

2.2.3.4. Product recovery

Distillation is the technology more utilized for ethanol recovery, and different technologies that will allow the economic recovery of dilute volatile products from streams containing a variety of impurities have been developed and commercially demonstrated [47].

However, ethanol can be distilled up to concentration of 95.6% because of the azeotrope formation of the mixture of ethanol with water, and further dehydration would be needed to achieve ethanol concentrations of ~99.6%. Other separation technologies include the removal of ethanol from a fermentation broth under vacuum even at a normal operating temperature [22]; extraction of ethanol with a solvent such as *n*-decanol when using immobilized cells of *S. cerevisiae* [48]; gas stripping of ethanol in an air-lift fermentor, which is a type of vessel originally developed for viscous microbial fermentation broths but it is also used for some of the more fragile and shear-sensitive mammalian cells in culture [49].

Figure 2.13 shows a generic block developed by Cardona and Sánchez [50] for fuel ethanol production from lignocellulosic biomass. Possibilities for reaction-reaction integration are shown inside shaded boxes: SHF, SSF and SSCF (as described previously); co-fermentation (CF); and consolidated bioprocessing (CBP). Main stream components are: cellulose, (C); hemicellulose, (H); lignin, (L); cellulases, (Cel); glucose, (G); pentoses, (P); inhibitors, (I); and ethanol, (EtOH).

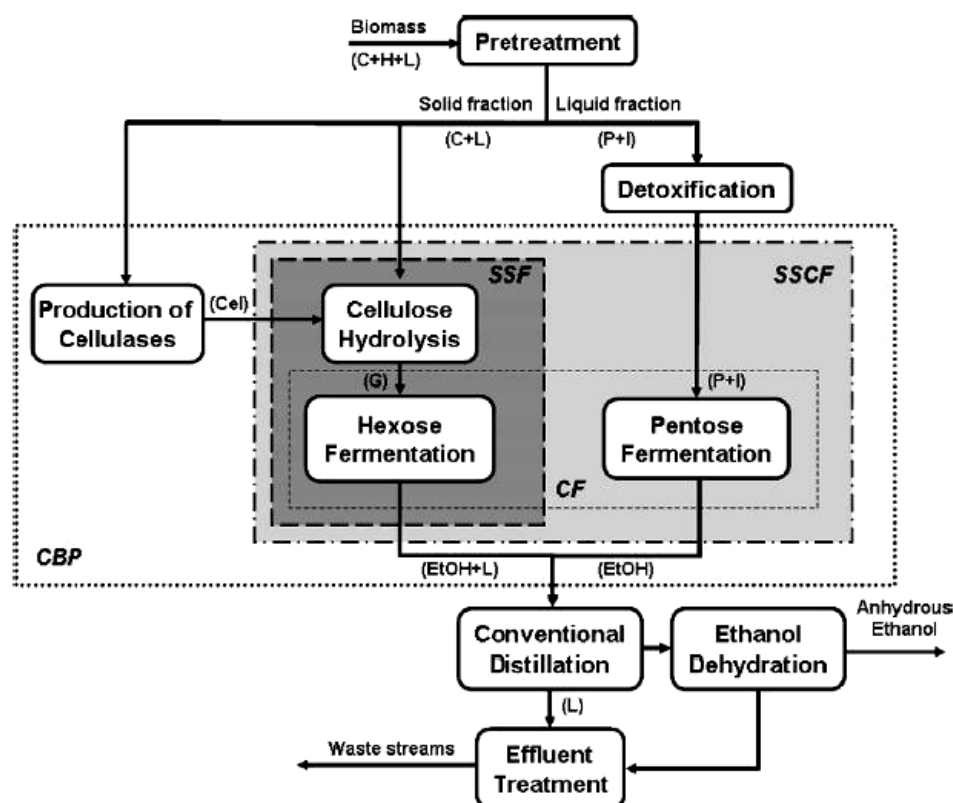


Figure 2.13 – Generic block diagram of fuel ethanol production from lignocellulosic biomass, from Cardona and Sánchez [50].

2.3. Biocatalysts for ethanol fermentation

Finding the right microorganisms to produce ethanol from the mixture of sugars resulting from the hydrolysis of lignocellulosic feedstocks is a major challenge in this bioprocess, because one of the main requirements is to metabolize the majority of sugars in solution to increase ethanol yield and process productivity. However, the best ethanol producers are incompetent at utilizing pentose sugars, whereas species that can efficiently utilize both pentoses and hexoses are less efficient at converting sugars to ethanol. Several microorganisms can efficiently ferment the glucose component in cellulose to ethanol, but conversion of the pentose sugars in the hemicellulose fraction, particularly xylose, remained a bottleneck in biomass-to-ethanol until a couple of years ago. Three options are suggested for actual processing, in order to find the best biocatalyst scheme: (i) endowing traditional yeast

ethanologens with novel traits, including the ability to utilize pentoses, (ii) “reforming” bacterial species and nonconventional yeasts to be more efficient at converting both pentoses and hexoses to ethanol, and (iii) devising conditions for mixed cultures to function synergistically with mixtures of major carbon substrates [2]. There are some essential traits in microorganisms used in bioethanol production, necessary to achieve high ethanol yields and concentration; microorganisms should ferment both hexoses and pentoses with ethanol as the sole fermentation product, tolerating high ethanol concentrations and inhibitory compounds as well typically present in dilute-acid hydrolysates, and should require hypoxic conditions (very low concentrations of oxygen).

Different strains of microbes have been utilized to produce ethanol, for both fuel and alcoholic purposes. Yeasts and bacteria are the preferred microbes although some fungus species such as *Paecilomyces sp.* NF1 have been also proposed to ferment all of the major sugars derived from hydrolysis of plant biomass to ethanol using the SSF configuration [51]. The microorganism more utilized along the history because of its advantages is the yeast *Saccharomyces cerevisiae*, but despite of such advantages it has some limitations that have motivated the search of other species to complement what *S. cerevisiae* lacks for an efficient ethanol production process.

2.3.1. Hexose-fermenting microbes

As mentioned above, *S. cerevisiae* is a well-known yeast strain used in alcoholic fermentations because of its ability to ferment glucose to ethanol as virtually the sole product, superior ethanol tolerance, and rapid fermentation rates under acidic conditions and resistance to the acetic acid found in lignocellulosic hydrolysates [52]. However, the main disadvantage of *S. cerevisiae* is its narrow substrate utilization range, because it cannot ferment pentoses due to the lack of both pentose-assimilation pathways and adequate levels of key pentose

phosphate pathway enzymes. Bacteria are much less widely known as ethanol producers than are yeasts, but *Escherichia*, *Klesbiella*, *Erwinia*, and *Zymomonas* species have all received serious and detailed considerations for industrial use. *Zymomonas mobilis* has extremely desirable features as an ethanologen with the advantage to grow at high sugar concentrations and to produce and tolerate ethanol at concentrations up to 13% mass/volume (w/v) [53].

2.3.2. Pentose-fermenting microbes

The lack of an effective pentose-assimilation pathway in efficient hexose-fermenting microbes and the need to take advantage of all sugars resulting from the hydrolysis of cellulose and hemicellulose, motivated several years ago the search of strains that could ferment xylose under strictly anaerobic conditions. Yeasts such as *Candida shehatae*, *Pachysolen tannophilus*, *Pichia stipitis*, and *Kluyveromyces marxianus* have been postulated to use a two-step pathway in which xylose is first reduced to xylitol by xylose reductase enzyme (XR), and then is oxidized to xylulose by xylitol dehydrogenase enzyme (XD). Xylulose is subsequently phosphorylated to form xylulose-5-phosphate and then metabolized to ethanol through the pentose phosphate and Embden-Meyerhoff-Parnas pathways [54]. *P. stipitis* reportedly provides the best overall performance in terms of complete sugar utilization, minimal coproduct formation, and insensitivity to temperature and substrate concentrations [55]. In bacteria, the pentose metabolic pathway is different, being the enzyme xylose isomerase (XI) the responsible for isomerization of xylose to xylulose directly without the production of xylitol. However, one limitation to the use of these yeasts on an industrial scale is their requirement for low levels of oxygen, and on the other hand, excess oxygen causes them to completely cease ethanol production and metabolize aerobically the substrate to form biomass. Therefore, the degree of control necessary to maintain the narrow range of

microaerophilic conditions that permit efficient ethanol production could be difficult and cost-prohibitive on an industrial scale.

2.3.3. Genetically engineered microbial strains

Some microorganisms have been genetically modified to change and improve their role in metabolism of substrates and consequently to produce ethanol with higher yields and productivities, but mainly to optimize the conversion of the various types of sugars after hydrolysis of lignocellulosic biomass. These changes include expression analysis of key genes in metabolic pathways for further inclusion of these genes in other microorganisms that naturally do not display them in their wild-type strains. The recent determination of the genome sequence for *P. stipitis* is important, as its genome characteristics and regulatory patterns could serve as guides for further development in this natural xylose-fermenting yeast or in engineered *S. cerevisiae*. In fact, *P. stipitis* has been the most widely used donor, probably because it shows relatively little accumulation of xylitol when growing on and fermenting xylose, thus wasting less sugar as xylitol [56]. For direct genetic manipulation of *S. cerevisiae*, the most used strategy has been to insert the two genes from *P. stipitis* coding for XR and XDH enzymes to conduct the intermediate metabolites through the pentose phosphate pathway with final ethanol production. In addition to this XR-XDH strategy, other option is the inclusion in of XI enzyme gene coming from bacteria or fungi such as *Piromyces*, in *S. cerevisiae* to metabolize xylose to ethanol. Some studies have been carried out to compare these two strategies, and results obtained by the group of Grauslund [57] reveal that despite a little xylitol accumulation, XR-XDH xylose utilization pathway provides faster ethanol production than using the XI pathway. However, in chemically defined medium, XI pathway showed the highest ethanol yield. Genetic manipulation of bacteria has been also carried out to utilize high-performance bacteria strains in the production of ethanol,

being *Escherichia coli*, *Klesbiella oxytoca* and *Zymomonas mobilis* the species assayed. Among them, *Z. mobilis* has shown the most promising results, when some strains were first engineered to catabolize xylose at the National Renewable Energy Laboratory in Colorado, United States. Genes for xylose utilization by *E. coli* were introduced into *Z. mobilis* [58].

Regardless the utilization of wild-type or genetically engineered hexose- and/or pentose-fermenting microbes, the complete degradation of glucose or xylose using yeasts, as the most abundant sugars in lignocellulosic hydrolysate, proceed along the metabolic pathways shown in Figure 2.14. Microorganisms used in the process have the ability to produce all of the enzymes required for each intermediate step in the corresponding metabolic pathways. The metabolic pathway shown in the left side of Figure 2.14 describes glucose degradation by means of glycolysis (dotted box to the left) with further catabolism of pyruvate produced in glycolysis to ethanol. The numbers between each intermediate step correspond to the enzymes that catalyze each reaction: (1) hexokinase, (2) phosphoglucose isomerase, (3) phosphofructokinase-1, (4) aldolase, (5) triose phosphate isomerase, (6) glyceraldehyde-3-phosphate dehydrogenase, (7) phosphoglycerate kinase, (8) phosphoglycerate mutase, (9) enolase, (10) pyruvate kinase, (11) pyruvate decarboxylase, and (12) alcohol dehydrogenase [59].

The right side of Figure 2.14 describes the yeast xylose degradation pathway, either by wild-type strains or genetically engineered yeast strains encoding genes to express enzymes for xylose degradation. In this pathway xylose is metabolized in two steps to form xylulose-5-phosphate and at this point begins the Pentose Phosphate Pathway (PPP) to yield fructose-6-phosphate and glyceraldehyde-3-phosphate, which enters into the glycolysis pathway to finally produce ethanol. The enzymes catalyzing xylose and PPP pathways are shown as letters between each intermediate step in Figure 2.14, and they are: (a) xylose reductase, (b) xylitol dehydrogenase, (c) xylulokinase, (d) transketolase, and (e) transaldolase [56].

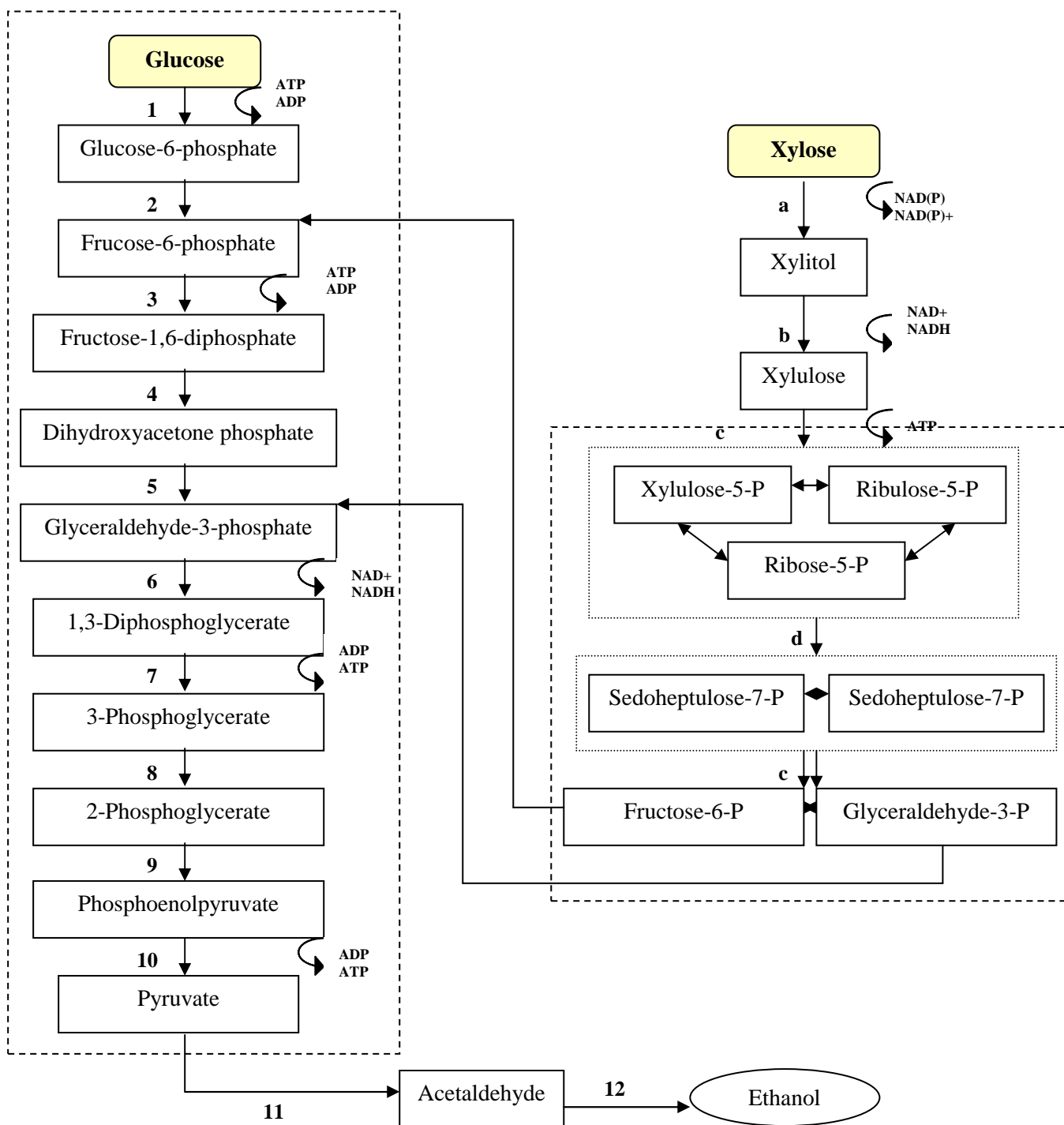


Figure 2.14 – Metabolic pathways to produce ethanol from glucose and xylose. (Adapted from Nelson and Cox [59]).

2.4. Fermentation of mixtures of glucose and xylose

After hydrolysis and detoxification of cellulose and hemicellulose, glucose and xylose are predominant in the resulting sugar solution. Depending on the type of feedstock used, and on the employed pre-treatment and hydrolysis methods as well, the proportion of glucose/xylose in hydrolysate can vary. However, the main objective is to ferment completely both sugars to improve ethanol yields. Various studies have focused in fermentation of glucose and xylose mixtures, with different initial ratios and methodologies, such as batch, fed-batch and continuous processes and the type of fermenting microorganisms used, where the most used are yeast and bacteria strains. Out of those, some included a given hexose- and xylose-fermenting, genetically engineered microorganisms as described in the previous section, or co-cultures of strains having the ability to ferment both sugars.

One important contribution in this regard is the study carried out by Agbogbo and co-workers [60] where different synthetic glucose/xylose mixtures with a total concentration of 60% (w/v) were fermented into ethanol using *P. stipitis* CBS 6054. The different percentage proportions of glucose/xylose mixtures used were respectively: 75/25, 50/50, 25/75, and also 100% of each single sugar. In all cases, glucose was the preferred substrate in the glucose/xylose mixtures; the high glucose fractions had higher cell biomass production rates and therefore higher substrate consumption rates and ethanol production rates as compared to high xylose fractions. However, the high xylose fractions had a slightly higher ethanol yields when compared to the high glucose fractions, because the xylose was channeled into ethanol production rather a cell biomass. These results are in agreement with studies by Meyrial and co-workers [61] where *P. stipitis* growth rate was higher on glucose than xylose, and no cell growth was observed for any of the glucose/xylose mixtures after a given period of time, but ethanol production continued until complete sugar depletion.

Other important contribution was made by Sánchez and co-workers, [62] with mixtures of glucose and xylose using *P. stipitis*, *C. shehatae* and *P. tannophilus*. Based on the parameters of specific production rate and overall yield, *P. stipitis* gave the best results for the transformation of substrates into ethanol, with yields of 0.42 and 0.47 g ethanol/g sugar for mixtures with ratios of glucose/xylose of 20/5 and 24/1, respectively. All of the mixtures showed sequential substrate consumption, initially using up glucose quite rapidly, followed by a period during which biomass production, substrate consumption and ethanol formation ceased or progressed only very slowly. Subsequently, xylose was consumed and further production of biomass and ethanol occurred. Also, during the first hours of culture, the higher the initial concentration of glucose, the closer the specific substrate consumption rates approached those obtained in the experiments with glucose alone as substrate.

The effect of operation conditions during fermentation have been also studied, such as agitation rate with suggested values ranging between 50-100 rpm according to Kongkiattikajorn [63]; and initial cell concentration studied by Agbogbo and co-workers. It was concluded that the rate of xylose consumption and ethanol production was high when the initial cell concentrations were high, being this last one possible since cells used the substrate for ethanol production rather than for cell growth [64].

Mixed sugar fermentations using microorganisms in a co-culture array is also a very important subject, because as mentioned in section 2.3, it is one of the suggested configurations in trying to find a suitable biocatalyst scheme. Results of experiments conducted with co-cultures of *S. cerevisiae* and *P. stipitis*, both wild-type strains show that there is no improvement in maximum ethanol concentration and yield when compared with single substrate-single yeast strain fermentations, but the fermentation time was certainly decreased [65]. In that work, the co-culture of *S. cerevisiae* and *P. stipitis* used with a culture medium containing 30 g/L of both glucose and xylose, 12 g/L of mannose and 8 g/L of

galactose had a yield of 0.41 g ethanol/g sugar, being this a 70% of theoretical yield. The co-culture of *P. stipitis* and *K. marxianus* had a high theoretical yield (80%) and also a high ethanol concentration. However, even with the potential of the co-culture process to maximize ethanol production, the development of the co-culture process to convert a glucose and xylose mixture into ethanol was confronted by several problems dealing with the necessity to co-cultivate two different yeast species. Interaction between strains must be verified to assure that each of the strains will metabolize both sugars efficiently and without inhibition effects of any type. Regarding this, Laplace and co-workers [66] have identified some strains of *P. stipitis* that have a negative impact on strains of *S. cerevisiae*, and this is strongly dependent upon physical parameters of the medium, such as pH. The inhibitory effect was mainly observed in the pH range 4.8-5.0. Other parameters affecting this relationship between strains is oxygen; a very low yield of ethanol from xylose can be obtained due to the limited oxygen supply to the xylose-fermenting yeast, and therefore, the use of a respiratory-deficient mutant of the hexose-fermenting yeast could be necessary [67].

2.5. Mathematical modeling of fermentation processes

Modeling a fermentation process presents some advantages such as process knowledge improvement, decreasing the cost of expensive industrial experimentation, mathematical optimization and process control. The mathematical equations describing fermentation processes have their origins in the intrinsic microbiological aspects and in mass balances applied to the process to describe properly the changes in concentration as a function of fermentation time. While in chemical reactors the process kinetics reflect the reaction rates at a molecular level, microbial process dynamics reflect the interaction between living cells and the culture environment. Mathematical models start with the quantification of cell growth, which can be viewed from various perspectives and with varying degrees of complexity,

depending whether we distinguish between individual cells in a reactor and whether we examine the individual metabolic reactions occurring within the cell. Cellular representations which are multicomponent are called structured, and single component representations are designated unstructured. Consideration of discrete, heterogeneous cells constitutes a segregated viewpoint, while an unsegregated perspective considers only averaged cellular properties [68]. The most idealized case is an unstructured-unsegregated model where cell population is treated as one-component solute, and a more realistic case is a structured-segregated model, where a multicomponent description of cell-to-cell heterogeneity is considered. Some models also take into account the effect of inhibition caused by substrates, products or toxic compounds present in medium constituents. Table 2.4 summarizes some unstructured models used to quantify fermentation kinetics. Unstructured models to describe multiple substrate kinetics are also available. However, as discussed in the next section, and according to the objectives of this research work, a structured model is a better approach to describe some processes.

In the simplest approach to modeling batch culture, it is supposed that the rate of increase in cell mass (X) is a function of the cell mass only. Thus:

$$\frac{dX}{dt} = f(X) \quad (2.4)$$

In the exponential phase of microbial growth, cells can multiply rapidly, and cell mass/cell number density increases exponentially with time. This is a period of balanced growth, in which all cells are assumed to grow, consume and produce products at the same rate. That is, the average composition of a single cell remains relatively constant during this phase of growth. Since the nutrient concentrations are large in this phase, the growth rate is

independent of nutrient concentration. The exponential growth rate is then a first order kinetic equation:

$$\frac{dX}{dt} = \mu X \quad \text{with } X = X_o \text{ at } t = 0 \quad (2.5)$$

where μ represents the specific growth rate of cells.

Table 2.4 – Unstructured models to quantify fermentation kinetics. Adapted from Sáez [38].

Name	Description	Kinetic expression (^a $r_i = \mu_i X$)
Monod	Substrate-limited	$r_1 = k S / (K + S)$
Mosser		$r_2 = k S^n / (K + S^n)$
Tessier		$r_3 = k [1 - \exp(-S / K)]$
Logistic law		$r_4 = k(1 - X / k)$
Noncompetitive	Substrate inhibition	$r_5 = k / (1 + K_s / S)(1 + S / K_I)$
Competitive		$r_6 = k S / (1 + S / K_I) + S$
Noncompetitive	Product inhibition	$r_7 = k / (1 + K_s / S)(1 + P / K_P)$
Competitive		$r_8 = k S / (1 + P / K_P) + S$
Noncompetitive	Toxic compound inhibition	$r_9 = k / (1 + K_s / S)(1 + I / K_I)$
Competitive		$r_{10} = k S / K_s (1 + I / K_I) + S$

^a The rate expression for growth on the i th substrate is given by $r_i = \mu_i X$.

2.5.1. Kinetics and modeling of single substrate fermentations

The simplest relationships describing exponential growth are unstructured models. The models that were first developed for cell growth did not account for the dependency of the exponential growth rate on nutrient concentration, they were devised to have a maximum achievable population built into the constitutive expressions employed. Such models find

applicability today when the growth-limiting substrate cannot be identified. One of the simplest models which include the effect of nutrient concentration is the model developed by Jacques Monod, based on observations of microbial growth at various initial glucose concentrations, assuming that only one substrate (the growth-limiting substrate, S) is important in determining the rate of cell proliferation denoted as μ . The form of the Monod equation is analog to that of the Michaelis-Menten enzyme kinetics, and is given by the following equation, where μ_{\max} is the maximum specific growth rate in h^{-1} , and K_s is the saturation constant in g/L, which is that value of the limiting nutrient concentration at which the specific growth rate is half its maximum value [68]:

$$\mu = \frac{\mu_{\max} S}{K_s + S} \quad (2.6)$$

Values of μ_{\max} vary with the type of organism and the value of K_s depends on the nature of substrate, and it is generally quite small, implying that the specific growth rate is near its maximum value for much of the period of batch growth. The parameters μ_{\max} , and K_s , named henceforth kinetic parameters, are obtained experimentally from the values of cell concentration and substrate concentration (X and S, respectively) during the fermentation time. For cell concentration the values chosen are only those belonging to the exponential phase, since the Monod model works under the assumption of balanced growth, which is achieved only at this growth stage. The parameter μ is calculated from the slope of the natural logarithm of cell concentration values in its exponential phase, plotted against fermentation time. The values of μ_{\max} and K_s can be obtained from several linearization methods of the Monod equation, including Lineweaver-Burk, Eadie-Hoffstee, Hanes-Woolf, or a “batch kinetics” equation as described by Shuler and Kargi [69].

To better describe microbial growth kinetics, it is necessary to define yield coefficients, the ones that relate the amount of products and cells formed per unit of substrate consumed by cells, giving the yield or efficiency in the process. A knowledge of yield coefficients allows us to design a growth medium that will supply all of the required nutrients in balanced amounts, so that a desired substrate can be made growth-rate limiting. Equations for yield coefficients can be found in literature [70] and they are defined on both molar and mass basis.

As mentioned before, optimization of ethanol fermentation processes could be based on the development of accurate growth and fermentation kinetic models, properly describing the consumption of substrates, and the production of extracellular products. Several kinetic models for growth of both *S. cerevisiae* and *P. stipitis* have been proposed previously in the literature, sometimes with the purpose of modeling only cell growth and substrate consumption, but also for modeling ethanol production simultaneously. *S. cerevisiae* growing on glucose has been the most studied case, and the effect of inhibition of both ethanol and substrate on the fermentation process has been the main object of those studies. Some modified Monod models that include terms for substrate and product inhibition were developed by these researchers [71, 72], achieving excellent fits between experimental data and simulations made with unstructured models. Other incident factors studied were substrate limitation effects, cell maintenance, effect of temperature, and these factors were studied in different culture modes such as batch, fed-batch and continuous. Novak and co-workers [71] obtained inhibition constants for ethanol, assaying ethanol added at the beginning of the fermentation and the ethanol produced along the process. Similar results were obtained by the group of Luong [72], where ethanol inhibition on the growth of *S. cerevisiae* was studied, showing that the maximum allowable ethanol concentration above which cells do not grow is 112 g/L and the level above which cells stop producing ethanol was 115 g ethanol/L. Models

for glucose fermentation with *S. cerevisiae* were also developed by Thatipamala and co-workers [73], studying the effect of both substrate and ethanol on the kinetics of biomass and product yields. These researchers proposed that inhibition occurs when glucose concentration in the culture medium increases above 150 g/L, and they also found that product inhibition does not have any effect on product yield, whereas substrate inhibition significantly affects the product yield. The reason for this substrate inhibition is because at higher substrate concentrations, catabolite inhibition of enzymes in the fermentative pathway becomes important, indicating the onset of substrate inhibition as a result of high osmotic pressure and low water activity [73]. Other studies have also proposed kinetic models on the basis of enzyme deactivation kinetics to explain the effect of temperature in cell mass growth and ethanol production [74]. A very important unstructured kinetic model was obtained by CIATEJ (Centro de Investigación y Asistencia en Tecnología y Diseño del Estado de Jalisco) in Mexico [75], and although the purpose of that process was the production of tequila, the same criteria can be easily applied for the process of fuel ethanol production. In this study, the combination of the Moser and Luong [76] kinetic model gave the best prediction for biomass, substrate and ethanol profiles with initial substrate concentrations ranging from 60 – 90 g/L. Kinetic parameters such as μ_{\max} , K_s , K_p , etc. were optimized simultaneously along the solution of non-linear differential equations describing mass balances for cells, substrate and product, with the objective to fit simulated data to experimental concentrations to minimize the error. Excellent linear correlations were obtained as a product of the validation of the proposed models. Other models different to that of Monod with or without inhibition terms have been utilized, and these models include the logistic equation which has a sigmoidal shape trend to represent cell growth, used to show the self-regression made by the increase in cell concentration characteristic of in batch fermentations. Wang and co-workers [76] used the logistic equation to describe fermentation kinetics of different sugars by *S. cerevisiae*,

achieving good predictions for the sugars utilized and a special analysis of different initial sugar concentrations. The model included the term for growth-associated products and the parameter of lag time in mass balance for ethanol, to describe the delay of ethanol production to cell growth.

In the case of modeling alcoholic fermentation of xylose with *P. stipitis* the research history is not as abundant as glucose with *S. cerevisiae*, but previous attempts to model fermentation with this yeast strain used the Monod model [77]. As mentioned previously in this chapter, *P. stipitis* is more vulnerable than *S. cerevisiae* to inhibitory effects of substrates, ethanol, secondary metabolites and toxic compounds from ethanol production stages prior to fermentation. Therefore these effects have to be accounted in kinetic models from several points of view, but moreover when experimental conditions require it. From literature it is known that substrate concentrations above 40 g/L inhibit the metabolism of *P. stipitis*, and ethanol concentrations above 64 g/L completely repress enzymatic synthesis for xylose degradation [78]. Research on xylose fermentation includes the work of Agbogbo and co-workers [63], studying the effect of initial cell concentration and the development of a model to predict the fermentation process. Results show that when initial cell concentration is high, the rate of xylose utilization, ethanol formation, and the ethanol yield increase. A two-parameter mathematical model was used to predict the cell population dynamics at the different initial cell concentrations, and these parameters coupled to the Monod model for cell growth equation were determined at the different initial cell concentrations used in the fermentation. The rates of substrate consumption and ethanol production were modeled using Leudeking-Piret kinetics involving parameters for cell maintenance and parameters associated with growth. The form of the empirical mathematical model used describes the population dynamics with just two parameters, which correlated very well with the initial cell

concentration used. From the results, the substrate consumption and ethanol production rate are both functions of the initial cell concentration.

Current technologies for ethanol production from lignocellulosic biomass require different approaches for the development of an efficient model that takes into account all the possible negative effects that intrinsic fermentation factors have on xylose degradation into ethanol. However, models can be as simple as using the Monod model and then incorporate appropriate parameters, the ones that can be obtained from statistical methodologies. Kumar and co-workers [79] studied the ethanol production from pentoses resultant of hydrolysis of hemicellulose present in a floating aquatic plant. The system developed can be described for the rate of biomass growth in which concentrations of sugar, ethanol production and cell activation are linked by coefficients of cell formation and inhibition, and working with the assumption that the rate or product formation is related both to the rate of cell growth and the concentration of microorganism present. The fitting between experimental data and simulated results from the model was statistically analyzed by means of residual plots, showing a right appropriateness of the model, since residuals were randomly distributed around the line of zero error. The model was also validated with correlation coefficients and the values obtained, above 0.98, imply that the proposed model was able to explain the experimental results.

2.5.1.1. Mass balances for batch fermentation

As mentioned above, kinetic models describing a fermentation process derive initially from the analysis of the cell population dynamics, choosing the appropriate model depending on the point of view to consider cell behavior in culture medium. Furthermore, cell growth, substrate consumption and product formation are monitored during the course of fermentation, therefore, the model to be developed has to be a function of time. For this reason, a complete analysis of the process inputs and outputs is necessary, and this analysis is

nothing but a mass balance, which depends on the configuration of the process (batch, fed-batch or continuous). Since this research work was made carrying out only batch processes, the mass balance describing this configuration does not involve the terms for “in” and “out” of material because no material is added or removed from the reactor and it is assumed that gas stripping of culture liquid is negligible, then the volume is constant. Cell death and maintenance are neglected because of the assumption of balanced growth, therefore the mass balance for each component reduces to:

$$Accumulation_i = production\ or\ consumption_i \quad (2.7)$$

or

$$\frac{dC_i}{dt} = r_i \quad (2.8)$$

Equation 2.7 is the general mass balance for each component i and equation 2.8 is its generic, showing that change in concentration of any component i , with respect to time is equal to the rate of formation or consumption of that component i . First it is necessary to define the rate of formation or consumption of each component, and beginning with cell mass we have the equation which describes the rate of cell production:

$$r_x = \mu X \quad (2.9)$$

where μ is the specific growth rate in h^{-1} , and X is cell concentration in g/L. Next, the rate of substrate consumption which accounts for both cell proliferation and product formation is described by the equation:

$$r_S = - \left[\frac{1}{Y_{X/S}} \mu X + Y_{P/X} \mu X \right] \quad (2.10)$$

note that the substrate rate is negative because substrate is being consumed, promoting cell growth and product formation. The terms $Y_{X/S}$ and $Y_{P/X}$ are the yield coefficient of cells based on substrate and the yield coefficient of product based on cells, in g/g [69]. The rate of product formation is given by the equation:

$$r_P = Y_{P/X} \mu X \quad (2.11)$$

Therefore, when equation 2.8 is applied to rate equations above described and using the Monod expression (Eq. 2.6) to represent the specific cell growth rate, without inhibition effects from any type (substrate, product, toxic compounds), the non-linear differential equation set for mass balances in a batch fermentation process is obtained:

$$\frac{dX}{dt} = \frac{\mu_{\max} [S]}{K_S + [S]} X \quad (2.12)$$

$$\frac{dS}{dt} = - \left[\frac{1}{Y_{X/S}} + Y_{P/X} \right] \frac{\mu_{\max} [S]}{K_S + [S]} X \quad (2.13)$$

$$\frac{dP}{dt} = Y_{P/X} \frac{\mu_{\max} [S]}{K_S + [S]} X \quad (2.14)$$

These equations are solved with an appropriate numeric method, employing kinetic parameters and yield coefficients obtained as described in Chapter 3, in order to obtain the profile concentrations for each component.

2.5.2. Kinetics and modeling of multiple substrate fermentations

Although empirical models, such as Monod's, describe microbial growth kinetics on a single substrate, they are not applicable to multisubstrate environments, and are very specific regarding system parameters. Simple unstructured models are developed to explain a particular set of experimental data and do not take into consideration the optimal nature of microbial growth on multiple substrates. Hence the predictive capability of such models remains within the bounds of the experiments they are based. In nature, microorganisms grow on multiple substrates, and different growth phenomena of microorganisms are observed in these environments: (i) sequential utilization of substrates, (ii) simultaneous consumption of substrates, and (iii) co-metabolism of substrates [80]. The diauxie phenomenon, discovered by Monod, is a well-known example of sequential utilization of two carbon substrates, with an intermediate lag phase between the two exponential growth phases. In this intermediate lag phase that precedes consumption of the next preferred substrate, the synthesis of enzymes needed for the metabolism of the next substrate is carried out.

Among the various proposed models to explain the microbial behavior in multiple substrates, one of the most studied and extensively utilized has been the cybernetic concept developed by Ramkrishna and Kompala [81]. This model views microorganisms as optimal strategists, that given a set of conditions, they have the ability to “think” and “decide” how best to utilize the resources so as to maximize a particular objective; cybernetic modeling translates the idea that cells regulate their activities by exerting control over the activities and the rates of synthesis of enzymes [82]. The cybernetic approach assumes that one key enzyme limits the growth rate achievable on a particular substrate, but this enzyme synthesis precedes that a particular substrate can be utilized for cell growth. Figure 2.15 shows a schematic diagram of the cybernetic model according to Narang and co-workers [83] with a binary mixture of substrates as two parallel enzyme-catalyzed growth reactions. S_i denotes the

i th substrate, E_i denotes the “lumped” system of inducible enzymes associated with growth on S_i , and B denotes the biomass or cell concentration. Substrate consumption and enzyme synthesis are based on Monod’s kinetics, but the model also takes into account the enzyme degradation stage, and the assumption for this stage is a first-order reaction.

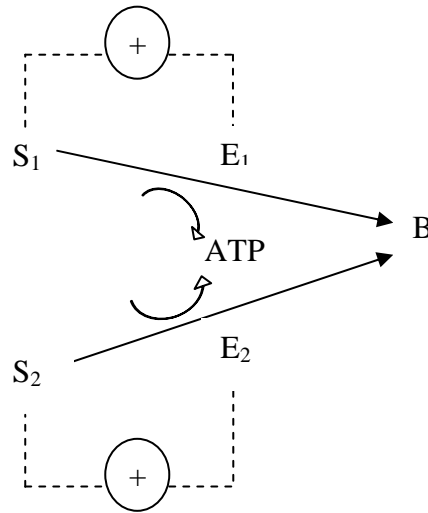
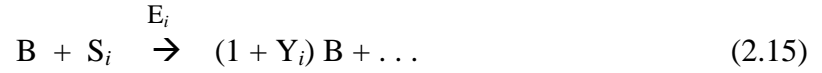


Figure 2.15 – Schematic diagram of the cybernetic model (Adapted from Venkatesh and co-workers [80]).

Cybernetic models have been able to successfully describe diauxic growth in batch, fed-batch and continuous cultures and the basic premise, the most important attribute of the modeling effort, is that information obtained from growth on single substrate experiments on each of the substrates will yield all of the information required for predicting growth in mixed substrates. The complete definition of the original cybernetic model along with modifications made, as a product of the application of the double matching law can be found in the literature, with the equations for cell growth, enzyme synthesis, substrate consumption and mathematical definition of cybernetic variables [84]. The salient features of the cybernetic modeling are represented with the assimilation of i th substrate S_i by the biomass B , and it is assumed to be catalyzed by a key enzyme E_i , representing the whole set of enzymes catalyzing the metabolic pathways of growth on S_i :



The key enzyme E_i , required for utilization of S_i , is induced in the presence of S_i , according to:



where Y_i is the biomass yield coefficient on substrate, and B' is the biomass excluding the key enzyme E_i . The rate equations for these two reactions sequences are similar to the Monod equation but also include special terms for the specific level e_i and the enzyme synthesis rate constant α_i , as described in equations 2.17 and 2.18. Therefore the expression μ_i is replaced by a mathematical relationship that will be discussed in Chapter 5 and the expression K_i replaces K_s in the unstructured Monod kinetics to bring out the influence of specific enzyme levels on the growth kinetics and to stand out the existence of more than one substrate. The equation rates describing the rates of biomass production and enzyme synthesis are:

$$r_{B,i} = \frac{\mu_i e_i [S_i] X}{K_i + [S_i]} \quad (2.17)$$

$$r_{E,i} = \frac{\alpha_i [S_i] X}{K_i + [S_i]} \quad (2.18)$$

The model development is complete and the equations are given below:

$$\frac{dX}{dt} = r_{B,i} v_i \quad (2.19)$$

$$\frac{dS_i}{dt} = \left(\frac{1}{Y_{X/S}} + Y_{P/X} \right) r_{B,i} v_i \quad (2.20)$$

$$\frac{dP}{dt} = Y_{P/X} r_{B,i} v_i \quad (2.21)$$

$$\frac{de_i}{dt} = r_{E,i} u_i - \beta e_i - e_i \frac{d \ln X}{dt} \quad (2.22)$$

The last equation describes the change of concentration of the enzyme levels as a function of time, and takes into account not only the rate of enzyme synthesis (first term) but also the first-order degenerative loss of the active enzyme E_i (second term) and the dilution of specific enzyme level due to cell growth (third term). The variables u_i and v_i are the cybernetic variables controlling the effects of regulation, where u_i regulates the rate of enzyme synthesis (induction/repression), and v_i regulates the growth rate (inhibition/activation). These two laws of regulation were referred to as the matching and proportional laws, respectively, and their derivation can be found in the literature [83, 84]. General equations are:

$$u_{i,j} = \frac{r_i}{\sum_j r_j} \quad (2.23)$$

$$v_{i,j} = \frac{r_i}{\max_j(r_j)} \quad (2.24)$$

where r_i represents the rate of biomass production due to the consumption of the i th substrate and r_j represents the particular rate of biomass production, due to substrate consumption from the i th to the j th alternative. The equations 2.19 – 2.24 will be extended in Chapter 5 in order to construct the complete cybernetic framework for the system studied in this work.

The first attempt to evaluate the cybernetic approach was made by the same authors of the model with the growth of *Klebsiella oxytoca* on mixed substrates containing glucose, xylose, arabinose, lactose and fructose [83], and the results were in accurate concordance with the experimental data, particularly with respect to the increasing rates during the second growth phase. Other modifications to the model have been proposed to describe simultaneous utilization of substrates, continuous culture, and specific mixtures of carbohydrates with other biopolymers [84-85]. Values for initial enzyme levels were proposed based on the past history of the inoculum, being 90% of the maximum specific level enzyme for fermentations in which the inoculum was precultured on the same substrate, and 18% of maximum specific enzyme level for fermentations with the less preferred substrate in which the inoculum was precultured on the preferred substrate [86]. Also, values for parameters α and β were proposed being 0.05 h^{-1} and $1.0\text{E-}3 \text{ h}^{-1}$, respectively. Doshi and Venkatesh [80] demonstrated simultaneous utilization of acetate, pyruvate and lactate using *Escherichia coli* K12, but the mixtures of glucose and lactose were unable to be demonstrated by means of the cybernetic model. Growth of *S. cerevisiae* on complex substrates such as melibiose and other carbohydrate mixtures including glucose, and galactose were also studied by means of the cybernetic model by Venkatesh and co-workers [85]. A novel feature of the model developed was the incorporation of dynamics of the regulation of enzymatic degradation of substrates, and in general, the model can be easily used to describe microbial growth on disaccharides. Other models have been proposed with different perspectives than the cybernetic framework, such as the one developed by Nakamura and co-workers [87] which involves equations for the

synthesis rate of inducible enzyme expressed as functions of promoter activity which at the same time is activated by a promoter activator and the operator activity is activated by the second substrate. The specific growth rate expressions for substrates 1 and 2 involve the effects of substrate and production inhibitions and maintenance coefficients. Because this model is not based on a cybernetic perspective, no cybernetic variables were used in the developed model, but simulations showed a good agreement with the experimental data. Also, the criteria used for incorporating the rates of inducible enzymes and promoter activator were another interesting approach in the efforts to model the behavior of mixed substrate fermentations. Other approach is the optimal model proposed by Venkatesh and co-workers [80], which features the ability to simulate both simultaneous and sequential utilization of limiting carbon sources in a growth medium. In this model, as successful as the cybernetic framework, the metabolic and genetic controls have been represented as constraints in the optimization scheme of the specific growth rate, and it has an additional advantage when compared to the cybernetic one, which is the requirement of less system parameters. This model was further used to simulate the behavior of *Lactobacillus rhamnosus* growing on glucose, citrate and lactate, being the first time that model was used also for product simulation, and the results of product formation, along with cell growth and substrate consumption were found to be very accurate to experimental data.

The majority of research performed in the topics previously discussed have emphasized in different approaches substantially important for the current research project, such as fermentation of a single substrate or a mixture of substrates using only one type of microorganism, the fermentation of mixtures of carbohydrates using a co-culture scheme, but lacking of a mathematical model to predict the trend of the fermentative process, and so on. Nonetheless, the specific case of mathematical modeling of glucose/xylose mixtures using co-culture of wild-type strains of *S. cerevisiae* and *P. stipitis*, with no genetic or metabolic

alterations at all, by means of a structured model, such as the cybernetic model, has not been reported yet at the moment when this documented was being written. Therefore, the contribution of this work to the vast topic of fuel ethanol production, hopefully is very relevant and useful for future works with similar objectives to the present ones but involving other process schemes, such as the modeling of a fed-batch or continuous process. Using as a reference the model proposed here with its corresponding modifications depending on the different conditions, or maybe attempting to use a co-culture with other yeast or bacteria strains, or any other alternative contributing to the study of the fermentation phase in the production of ethanol.

2.6. References cited

- [1] McGovern, P.E. (2003). Ancient wines: The search for the origins of viniculture. *Princeton University Press*. Princeton, NJ. **Chapter 3**.
- [2] Mousdale, D.M. (2008). Historical development of bioethanol as a fuel. *Biofuels: Biotechnology, Chemistry and Sustainable Development*. First Edition. CRC Press, Taylor & Francis Group. **Chapter 1**:1-44.
- [3] McCarthy, T. (2001). The coming wonder? Foresight and early concerns about the automobile. *Environ. History*. **6**:46.
- [4] Thomas, D.E. (1987). Diesel: Technology and society in industrial Germany. *University of Alabama Press, Tuscalosa*. **Chapter 5**.
- [5] BNDES and CGEE. (2008). Sugarcane-based bioethanol: Energy for Sustainable Development. *PDF version*.
- [6] Cheremisinoff, N.P. (1979). Gasohol for Energy Production. *Ann Arbor Science Publishers, Ann Arbor*. **Chapter 6**.
- [7] Melges de Andrade, A.; Morata de Andrade, C.A.; and Bodinaud, J.A. (1998). Biomass energy use in Latin America: focus on Brazil. *Biomass Energy: Data, Analysis and Trends*. International Energy Agency, Paris. 87.
- [8] ANFAVEA. (Associação Nacional dos Fabricantes de Veículos Automotores). <http://www.anfavea.com.br> Access date: October 2009.

- [9] BP Statistical Review of World Energy. British Petroleum. London (2007). <http://www.bp.com/printsectiongenericarticle.do?categoryId=9023773&contentId=7044469> Access date: October 2009.
- [10] Martines-Filho, J.; Burnquist, H.L.; and Vian, C.E.F. (2006). Bioenergy and the rise of sugarcane-based ethanol in Brazil. *Choices*. **21**(2):91.
- [11] The Research Institute for Sustainable Energy, RISE. <http://www.rise.org.au/info/Res/biomass/index.html> Access date: October 2009.
- [12] Energy Information Administration, U.S. Department of Energy. <http://eia.doe.gov>
- [13] Farrell, A.E.; Plevin, R.J.; Turner, B.T.; Jones, A.D.; O'Hare, M.; Kammen, D.M. (2006). Ethanol can contribute to energy and environmental goals. *Science*. **311**:506-508.
- [14] Lynd, L.R.; Cushman, J.H.; Nichols, R.J.; Wyman, C.E. (1991). Fuel ethanol from cellulosic biomass. *Science*. **251**:1318-1323.
- [15] Owen, K. (1990). Automotive Fuels Handbook. *Society of Automotive Engineers*. Warrendale, PA.
- [16] Chandel, A. K.; ES, C.; Rudravaram, R.; Narasu, M. L.; Rao, V.; Ravindra, P. (2007). Economics and environmental impact of bioethanol production technologies: an appraisal. *Bioetchnol. Molec. Biol. Review*. **2**(1):014-032.
- [17] Wilke, C.R.; Yang, R.D.; Scamanna, A.F.; and Freitas, R.P. (1981). Raw material evaluation and process development studies for conversion of biomass to sugars and ethanol. *Biotechnol. Bioeng*. **23**:163-183.
- [18] Bohlmann, G.M. (2006). Process economic considerations for production of ethanol from biomass feedstocks. *Industrial Biotechnol*. **2**, 14.
- [19] Hamelinck, C.N.; vanHooijdonk, G.; and Faaij, A.P.C. (2005). Ethanol from lignocellulosic biomass: techno-economic performance in short-, middle- and longer-term. *Biomass Bioenergy*. **28**:384.
- [20] Hill, J. et al. (2006). Environmental, economic, and energetic costs and benefits of biodiesel and ethanol biofuels. *Proc. Natl. Acad. Sci. USA*. **103**:11206.
- [21] Wang, M.; Wu, M.; and Huo, H. (2007). Life-cycle energy and greenhouse gas emission impacts of different corn ethanol plant types. *Environmental Research Letters*. **2**:1-13.
- [22] Balat, M.; Balat, H.; Öz, C. (2007). Progress in bioethanol processing. *Progress in Energy and Combustion Science*. **34**:551-573.
- [23] Renewable Energy Policy Network (REN21). Renewables-2006: global status report. Paris and Washington, DC: REN21 and Worldwatch Institute (2006).

- [24] Claasen, P.A.M.; van Lier, J.B.; López Contreras, A.M.; van Niel, E.W.J.; Sijtsma, L.; Stams, A.J.M.; de Vries, S.S.; Weusthuis, R.A. (1999). Utilization of biomass for the supply of energy carriers. *Applied Microbiology and Technology*. **52**:741-755.
- [25] Kosaric, N.; Velikonja, J. (1995). Liquid and gaseous fuels from biotechnology: challenge and opportunities. *FEMS Microbiology Reviews*. **16**:111-142.
- [26] Dutch Sustainable Development Group (DSD). (2005). Feasibility study on an effective and sustainable bioethanol production program by Least Developed Countries as alternative to cane sugar export, DSD group; study report on bioethanol production in LDC's, the Netherlands. [cited; available from: www.swilion.nl/documenten/DSD%20rAPPORT].
- [27] Mabee, W.E.; Saddler, J.N.; Nielsen, C.; Nielsen, L.H.; Jensen, E.S. (2006). Renewable-based fuels for transport. In: Renewable energy for power and transport. Riso energy report 5. 47-50.
- [28] Shigechi, H.; Koh, J.; Fujita, Y.; Matsumoto, T.; Bito, Y.; Ueda, M. (2004). Direct production of ethanol from raw corn starch via fermentation by use of a novel surface-engineered yeast strain codisplaying glucoamylase and α -amylase. *Appl. Environ. Microbiol.* **70**:5037-5040.
- [29] Bohlmann, G.M. (2006). Process economic considerations for production of ethanol from biomass feedstocks. *Ind. Biotechnol.* **2**:14-20.
- [30] Demirbas, A. (2005). Estimating of structural composition of wood and non-wood biomass samples. *Energy Sources*. **27**:761-767.
- [31] Ann, G.; Demirbas, A. (2004). Mathematical modeling the relations of pyrolytic products from lignocellulosic materials. *Energy Sources*. **26**:1023-1032.
- [32] Rubin, E.M. (2008). Genomics of cellulosic biofuels. *Nature. International weekly journal of science*. **454**:841-845.
- [33] Mohan, D.; Pittman, C.U.; Steele, P.H. (2006). Pyrolysis of wood/biomass for bio-oil: a critical review. *Energy Sources*. **20**:848-889.
- [34] Zaldivar, J.; Nielsen, J.; Olsson, L. (2004). Fuel ethanol production from lignocellulose: a challenge for metabolic engineering and process integration. *Appl. Microbiol. Biotechnol.* **56**:17-34.
- [35] The Royal Society of Chemistry. Carbohydrate Section. <http://www.rsc.org/education/teachers/learnnet/cfb/carbohydrates.htm> Access date: October 2009.
- [36] Sigma Aldrich Lifesciences. Carbohydrate Analysis Section. <http://www.sigmaaldrich.com/life-science/metabolomics/enzyme-explorer/learning-center/carbohydrate-analysis/carbohydrate-analysis-ii.html> Access date: October 2009.

- [37] The University of Waikato. Science on the farm. <http://sci.waikato.ac.nz/farm/content/plantstructure.html> Access date: October 2009.
- [38] Saez-Miranda, J.C. (2006). Kinetic, intracellular ATP growth and maintenance studies, and modeling of metabolically engineered *Zymomonas mobilis* fermenting glucose and xylose mixtures. Ph.D. thesis, University of Puerto Rico, Mayagüez Campus.
- [39] Shahbazi, A.; Li, Y.; Mims, M.R. (2005). Application of sequential aqueous steam treatments to the fractionation of softwood. *Appl. Biochemistry and Biotechnol.* 973-987.
- [40] Laser, M.; Schulman, D.; Allen, S.G.; Lichwa, J.; Antal Jr.; Lynd, L.R. (2002). A comparison of liquid hot water and steam pretreatments of sugar cane bagasse for bioconversion to ethanol. *Bioresource Technol.* **81**:33-44.
- [41] Zhang, Y.-H.P.; Lynd, L.R. (2004). Toward an aggregated understading of enzymatic hydrolysis of cellulose: noncomplexed cellulose systems. *Biotechnol. Bioeng.* **8**(7):797-824.
- [42] Sánchez, O.; Cardona, C.A. (2007). Trends in biotechnological production of fuel ethanol from different feedstocks. *Bioresource Technology.* **99**:5270-5292.
- [43] Demirbas, A. (2005). Bioethanol from cellulosic materials: a renewable motor fuel from biomass. *Energy Sources.* **27**:327-337.
- [44] Katahira, S.; Mizuike, A.; Fukuda, H.; Kondo, A. (2006). Ethanol fermentation from lignocellulosic hydrolysate by a recombinant xylose- and celooligosaccharide-assimilating yeast strain. *Appl. Microbiol. Biotechnol.* **72**:1136-1143.
- [45] Hahn.Hagerdal, B.; Galbe, M.; Gorwa-Grauslund, M.F.; Liden, G.; Zacchi, G. (2006). Bioethanol – the fuel of tomorrow from the residues of today. *Trends. Biotechnol.* **24**:549-556.
- [46] Moiser, N.; Wyman, C.; Dale, B.; Elander, R.; Holtzapple, YYLM; Ladisch, M. (2005). Features of promising technologies for pretreatment of lignocellulosic biomass. *Bioresource Technol.* **96**:673-686.
- [47] Madson, P.W.; Lococo, D.B. (2000). Recovery of volatile products from dilute high-fouling process streams. *Appl. Biochem. Biotechnol.* **84-86**:1049-1061.
- [48] Minier, M.; Goma, G. (1982). Ethanol production by extractive fermentation. *Biotechnol. Bioeng.* **24**:1565.
- [49] Dominguez, J.M. et al. (2000). Ethanol production from xylose with the yeast *Pichia stipitis* and simultaneous product recovery by gas stripping using a gas-lift fermentor with attached side-arm (GLSA). *Biotechnol. Bioeng.* **67**: 336.
- [50] Cardona, C.A.; Sánchez, O.J. (2007). Fuel ethanol production: Process design trends and integration opportunities. *Bioresource Technology.* **98**:2415-2457.

- [51] Wu, J.F.; Lastick, S.M.; Updegraff, D.M. (1986). Ethanol production from sugars derived from plant biomass by a novel fungus. *Nature: International Weekly Journal of Science*. **321**:997-888.
- [52] Linden, T.; Hahn-Hägerdal, B. (1989). Fermentation of lignocellulosic hydrolysates with yeasts and xylose isomerase. *Enz. Microbiol. Tech.* **11**:583-589.
- [53] Rogers, P.L.; Lee, K.L.; Tribe, D.E. (1979). Kinetics of alcohol production by *Zymomonas mobilis* at high sugar concentrations. *Biotech. Lett.* **1**:165-170.
- [54] Gong, C.S.; Chen, L.F.; Chiang, L.C.; Flickenger, M.C.; Tsao, G.T. (1981). Production of ethanol from D-xylose by using D-xylose isomerase and yeast. *Appl. Environ. Microbiol.* **56**:120-126.
- [55] McMillan, J.D. (1993). Xylose fermentation to ethanol: A review. TP-421-4944, Golden, CO. National Renewable Energy Laboratory.
- [56] Skoog, K.; Hahn-Hägerdal, B. (1990). Effect of oxygenation on xylose fermentation by *Pichia stipitis*. *Appl. Environ. Microbiol.* **56**:3389.
- [57] Grauslund, F.G.; Karhumaa, K.; Garcia-Sanchez, R.; Hahn-Hägerdal, B. (2007). Comparison of the xylose reductase-xylitol dehydrogenase and the xylose isomerase pathways for xylose fermentation by recombinant *Saccharomyces cerevisiae*. *Microbial Cell Factories*. **6**(5):1-10.
- [58] Zhang, M. et al. (1995). Metabolic engineering of a pentose metabolism pathway in ethanologenic *Zimomonas mobilis*. *Science*. **267**:240.
- [59] Nelson, D.L.; Cox, M.M. (2005). Lehninger Principles of Biochemistry. *Freeman*. 4th edition. **Chapter 14**:521-551.
- [60] Agbogbo, F.K.; Coward-Kelly, G.; Torry-Smith, M.; Wenger, K.S. (2006). Fermentation of glucose/xylose mixtures using *Pichia stipitis*. *Process Biochemistry*. **41**:2333-2336.
- [61] Meyrial, V.; Delgenes, J.P.; Romieu, C.; Moletta, R.; Gounot, A.M. (1995). Ethanol tolerance and activity of plasma membrane ATPase in *Pichia stipitis* grown on D-xylose or on D-glucose. *Enzyme Microb. Technol.* **17**:535-540.
- [62] Sánchez, S.; Bravo, V.; Castro, E.; Moya, A.J.; Camacho, F. (2002). The fermentation of mixtures of D-glucose and D-xylose by *Candida shehatae*, *Pichia stipitis* or *Pachysolen tannophilus* to produce ethanol. *Journal of Chem. Technol. and Biotechnol.* **77**:641-648.
- [63] Kongkiattikajorn, J.; Rodmui, A.; Dandusitapun, Y. (2007). Effect of agitation rate on batch fermentation of mixture culture of yeasts during ethanol production from mixed glucose and xylose. *Thai Journal of Biotechnol.* 1-4.

- [64] Agbogbo, F.; Coward-Kelly, G. Torry-Smith, M.; Wenger, K.; Jeffries, T.W. (2007). The effect of initial cell concentration on xylose fermentation by *Pichia stipitis*. *Appl. Biochem. Biotechnol.*, **136**:653-662.
- [65] Rouhollah, H.; Iraj, N.; Giti, E.; Sorah, A. (2007). Mixed sugar fermentation by *Pichia stipitis*, *Saccharomyces cerevisiae*, and an isolated xylose-fermenting *Kluyveromyces marxianus* and their co-cultures. *African Journal of Biotechnology*. **6**(9): 1110-1114.
- [66] Laplace, J.M.; Delgenes, J.P.; Moletta, R. (1992). Alcoholic glucose and xylose fermentation by the coculture process: compatibility and typing of associated strains. *Canadian Journal of Microbiology*. **38**:654-658.
- [67] Taniguchi, M.; Tohma, T.; Itaya, T.; Fujii, M. (1997). Ethanol production from a mixture of glucose and xylose by co-culture of *Pichia stipitis* and a respiratory-deficient mutant of *Saccharomyces cerevisiae*. *Journal of Fermentation and Biotechnology*. **83**(4):364-370.
- [68] Bailey, J.E.; Ollis, D.F. (1986). Applied Enzyme Catalysis. *Biochemical Engineering Fundamentals*. Second Edition. McGraw-Hill, Inc. **Chapter 4**:157-226.
- [69] Shuler, M.L.; Kargi, F. (2002). Enzyme Kinetics. *Bioprocess Engineering – Basic Concepts*. Second Edition. Prentice Hall. **Chapter 3**:80-95.
- [70] Blanch, H.W.; Clark, D.S. (1996). Microbial Growth. *Biochemical Engineering*. First Edition. Marcel Dekker, Inc. **Chapter 3**:173-244.
- [71] Novak, M.; Strehaiano, P.; Moreno, M. Goma, G. (1981). Alcoholic fermentation: On the inhibitory effect of ethanol *Biotechnol. Bioeng.* **23**:201-211.
- [72] Luong, J.H.T. (1984). Kinetics of ethanol inhibition in alcohol fermentation. *Biotechnol. Bioeng.* **28**:280-285.
- [73] Thatipamala, R.; Rohani, S.; Hill, G.A. (1992). Effects of high product and substrate inhibitions on the kinetics and biomass and product yields during ethanol batch fermentation. *Biotechnol. Bioeng.* **40**:289-297.
- [74] Nanba, A.; Nishizawa, Y.; Tsuchiya, Y.; Nagai, S. (1987). Kinetic analysis for batch ethanol fermentation of *Saccharomyces cerevisiae*. *J. Ferment. Technol.* **65**(3):277-283.
- [75] Arellano-Plaza, M.; Herrera-López, E.J.; Díaz-Montaña, D.M.; Moran, A.; Ramírez-Córdova, J.J. (2007). Unstructured kinetic model for tequila batch fermentation. *Int. J. Mathem. Comput. Simulation*. **1**(1):1-6.
- [76] Wang, D.; Xu, Y.; Hu, J.; Zhao, G. (2004). Fermentation kinetics of different sugars by apple wine yeast *Saccharomyces cerevisiae*. *Journal of the Institute of Brewing*. **110**(4):340-346.
- [77] Dominguez, H.; Nuñez, M.N.; Chamy, R.; Lema, J.M. (1993). Determination of kinetic parameters of fermentation processes by a continuous unsteady-state method:

- Application to the alcoholic fermentation of D-xylose by *Pichia stipitis*. *Biotechnol. Bioeng.* **41**(11):1129-1132.
- [78] Slininger, P.J.; Branstrator, L.E.; Bothast, R.J.; Okos, M.R.; Ladisch, M.R. (2005). Growth, death, and oxygen uptake kinetics of *Pichia stipitis* on xylose. *Biotechnol. Bioeng.* **37**(10):973-980.
 - [79] Kumar, A.; Singh, L.K.; Ghosh, S. (2009). Bioconversion of lignocellulosic fraction of water-hyacinth (*Eichhornia crassipes*) hemicellulose acid hydrolysate to ethanol by *Pichia stipitis*. *Bioresource Technology.* **100**:3293-3297.
 - [80] Bajpai-Dikshit, J.; Suresh, A.K.; Venkatesh, K.V. (2003). An optimal model for representing the kinetics of growth and product formation by *Lactobacillus rhamnosus* on multiple substrates. *Journal of Bioscience and Biotechnology.* **96**(5):481-486.
 - [81] Kompala, D.S.; Ramkrishna, D.; Tsao, G.T. (1984). Cybernetic modeling of microbial growth on multiple substrates. *Biotechnol. Bioeng.* **26**:1272-1281.
 - [82] Patnaik, P.R. (2000). Are microbes intelligent beings?: An assessment of cybernetic modeling. *Biotechnology Advances.* **18**:267-288.
 - [83] Narang, A.; Konopka, A.; Ramkrishna, D. (1996). Dynamic analysis of the cybernetic model for diauxic growth. *Chem. Eng. Science.* **52**(15):2567-2578.
 - [84] Kompala, D.S.; Ramkrishna, D. (1986). Investigation of bacterial growth on mixed substrates: Experimental evaluation of cybernetic models. *Biotechnol. Bioeng.* **28**:1044-1055.
 - [85] Ramakrishna R.; Ramakrishna, D. (1996). Cybernetic modeling of growth in mixed, substitutable substrate environments: Preferential and simultaneous utilization. *Biotechnol. Bioeng.* **52**:141-155.
 - [86] Gadgil, Ch.J.; Bhat, P.J.; Venkatesh, K.V. (1996). Cybernetic model for the growth of *Saccharomyces cerevisiae* on melibiose. *Biotechnol. Prog.* **12**:744-750.
 - [87] Nakamura, Y.; Sawada, T.; Inoue, E. (2001). Mathematical model for ethanol production from mixed sugars by *Pichia stipitis*. *Journal of Chem. Technol. Biotechnol.* **76**:586-592.

3. MATERIALS AND METHODS

3.1. Microorganisms

Four yeast strains were used in this research work: *Candida shehatae* NRRL Y-1285, *Pachysolen tannophilus* NRRL Y-12885, *Pichia stipitis* NRRL Y-11545, obtained from the National Renewable Resources Laboratory, Peoria, Illinois, and a commercial strain of *Saccharomyces cerevisiae* Montrachet, provided by Dr. Govind Nadathur from the Department of Marine Sciences, University of Puerto Rico, Mayagüez Campus. Stock cultures were stored in 1.5 mL microvials at -80°C in a 60% (v/v) glycerol aqueous solution and fresh colonies were aseptically transferred every 10 days spread on petri dishes containing YPD Agar culture media (Difco, BD Co., France)

Preliminary screening of xylose-fermenting yeast strains was carried out using *C. shehatae*, *P. tannophilus* and *P. stipitis*, but this last yeast strain proved to be the higher ethanol producing strain from xylose as a carbon source, and therefore was used with *S. cerevisiae* in all the experiments whose results are detailed in Chapters 4 and 5.

3.2. Inoculum preparation

3.2.1. Inocula for single substrate fermentations

Stock cultures were maintained on 60% glycerol at -80°C. Approximately 100 µL were cultivated on YPD agar plates containing the following components (amounts in g/L): glucose, 20; peptone, 20; yeast extract, 10; and agar, 15. Petri dishes were incubated in an Imperial III static incubator (Lab-Line) at 32°C for 72-90 hours in order to obtain fresh and well defined colonies, and also to obtain viable cells at the exponential phase for all the experiments [1-2]. A loopfull of the strain assayed was added to 30 mL filter sterilized media

in a 125 mL autoclaved baffled culture flask, comprising the following components (in g/L): yeast extract, 3; peptone, 5; malt extract, 3; $\text{MgSO}_4 \cdot 7\text{H}_2\text{O}$, 2; $(\text{NH}_4)_2\text{SO}_4$, 3, KH_2PO_4 , 2; and sugar (glucose or xylose), 25. The medium composition was an average of the proportions suggested by several previous works [2-5]. Cultures were aerobically incubated for 12-18 hours, 32°C and 185 rpm until mid-exponential growth phase was achieved, in a temperature controlled orbital Innova 4000 shaker (New Brunswick, NJ), according to Figure 3.1

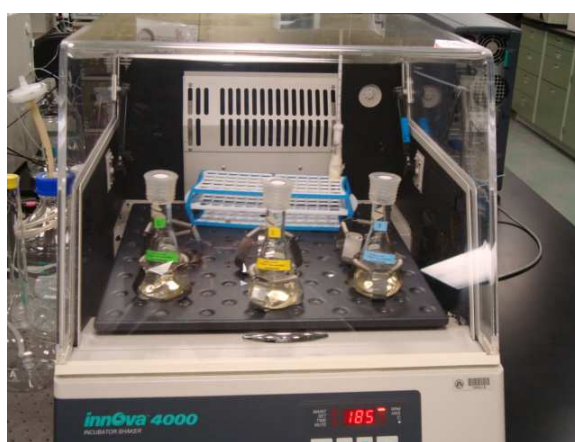


Figure 3.1 - Inoculum preparation for single substrate fermentations in an Innova 4000 incubator shaker.

3.2.2. Inocula for mixed substrate and mixed strains fermentations

Culture media compositions for inocula in co-fermentations are the same as those described in section 3.2.1 for both solid agar and liquid media, with a total sugar concentration of 25 g/L in liquid medium, varying the proportions between glucose and xylose in the following patterns. The difference in method is one additional pre-culturing step in the preparation chain, similar to the methodology described by Sáez [6]. Two loopfulls were taken from petri dishes incubated for 72-90 hours, at 32°C containing *S. cerevisiae* and *P. stipitis*, respectively. Loopfulls were added to 30-mL filter sterilized culture medium in a 125 mL autoclaved baffled culture flask and were cultivated for 9-12 hours, at 32°C and 150

rpm in a temperature-controlled orbital Innova 4000 incubator shaker. These cultures were transferred into an autoclaved baffled polycarbonate-polypropylene 300 mL (150 mL working volume) shake flask (TunAir, AVP Caribe, PR) containing the same mixed sugar nutrient as described above and incubation was continued in the same incubator shaker for 12-16 hours, at 32°C and 200 rpm. Figure 3.2 shows the scheme for inoculum preparation.

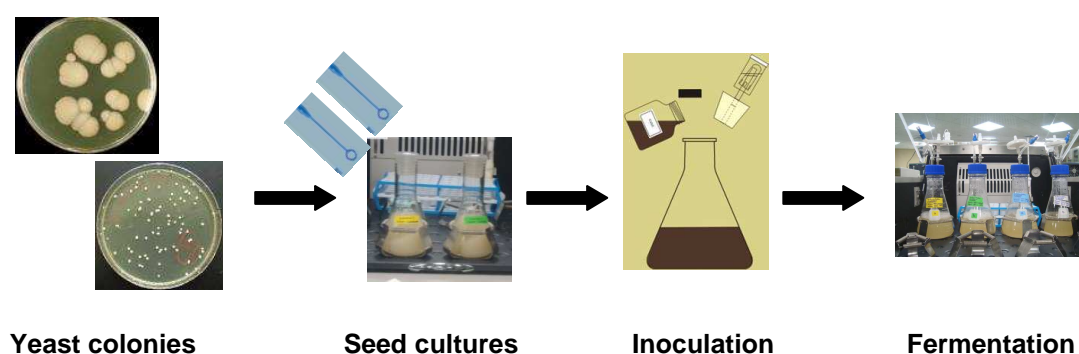


Figure 3.2 - Inoculum preparation for co-fermentations in an Innova 4000 incubator shaker.

3.3. Batch fermentations

In efforts to achieve the necessary conditions for a vigorous inoculum, and having a high initial cell concentration in fermentation, inocula as described above were transferred at a 10% (v/v) [7] to a 500-mL autoclaved bioreaction system consisting of one semi-baffled culture flask (Pyrex, Fisher Scientific) along with a sampling-venting assembly integrated by a polypropylene thread cap and a two-port stainless steel base (Bellco Company, NJ). One port was used to provide the low-oxygen levels necessary for ethanol fermentation, especially when using xylose-fermenting yeast strains [8]. Hence, air exchange was achieved by plugging a polypropylene filter disk containing a 0.2 μm nitrocellulose membrane to the shortest tube of the stainless steel assembly. The left port was connected to one sterile C-flex

tubing (Wave Biotech, GE Lifesciences) provided with a septum valve in the outer end, to aseptically collect samples along the fermentation culture. The culture flask contained 270 mL of the same filter-sterilized culture media described in section 3.2.1, which was mixed with the 30 mL of inoculum to give 300 mL of total fermentation volume. The bioreactor was inoculated to achieve an initial cell concentration of at least 0.5 g/L and an initial pH 5.00 [9] and was incubated in the Innova 4000 shaker at 32°C [9] and 100 rpm [10] for the time necessary until complete sugar depletion. The elapsed time ranged between 8 and 72 hours, depending on the combination of sugar and yeast strain, being 8 hours for system glucose - *S. cerevisiae* and 72 hours for the system xylose - *P. stipitis*. All the experiments were conducted by triplicate and were carried out at an initial sugar substrate concentration of 25 g/L (using either pure glucose, pure xylose, or mixtures with the following proportions of glucose and xylose, respectively, expressed as percentages: 25/75, 50/50 and 75/25). Samples were collected periodically throughout the course of the fermentations using standard methods (withdrawing 5 mL of culture broth through a syringe inserted in the septum at the outer end of the C-flex tube). Samples were analyzed to determine the concentrations of sugars (glucose and xylose), using HPLC and the YSI Biochemistry Analyzer, ethanol and byproducts (i.e., xylitol, lactic acid, glycerol and acetic acid), using HPLC and cell mass using spectrophotometry and the gravimetric method to determine dry cell mass.



Figure 3.3 - Batch fermentation in an Innova 4000 incubator shaker.

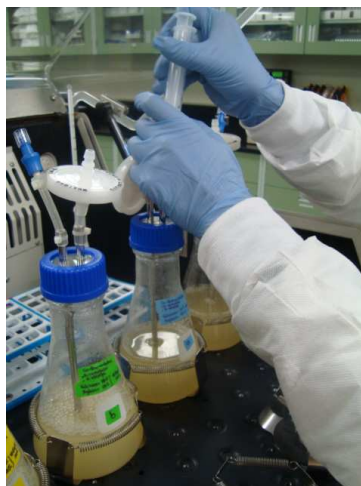


Figure 3.4 - Aseptic sampling throughout the course of fermentation.

3.4. Cell growth and cell mass concentration

One milliliter of the total sample volume was used to measure cell growth, as optical density (OD) at 600 nm in a Genesys 6 UV-Vis spectrophotometer (Thermo Scientific). Dilutions were required when the OD₆₀₀ value was higher than 0.850 absorbance units, using sterile medium as sample diluent and also as the blank to “zero” the spectrophotometer at the

beginning of each measurement. Cell mass concentration was calculated as dry cell mass, DCM (g/L) from the sample dry weights (knowing the sample volumes) with a manifold filtration unit (Cole Parmer Instruments) following the gravimetric method, as shown in Figure 3.5. Three milliliters of yeast whole broth samples were filtered on to preweighed cellulose acetate Advantec-25mm, 0.2 μm filter mats, (Cole Parmer Instruments) retaining the cells, and washed twice with deionized water, and then dried in an static Imperial III incubator (Labline) overnight until constant weight was attained.



Figure 3.5 - Manifold filtration unit used for cell filtration.

A linear correlation between OD and cell mass concentration was estimated for each of the strains utilized to evaluate the consistency of direct and indirect methods for cell concentration measurement and also for further cell mass concentration measurements from OD using a correlation factor, as shown in Figures 3.6 – 3.9.

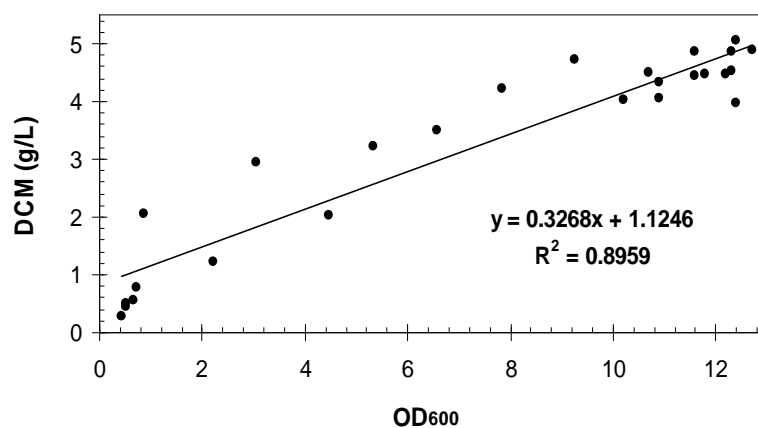


Figure 3.6 – Linear correlation between DCM concentration (g/L) and OD at 600 nm for glucose with *Saccharomyces cerevisiae*.

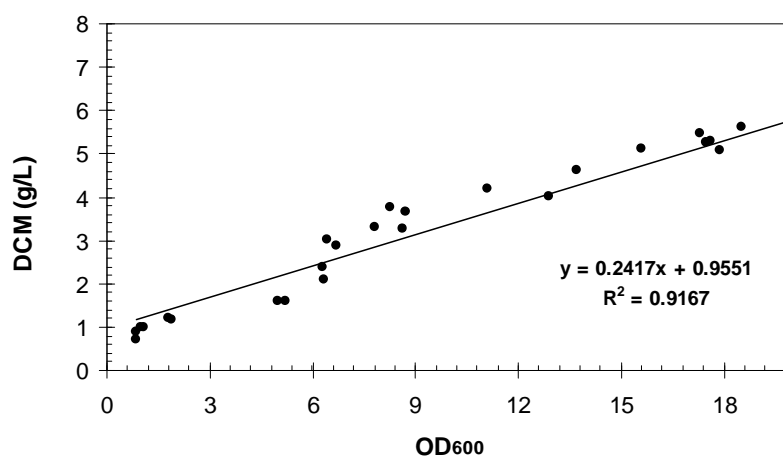


Figure 3.7 – Linear correlation between DCM concentration (g/L) and OD at 600 nm for glucose with *Pichia stipitis*.

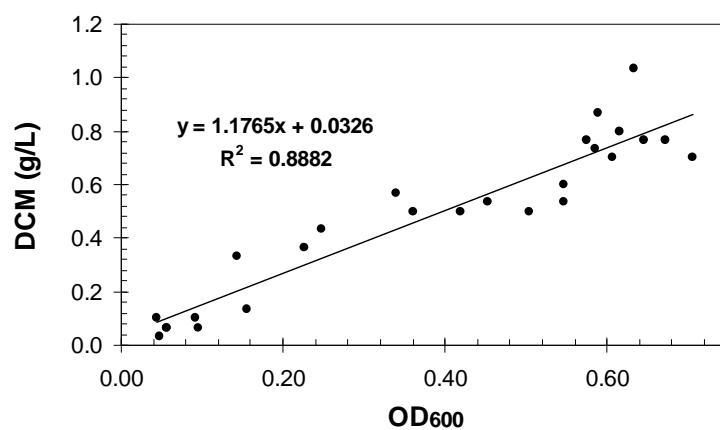


Figure 3.8 – Linear correlation between DCM concentration (g/L) and OD at 600 nm for xylose with *Saccharomyces cerevisiae*.

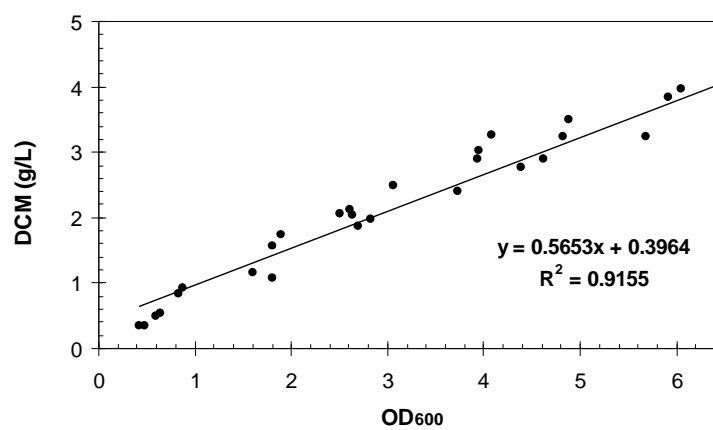


Figure 3.9 – Linear correlation between DCM concentration (g/L) and OD at 600 nm for xylose with *Pichia stipitis*.

3.5. Sugar, ethanol, and by-product concentrations

The concentration of sugars (glucose and xylose), ethanol, and by-products xylitol, lactic acid, glycerol and acetic acid were determined using a high performance liquid chromatography (HPLC) Shimadzu LC-10ATVP unit as shown in Figure 3.10. Samples withdrawn from the bioreactor flasks were centrifuged using a microcentrifuge (Eppendorf, model 5415C) at 7000 rpm by 5 minutes. The supernatant was filtered using a 0.20 μm Fisherbrand nylon membrane (Fisher Scientific) and was then analyzed using HPLC with an Aminex BioRad HPX-87H, 300 mm organic acids column (BioRad Labs, CA) operating at 45°C. A refractive index detector was used for compound detection and dilute sulfuric acid (0.001 M) at a flow rate of 0.6 mL/min was the mobile phase. Mixed standard solutions of ethanol and sugar (only glucose, only xylose or glucose/xylose mixtures) were run to construct a calibration curve, and standards of glucose and xylose were periodically injected to the HPLC to verify calibration accuracy.



Figure 3.10 - High performance liquid chromatography device (Shimadzu LC-10ATVP) for analysis of sugars, ethanol and byproduct concentrations.

Sugar concentration was also analyzed throughout fermentation time by means of YSI 2700 Biochemistry Analyzer (YSI, OH). This analysis gave excellent and accurate real-time information about the consumption of sugar, either as sole carbon source or in mixtures of glucose/xylose. The sample -approximately 0.5 mL- was centrifuged and filtered as described above and processed in the YSI 2700 sample station, which aspirates only 13 μL and gives directly the sugar concentration in less than one minute.

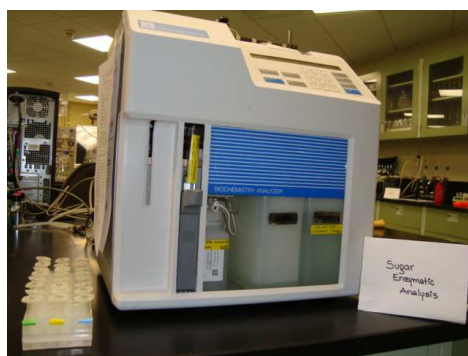


Figure 3.11 – Biochemistry Analyzer device (YSI 2700) for sugar monitoring.

3.6. Profile concentrations model development and simulation

3.6.1. Single substrate fermentations

The model proposed to simulate single substrate fermentations derives from the basis of mass balances applied to a batch fermentation system taking into account that limiting substrate is consumed for both cell proliferation and ethanol production and considering the cells as a single species in solution, assuming fixed composition which is equivalent to assuming balanced growth; this is the basic assumption of an unstructured model [11]. Prior to construct the complete set of equations, kinetic parameters such as maximum cell growth rate (μ_{\max}) and saturation kinetic constant (K_s) must be calculated. The values for μ_{\max} are determined from cell growth experimental data, taking only those cell concentrations that fall inside the exponential growth phase and applying an exponential regression to fit the data, as

shown in Figure 3.12. The slope of the model which describes the exponential trend of the plotted data is the numeric value for μ , which according to Shuler and Kargi [12] can be approximated to μ_{\max} . However, the value of μ_{\max} was further obtained using optimization techniques.

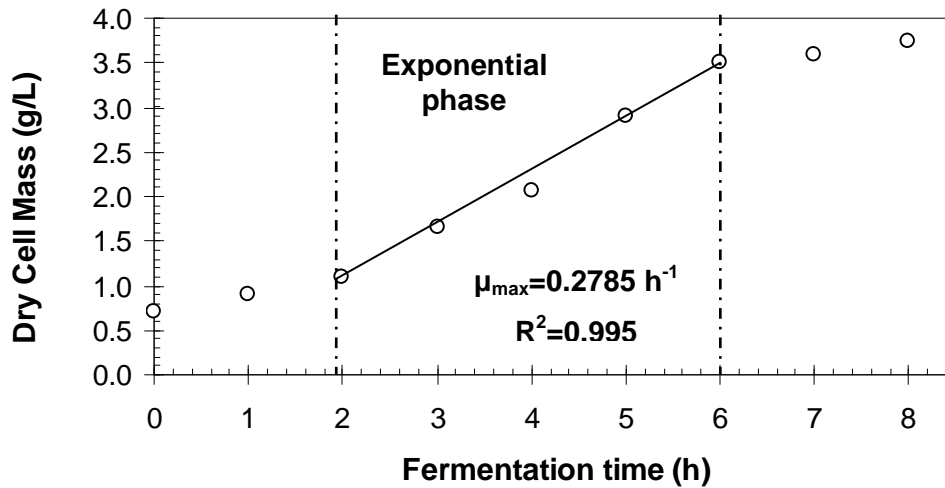


Figure 3.12 – Growth curve and maximum specific growth rate determination for one run of glucose fermentation with *S. cerevisiae*.

The K_s value is determined from the various linearized expressions between substrate concentration and μ_{\max} such as Lineweaver-Burk, Eadie-Hofstee, Hanes-Woolf or Batch Kinetics, the ones that are based in enzymatic kinetics [12]. This value was later optimized while solving the mass balance equations, along with the optimization of the μ_{\max} value.

Finally, the remaining experimental parameters to be determined were the yield coefficients: $Y_{X/S}$, $Y_{P/X}$ and $Y_{P/S}$ corresponding to cell growth with respect to substrate consumption, ethanol production with respect to cell growth, and ethanol production with respect to substrate consumption, respectively. Yield coefficients are defined based on the amount of consumption of another material and an appropriate method to obtain them is to plot experimental data according to yield relationship desired, and then obtain the slope for

the linear correlation between them. Figure 3.13 shows the procedure utilized to calculate ethanol mass yield coefficient with respect to cell growth, $Y_{P/X}$ for a particular case along this research work. Note that a linear trend was proposed for the relationship between ethanol concentration versus cell concentration and the slope of such linear model results in the value of $Y_{P/X}$.

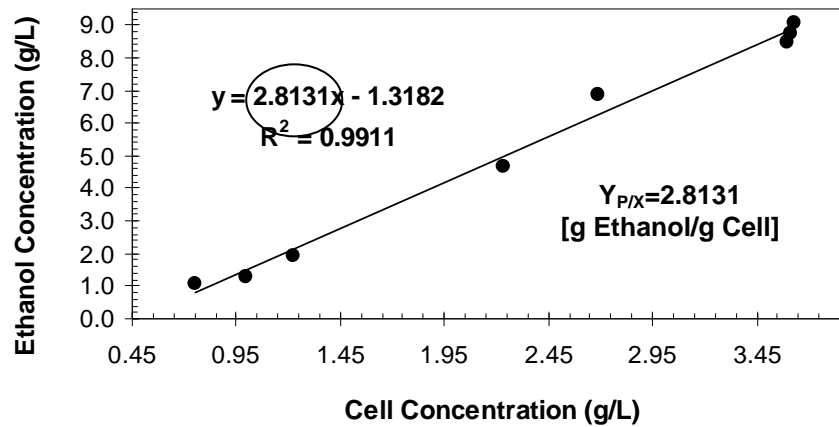


Figure 3.13 – Linear regression between ethanol and cell mass concentrations for yield coefficient $Y_{P/X}$. The slope of the regression equation represents the value of the yield coefficient, $Y_{P/X}$.

As mentioned in Chapter 2, mass balance equations describing the batch fermentation process for cell mass production, sugar utilization and ethanol production respectively, are described by equations (2.12 – 2.14). In the formulation of these mass balances, it was assumed that the growth kinetics would show no inhibition effects, from substrate or product, due to the relatively low concentration of both along the batch fermentation process. These equations, along with kinetic parameters and yield coefficients obtained as described previously require being solved simultaneously using the initial conditions experimentally at the start of fermentation process. Because of the non-linear characteristics of the ordinary differential equations system it was necessary to solve it using an appropriate method. The method used in this work is the fourth-order Runge-Kutta algorithm, known as RK4 which is

a reasonably simple and robust method. RK4 is an excellent procedure for numerical solution of a set of non-linear differential equations when combined with an intelligent adaptive step-size routine [13]. The software utilized to solve the different sets of equations was MATLAB (version 7.8.0.347, The MathWorks Inc., MA) using the ode45 function, which is based on an explicit 4th or 5th order-Runge-Kutta method, and it is believed to be a suitable method for most problems [14]. Figure 3.14 shows the basic algorithm in which the above described non-linear differential system is proposed and later solved:

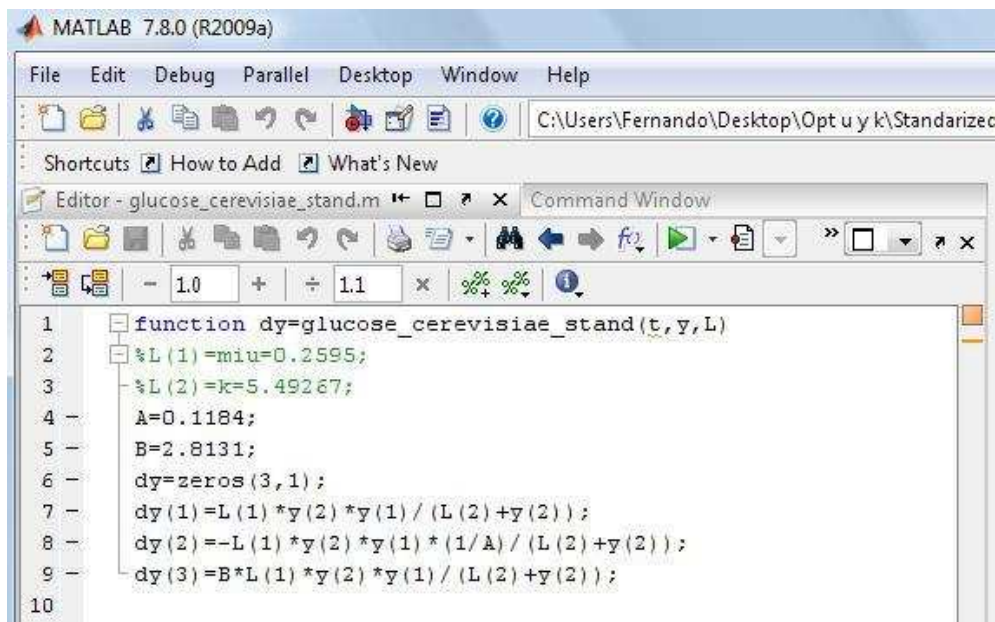


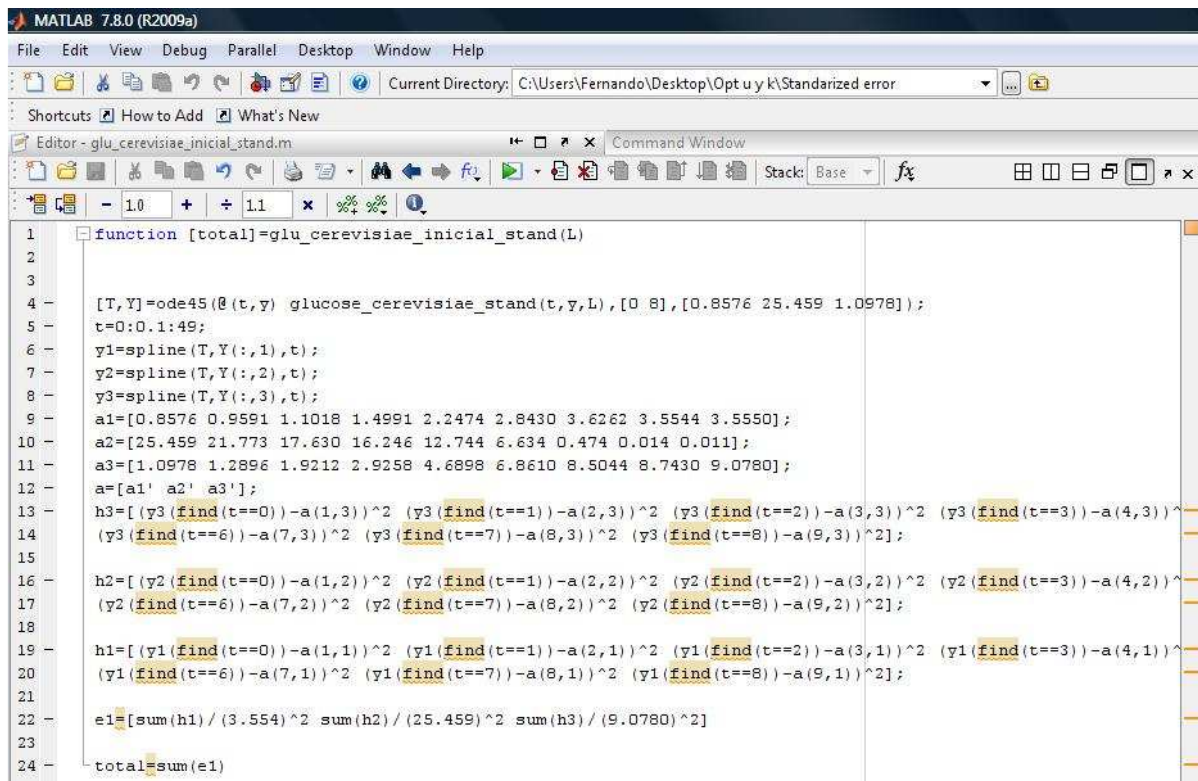
Figure 3.14 – Matlab Editor Window with proposed ordinary differential system.

Figure 3.15 shows the algorithm implemented to solve the non-linear differential system proposed in Figure 3.14, for batch fermentation mass balances along with a simultaneous optimization routine to obtain the optimum values of the parameters μ_{\max} and K_s . The optimization routine minimizes the objective error function $E(\theta)$, between the experimental data points and the values determined by the Runge-Kutta solution. This

objective function, used previously in optimization techniques for parameter estimation [15] is:

$$E(\theta) = \sum_{n=1}^n \left[\frac{(X_s - X_e)^2}{X_{e,\max}^2} + \frac{(S_s - S_e)^2}{S_{e,\max}^2} + \frac{(P_s - P_e)^2}{P_{e,\max}^2} \right] \quad (3.1)$$

where the subscripts s, e and max correspond to simulated, experimental and maximum measured concentrations in g/L, respectively, for cell mass (X), sugar (S) and ethanol (P), and n is the number of sampling points. The objective function was further minimized using the function “fmincon” included in the Optimization Toolbox of MATLAB version 7.8.0.347.



```

1 function [total]=glu_cerevisiae_inicial_stand(L)
2
3
4 [T,Y]=ode45(@ (t,y) glucose_cerevisiae_stand(t,y,L),[0 8],[0.8576 25.459 1.0978]);
5 t=0:0.1:49;
6 y1=spline(T,Y(:,1),t);
7 y2=spline(T,Y(:,2),t);
8 y3=spline(T,Y(:,3),t);
9 a1=[0.8576 0.9591 1.1018 1.4991 2.2474 2.8430 3.6262 3.5544 3.5550];
10 a2=[25.459 21.773 17.630 16.246 12.744 6.634 0.474 0.014 0.011];
11 a3=[1.0978 1.2896 1.9212 2.9258 4.6898 6.8610 8.5044 8.7430 9.0780];
12 a=[a1' a2' a3'];
13 h3=[(y3(find(t==0))-a(1,3))^2 (y3(find(t==1))-a(2,3))^2 (y3(find(t==2))-a(3,3))^2 (y3(find(t==3))-a(4,3))^2
14 (y3(find(t==6))-a(7,3))^2 (y3(find(t==7))-a(8,3))^2 (y3(find(t==8))-a(9,3))^2];
15
16 h2=[(y2(find(t==0))-a(1,2))^2 (y2(find(t==1))-a(2,2))^2 (y2(find(t==2))-a(3,2))^2 (y2(find(t==3))-a(4,2))^2
17 (y2(find(t==6))-a(7,2))^2 (y2(find(t==7))-a(8,2))^2 (y2(find(t==8))-a(9,2))^2];
18
19 h1=[(y1(find(t==0))-a(1,1))^2 (y1(find(t==1))-a(2,1))^2 (y1(find(t==2))-a(3,1))^2 (y1(find(t==3))-a(4,1))^2
20 (y1(find(t==6))-a(7,1))^2 (y1(find(t==7))-a(8,1))^2 (y1(find(t==8))-a(9,1))^2];
21
22 e1=[sum(h1)/(3.554)^2 sum(h2)/(25.459)^2 sum(h3)/(9.0780)^2]
23
24 total=sum(e1)

```

Figure 3.15 – MATLAB Editor Window with the ode45 Runge-Kutta solver method and simultaneous optimization for μ_{\max} and K_s value based in minimization of Equation 3.1.

Other software was also used along with MATLAB, because of its simplicity, to solve the differential equations system when no optimization is required. This alternative software is Polymath (Polymath 6.0 Educational Release). It also incorporates a 4th-order Runge-Kutta method in its algorithm RKF45 [16] and the results obtained are quite similar to those obtained with MATLAB. Figure 3.16 shows a routine created in Polymath to solve a differential equation system for glucose fermentation with *S. cerevisiae*.

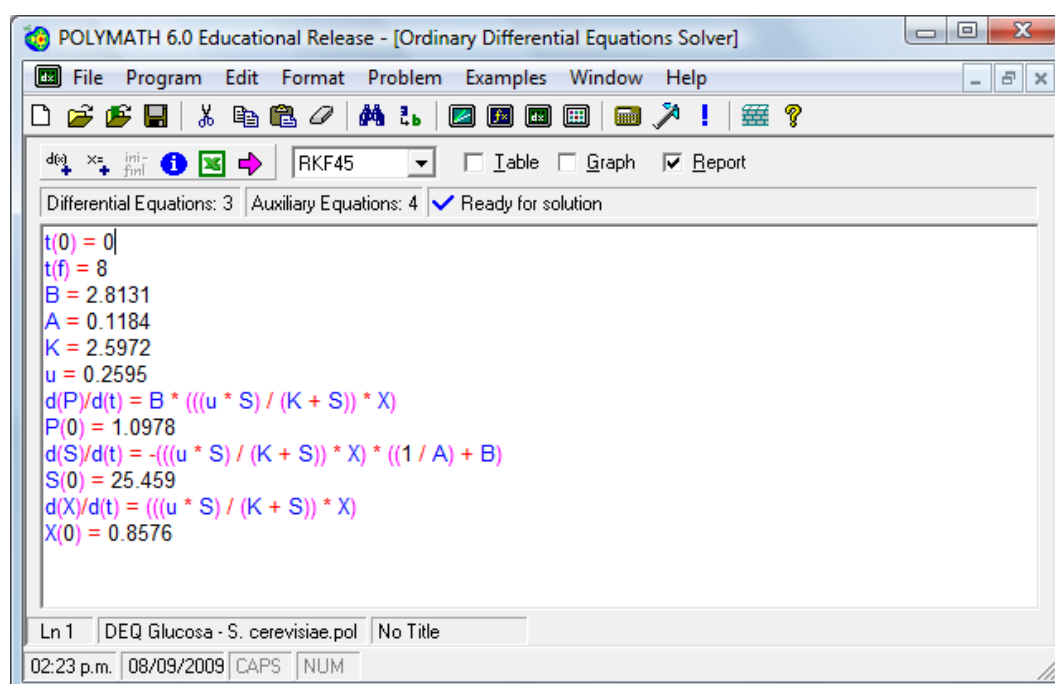


Figure 3.16 - Polymath Editor Window with the RK45 solver method for the system Glucose – *S. cerevisiae*.

3.6.2. Co-fermentations of glucose/xylose mixtures

Once analyses for single substrate fermentations were finished, the optimized kinetic parameters and yield coefficients were used to construct the structured model to predict the behavior of profile concentrations in batch fermentations with mixtures of glucose and xylose,

starting with the mixture models for each yeast strain and then a consolidated model for the mixtures using co-cultures of the two yeast strains.

As described in Chapter 2, structured models recognize the complex set of metabolic reactions occurring within the cell. Therefore the mass balances presented previously still apply, but it is necessary to add equations for the rates of key enzyme synthesis of both yeast strains and to modify the equations for the rate of cell growth. According to the equations 2.17 - 2.24, the structured differential system which models a mixture of two substrates using two different yeast strains, including the enzyme balances and the cybernetic variables was solved using MATLAB version 7.8.0.347 with the same 4th order Runge-Kutta method used for the single substrate fermentations differential system.

Following all of the considerations and assumptions found in the literature for the analysis of the cybernetic models [17,18,19], and as explained in Chapter 2, with appropriate and reasonable expressions and values for the cybernetic variables and initial conditions of the six components, the system was solved. Figure 3.17 shows the MATLAB algorithm to solve the differential equation system corresponding to a structured model for a mixture of glucose and xylose with *P. stipitis*, including the optimization of cellular resources, which is mathematically described by the cybernetic variables.

```

1 function dy=Ps_glu_xyl_NoB(t,y)
2 % 1 belongs to glucose
3 % 2 belongs to xylose
4 miu=[0.1766 0.054];
5 K=[25 25];
6 A=[0.0941 0.0831];
7 B=[3.208 3.5945];
8 alpha=0.001; beta=0.05;
9 rate_1=(miu(1)*y(2))/(K(1)+y(2));
10 rate_2=(miu(2)*y(3))/(K(2)+y(3));
11 if rate_1>rate_2
12     max=rate_1;
13 else max=rate_2;
14 end
15 v1=((miu(1)*y(2))/(K(1)+y(2)))/max;
16 v2=((miu(2)*y(3))/(K(2)+y(3)))/max;
17 u1=((miu(1)*y(2))/(K(1)+y(2)))/((miu(1)*y(2))/(K(1)+y(2))+(miu(2)*y(3))/(K(2)+y(3)));
18 u2=((miu(2)*y(3))/(K(2)+y(3)))/((miu(1)*y(2))/(K(1)+y(2))+(miu(2)*y(3))/(K(2)+y(3)));
19
20 Z=[t' v1' v2' u1' u2'];
21 xlsxwrite('Ps_glu_xyl_NoB_cybernetic.xls',Z);
22
23 dy=zeros(6,1);
24 dy(1)=(miu(1)*y(2)*y(1))/(K(1)+y(2))*((miu(1)*y(2))/(K(1)+y(2)))/max+(miu(2)*y(3)*y(1))/(K(2)+y(3))*((miu(2)*y(3))/(K(2)+y(3)))/max;
25 dy(2)=-(1/A(1))*((miu(1)*y(2)*y(1))/(K(1)+y(2))*((miu(1)*y(2))/(K(1)+y(2)))/max);
26 dy(3)=-(1/A(2))*((miu(2)*y(3)*y(1))/(K(2)+y(3))*((miu(2)*y(3))/(K(2)+y(3)))/max);
27 dy(4)=B(1)*((miu(1)*y(2)*y(1))/(K(1)+y(2))*((miu(1)*y(2))/(K(1)+y(2)))/max+(B(2)*((miu(2)*y(3)*y(1))/(K(2)+y(3))*((miu(2)*y(3))/(K(2)+y(3)))/max);
28 dy(5)=alpha*y(2)/(K(1)+y(2))*((miu(1)*y(2))/(K(1)+y(2)))/((miu(1)*y(2))/(K(1)+y(2))+(miu(2)*y(3))/(K(2)+y(3)));
29 dy(6)=alpha*y(3)/(K(2)+y(3))*((miu(2)*y(3))/(K(2)+y(3)))/((miu(1)*y(2))/(K(1)+y(2))+(miu(2)*y(3))/(K(2)+y(3)));
30

```

Figure 3.17 - MATLAB Editor Window with a set of non-linear ordinary differential equations for a mixture of glucose and xylose with *P. stipitis*, including a rate maximization subroutine in the calculation of the cybernetic variables.

3.7. References cited

- [1] Agbogbo, F.K; Coward-Kelly, G.; Torry-Smith, M.; Wenger, K.S. (2006). Fermentation of glucose/xylose mixtures using *Pichia stipitis*. *Process Biochemistry*. **41**:2333-2336.
- [2] Sánchez, S.; Bravo, V.; Castro, E.; Moya, A.J.; Camacho, F. (2002). The fermentation of mixtures of D-glucose and D-xylose by *Candida shehatae*, *Pichia stipitis* or *Pachysolen tannophilus* to produce ethanol. *Journal of Chem. Technol. and Biotechnol.* **77**:641-648.
- [3] Zaho, L.; Zhang, X.; and Tan, T. (2008). Influence of various glucose/xylose mixtures on ethanol production by *Pachysolen tannophilus*. *Biomass and Bioenergy*. **32**:1156-1161.

- [4] Wilkins, M.R.; Mueller, M.; Eichling, S.; and Banat, I.M. (2008). Fermentation of xylose by the thermotolerant yeast strains *Kluyveromyces marxianus* IMB2, IMB4, and IMB5 under anaerobic conditions. *Process Biochem.* **43**:346-350.
- [5] Rouhollah, H.; Iraj, N.; Giti, E.; and Sorah, A. (2007). Mixed sugar fermentation by *Pichia stipitis*, *Saccharomyces cerevisiae* and an isolated xylose-fermenting *Kluyveromyces marxianus* and their cocultures. *African Journal of Biotechnol.* **6**(9):1110-1114.
- [6] Sáez-Miranda, J.C.; Saliceti-Piazza, L.; and McMillan, J.D. (2006). Measurement and analysis of intracellular ATP levels in metabolically engineered *Zymomonas mobilis* fermenting glucose and xylose mixtures. *Biotechnol. Prog.* **22**:359-368.
- [7] Wyman, C.E. (1996). Handbook on Bioethanol: Production and Utilization. *Taylor & Francis*. **1st Ed**: 163-178.
- [8] Skoog, K.; Hahn-Hägerdal. (1990). Effect of oxygenation on xylose fermentation by *Pichia stipitis*. *Applied and Environmental Microbiology.* **56**(11):3389-3394.
- [9] Slininger, P.J.; Bothast, R.J.; Ladisch, M.R.; and Okos. M.R. (1989). Optimim pH and temperature conditions for xylose fermentation by *Pichia stipitis*. *Biotechnol. Bioeng.* **35**:727-731.
- [10] Kongkiattikajorn, J.; Rodmui, A.; and Dandusitapun, Y. (2007). Effect of agitation rate on batch fermentation of mixture culture of yeasts during ethanol production from mixed glucose and xylose. *Thai Journal of Biotechnology.* 1-4.
- [11] Blanch, H.W.; Clark, D.X. (1996). Biochemical Engineering. *Marcel Dekker Inc.* **1st. Ed**:162-275.
- [12] Shuler, M.L.; Kargi, F. (2006). Bioprocess Engineering – Basic Concepts. *Prentice Hall.* **2nd Ed**:175-209.
- [13] Goeken, D.; Johnson, O. (1999). Fifth-order Runge-Kutta with higher order derivative approximations. *Electronic Journal of Differential Equations*:1-9.
- [14] Dormand, J.R.; Prince, P.J. (1980). A family of embedded Runge-Kutta formulae. *J. Compl. Appl. Math.* **6**:19-26
- [15] Ccopa Rivera, E.; Costa, A.C.; Atala, D.I.P.; Maugeri, F.; Wolf Maciel, M.R.; Maciel Filho, R. (2006). Evaluation of optimization techniques for parameter estimation: Application to ethanol fermentation considering the effect of temperature. *Process Biochemistry.* **41**:1682-1687.
- [16] Forsythe, G.E.; Malcolm, M.A.; and Moler, C.B. (1977). Computer Methods for Mathematical Computation. *Prentice Hall, Englewood Cliffs.*

- [17] Kompala, D.; Ramakrishna, D. (1986). Investigation of bacterial growth on mixed substrates: Experimental evaluation of cybernetic models. *Biotechnol. Bioeng.* **28**:1044-1055.
- [18] Kompala, D.; Ramakrishna, D.; Tsao, G. (1984). Cybernetic modeling of microbial growth on multiple substrates. *Biotechnol. Bioeng.* **26**:1272-1281.
- [19] Ramakrishna, D.; Ramakrishna, D. (1996). Cybernetic modeling of growth in mixed, substitutable substrate environments: Preferential and simultaneous utilization. *Biotechnol. Bioeng.* **52**:141-151.

4. SINGLE SUBSTRATE FERMENTATIONS

This chapter presents kinetic information and mathematical modeling, which is regarded as an indispensable step in developing a fermentation process with advantages such as process knowledge improvement, decreasing the cost of expensive industrial experimentation, mathematical optimization and process control strategies. The main goal of this work is to develop a mathematical model able to successfully predict the behavior of batch fermentations using a mixture of carbohydrates in a co-culture configuration for bioethanol production. To achieve this, and taking into account the cell optimization nature in which the structured model is based, both sugars (glucose and xylose) and the two yeast strains (*Saccharomyces cerevisiae* and *Pichia stipitis*) were analyzed individually in four isolated systems (one carbohydrate-one yeast strain). Thus the kinetic parameters were obtained to construct both unstructured and structured models to describe individual and mixed sugar fermentations, respectively. The four individual systems analyzed and discussed in this chapter are: glucose-*P. stipitis*, glucose-*S. cerevisiae*, xylose-*P. stipitis* and xylose-*S. cerevisiae*. This last system was carried out only as a control monitoring, since wild type-strains of *S. cerevisiae* do not have metabolic capacity to efficiently utilize xylose as the sole carbon source and ferment it to ethanol. However, several research works have been dedicated to develop improved *S. cerevisiae* strains by means of genetic engineering, encoding genes of naturally pentose-fermenting yeast strains, resulting in ethanol yields at near theoretical yields of 0.51 g ethanol/g sugar, but with low maximal productivities [1].

Each of the individual fermentations started with a maximum initial sugar concentration ranging from 20-25 g/L, therefore the maximum ethanol concentration achievable is ~12.5 g/L if reaction would yield 100% with respect to the theoretical yield for fermentation systems using yeast strains. A simple unstructured model is good enough to simulate these individual fermentation systems, since the range of concentrations of both

substrates and products do not cause the inhibition as studied by some authors. These studies suggest that substrate inhibition should begin with sugar concentrations above 40 g/L for *P. stipitis* [3] and 150 g/L for *S. cerevisiae*, because at higher substrate concentrations catabolite inhibition of enzymes in the fermentative pathway becomes important, indicating the onset of substrate inhibition as a result of high osmotic pressure and low water activity [4]. Product inhibition takes place when ethanol produced reaches levels at which cells do not grow anymore. These concentrations have been found to be 64 g/L for *P. stipitis* [3] and 105 g/L for *S. cerevisiae* [5]. This is the reason why all the systems discussed in this chapter are on the basis of the Monod model with no substrate or product inhibition terms.

4.1. Fermentation kinetics and experimental profiles

Determination of fermentation kinetics for the four systems previously described started by determining the values of the maximum cell growth rate, μ_{\max} . For this purpose the exponential growth phases were located and the procedure suggested by Shuler, described in section 3.6.1 was followed, which stipulates that the slope resulting from the exponential regression applied to the set of experimental data that lie in the exponential growth phase belongs to the numeric value of μ , as shown in Figures 4.1 – 4.3. According to Figure 4.1, the ability of *S. cerevisiae* to grow in glucose is easily and efficiently proved, displaying a steep exponential ramp which involves the highest specific growth rate of all the four systems under study, 0.2595 h^{-1} . This well known efficiency is the result of *S. cerevisiae*'s outstanding features such as larger size, thicker cell wall, better growth at low pH, less stringent nutritional requirements, and greater resistance to contamination [6]. Also, glucose fermentation with *P. stipitis* showed a higher specific growth rate when compared to xylose as a substrate for the same experimental conditions, which has been observed previously in the literature. However, the lowest specific cell growth rate was achieved in the system xylose –

P. stipitis, which is in complete agreement with the results presented by other authors [7], but opposite to results presented by Sánchez and co-workers [8]. As discussed later on this chapter, xylose uptake is slower than glucose uptake for a given microorganism under the same experimental conditions, and this situation was early observed through the values of μ when comparing Figures 4.1 – 4.3, where it is obvious that μ for glucose is threefold of μ for xylose, under the same experimental conditions, and virtually the same initial cell concentration. According to Figure 2.14 which shows the metabolic pathways for ethanol production from both glucose and xylose, the net energetic yield when glucose is the carbon source is 2 moles of ATP per mole of glucose, which favors the glucose metabolism over that of xylose, which yields ~1.67 moles of ATP per mole of xylose. Also, some nuclear magnetic resonance studies prove that cell growth rate is faster in glucose than xylose, concluding that xylose metabolism is less energized than the glucose one, with cells consuming glucose having higher levels of nucleoside triphosphates (NTP) and sugar diphosphatases (UDP) than those cells cultured in xylose. This is important because NTP (mostly ATP) are cellular energy reserve materials and UDP sugar levels are indicative of cell growth potential; thus, cells metabolizing xylose would have less energy for growth than cells metabolizing glucose [9].

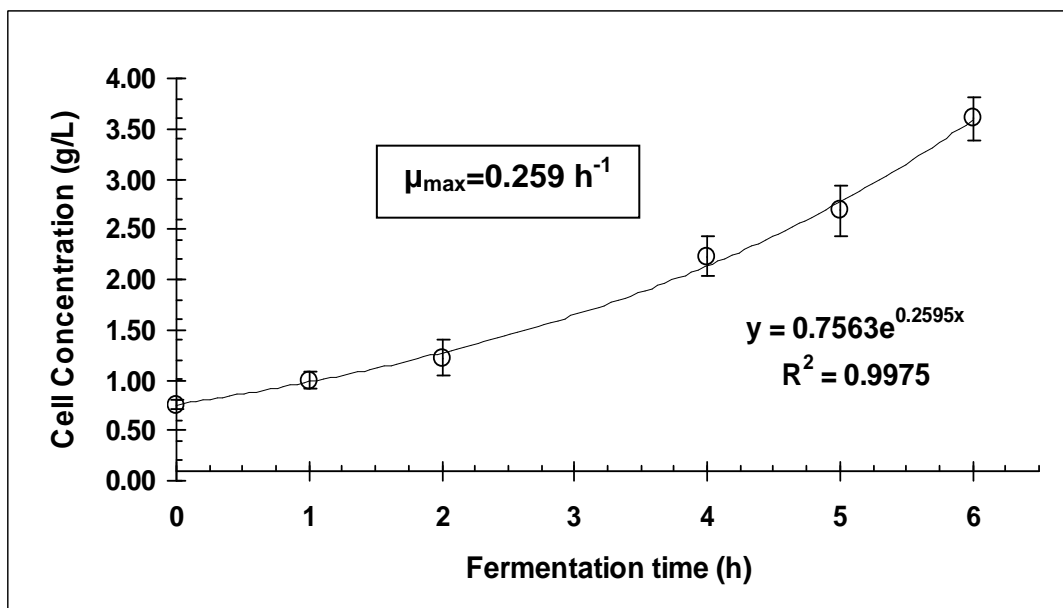


Figure 4.1 – Determination of μ_{\max} for glucose fermentation with *S. cerevisiae*. Error bars are ± 1 standard deviation of 3 replicates.

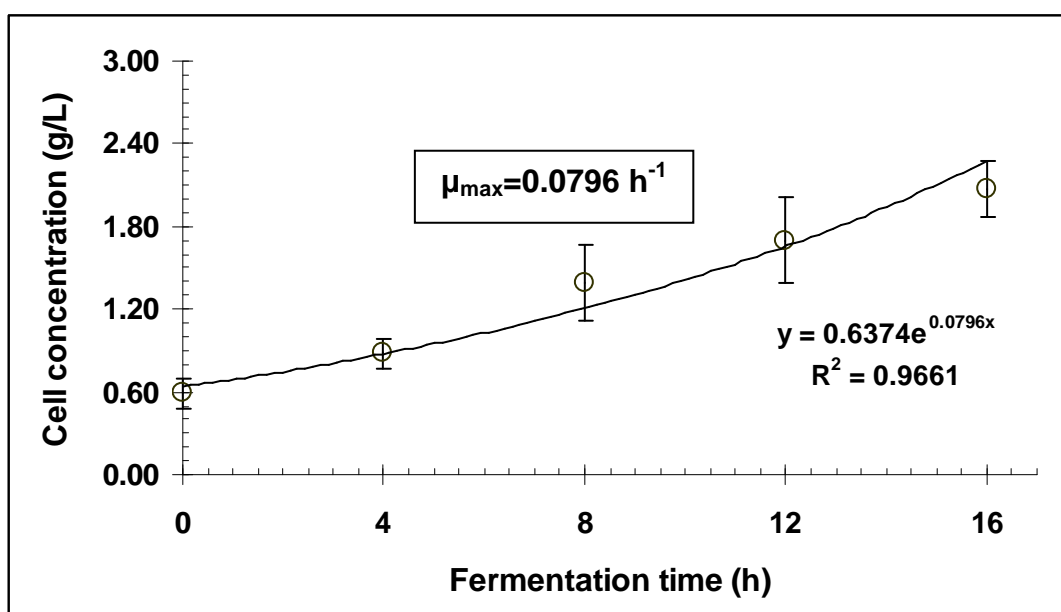


Figure 4.2 – Determination of μ_{\max} for glucose fermentation with *P. stipitis*. Error bars are ± 1 standard deviation of 3 replicates.

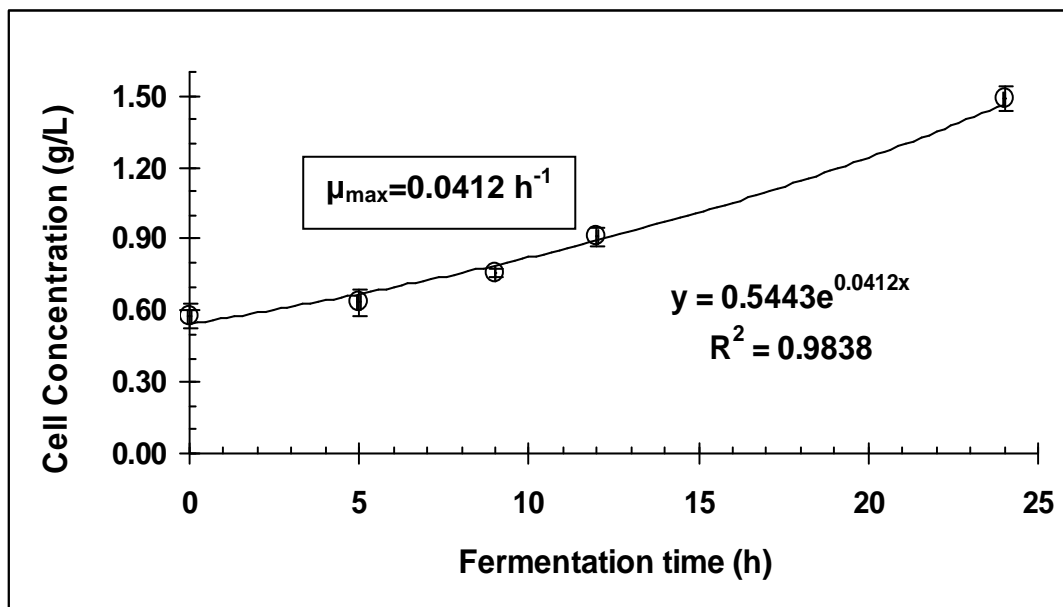


Figure 4.3 – Determination of μ_{\max} for xylose fermentation with *P. stipitis*. Error bars are ± 1 standard deviation of 3 replicates.

Figure 4.4 belongs to the system xylose – *S. cerevisiae*. As mentioned above, this one was only a control-system, and it was proven that this wild-type yeast strain did not produce measurable quantities of ethanol but showed an apparent cell growth. However, an exponential growth phase was identified suggesting the existence of this apparent growth. Indeed, this is not comparable to the growth trend found in the other three systems because by analyzing the scale of cell concentration, the present system has cell concentrations ranging between 0 and 0.5 g/L, while the other systems achieved up to 3.5 g/L of biomass. Although *S. cerevisiae* cannot metabolize xylose, it takes up this pentose through its glucose transporters even though their affinity for this sugar is very low and competition with glucose restricts xylose assimilation [6]. Likewise, this slight growth is also due to the contribution of other medium components, such as malt extract which contains more than 90% of sugars like

glucose, fructose and sucrose, and these sugars are easily metabolized by *S. cerevisiae*. Nonetheless, the malt extract proportion with respect to the main carbon source in culture medium is very low (Section 3.2.1), reason why even with the complete degradation of the sugars present in it, cell growth is not significant.

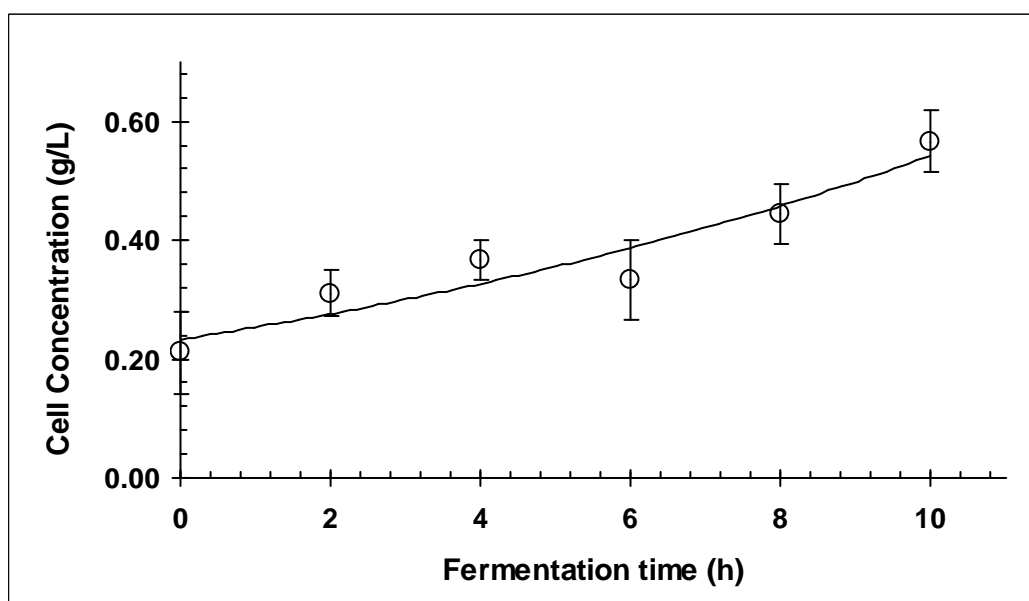


Figure 4.4 – Apparent exponential phase for xylose culture medium with *S. cerevisiae*. Error bars are ± 1 standard deviation of 3 replicates.

Along with the mathematical determination of μ , and after tabulating the complete set of cell mass, sugars and ethanol concentrations from periodically and aseptically sampling throughout the fermentation course, the experimental profiles were constructed as a function of fermentation time. The ± 1 standard deviation error bars represent the average of three replicates that were carried out in each of the single substrate fermentation experiments, showing a good run-to-run reproducibility for all the components. Figure 4.5 proves the discussed previously about the null consumption of xylose by *S. cerevisiae*, having an apparent growth as a result of the consumption of sugar available in malt extract. Some

studies have also demonstrated slight growth of *S. cerevisiae* on xylose as a sole carbon source under both aerobic and anaerobic conditions [10].

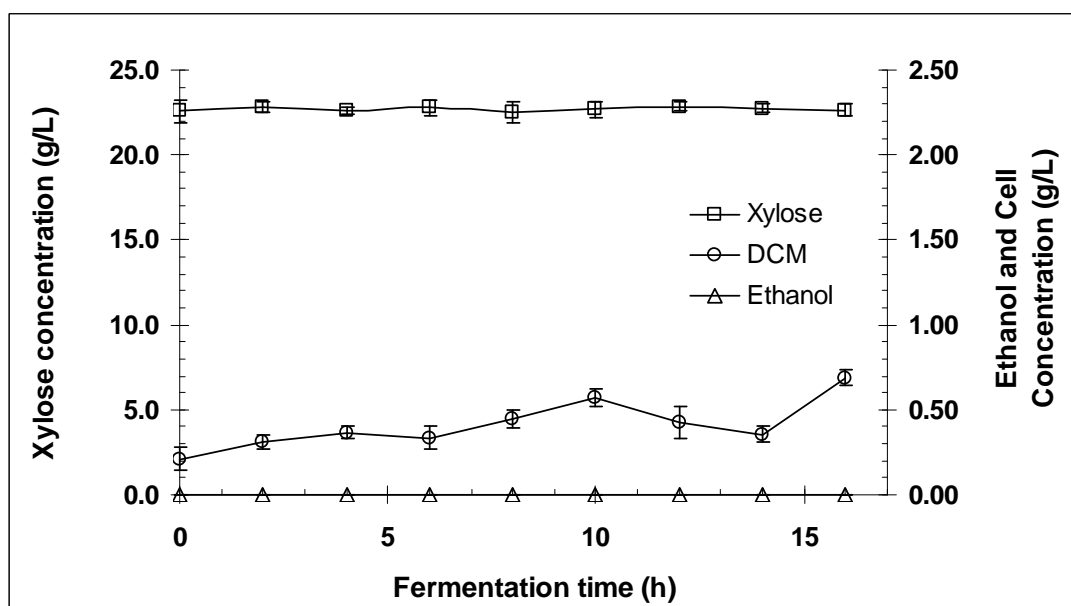


Figure 4.5 – Experimental profile concentration for xylose fermentation with *S. cerevisiae*. Error bars are ± 1 standard deviation of 3 replicates.

The existence of xylose reductase (XR) and xylose dehydrogenase (XDH) enzymes in *P. stipitis* was then tested when culturing this yeast strain with xylose, as shown in Figure 4.6. Sugar consumption started from ~ 20 g/L and it was decreasing slowly in the first 12 hours of fermentation, but from this moment on, consumption rate increased mildly, but keeping the typical slow kinetics reported for this sugar. It was able to have a measurable quantity of ethanol from the beginning of the fermentation, this is at $t=0$, because the inoculum was pre-cultured using the same carbon source, and even under aerobic conditions a small proportion of sugar was converted to ethanol. Ethanol concentration was increasing slowly, having an accumulation that was proportional to the consumption of xylose, suggesting that the relatively low protein synthesis of the xylose transporters system for *P. stipitis* preclude rapid production of ethanol from xylose in this organism [11]. The maximum ethanol concentration

achieved was 4.194 g/L, but this is not certainly the highest concentration that could be reached since xylose was not totally consumed in this experiment. Instantaneous monitoring of sugar concentration for this research work was carried out by means of an enzymatic biochemistry analyzer as described in Chapter 3, but for this experiment the improved membranes for xylose assay were not yet available, therefore after 72 hours of fermentation, and having the cell growth in apparent stationary phase, the experiment was concluded.

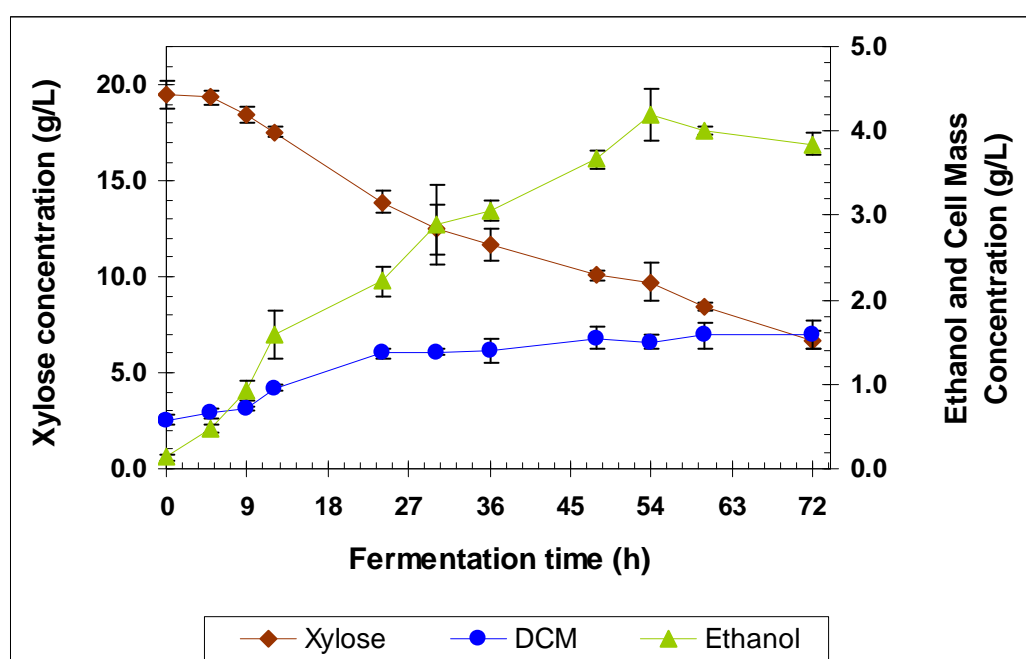


Figure 4.6 – Experimental profile concentration for xylose fermentation with *P. stipitis*. Error bars are ± 1 standard deviation of 3 replicates.

Further HPLC analysis of the samples showed a considerable xylose concentration remaining in the culture medium, having the potential to produce more ethanol even with the cells in a post-exponential phase linear growth period which has been detected by others [8,13] and this is characteristic of the kinetic control of the bioprocess residing in the transfer of oxygen within the cell suspension, since *P. stipitis* requires hypoxic conditions for better fermentative performance. Also, a characteristic of fermentation systems with xylose as the

sole carbon source, or mixtures of glucose and xylose is the uncoupling of ethanol production from cell growth that occurs towards the end of batch fermentation [13]. When the uncoupling behavior is observed the cell growth rate decreases even close to zero while the remaining carbohydrate present in solution is slowly fermented to ethanol. This uncoupled ethanol production was observed after 36 hours of fermentation because cell growth decreased virtually near to zero while ethanol kept its production rate. However, regardless the availability of sugar, ethanol yield could be determined successfully because the yield coefficient is obtained by matching the concentration of both substrate and product for each sampling time, and this coefficient is assumed to stay constant throughout the fermentation for a given initial sugar concentration. Fermentation yields will be discussed later in this chapter. The total volumetric consumption and production rates for xylose and ethanol were 0.19 g xylose/L-h and 0.07 g/L ethanol-h, respectively, being these the smallest volumetric rates for all the single substrate fermentations, but not necessarily the smallest yields because yields and productivities are not directly related since their calculation basis are different. As discussed above, xylose transport into the cell is a good indicative for these low rates, because the uptake of this sugar is rate-limiting for catabolism and at least two transport systems differing in their affinity for xylose are responsible for the sugar uptake [12].

It is important to emphasize that, according to the work developed by Busturia and Lagunas [14] xylose is presumably transported by the same system as glucose for any given type of cell, but with a 200-fold lower affinity and this results, as mentioned above, in a slower ethanol production rate. After xylose fermentation with *P. stipitis* was analyzed, the performance of this yeast strain can be compared when culturing it with glucose as the main carbon source, as shown in Figure 4.7. Fermentation started with an initial glucose concentration of 25 g/L and the exponential growth phase represented one third of the total fermentation time. Within this lapse (first 16 hours) it was observed that along with cell

growth both glucose consumption and ethanol production had a high rate, with an ethanol production of almost 50% with respect to the total ethanol accumulated in this period and a proportional percentage of glucose was consumed as well. Again, the linear post-exponential cell growth phase was observed but unlike xylose fermentation, this phase was extended all over the two thirds of total fermentation time. Even though biomass proliferation was substantially lower if compared to the exponential phase, the remaining half of total ethanol produced took place during this post-exponential phase. This observation is consistent with that reported in literature, where it is discussed that when working with microorganisms requiring low dissolved oxygen concentrations, ethanol production occurs between two different stages, and one of them does not necessarily imply an exponential cell growth [8].

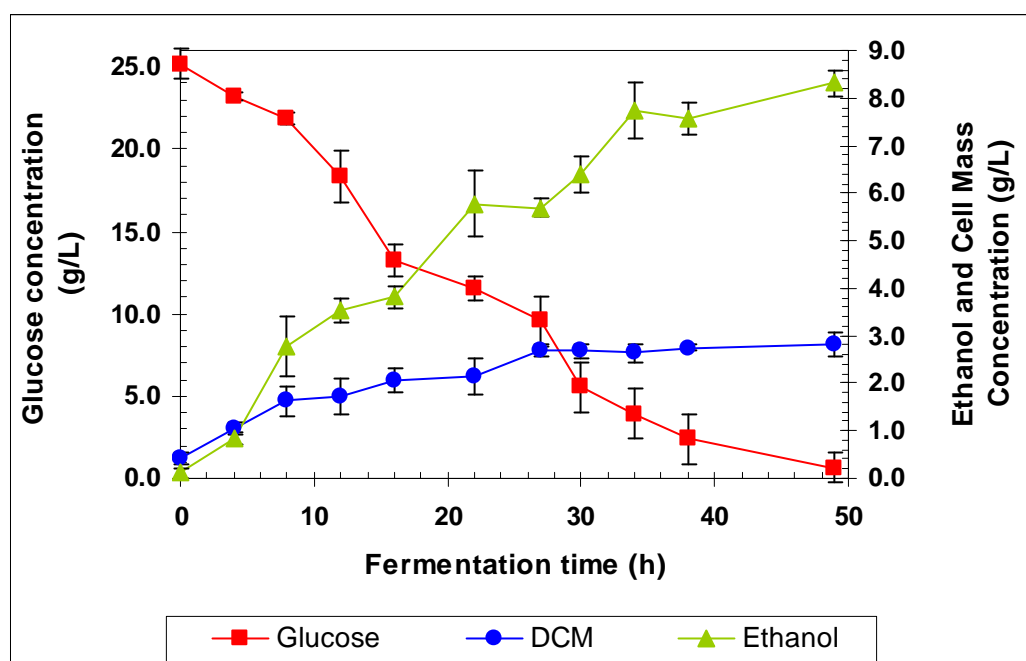


Figure 4.7 – Experimental profile concentration for glucose fermentation with *P. stipitis*. Error bars are ± 1 standard deviation of 3 replicates.

The uncoupled ethanol production during the slight post-exponential cell growth phase was observed again, showing that uncoupling is not only a characteristic of xylose

fermentation but an inherent phenomenon of the xylose-fermenting yeast strains. This phenomenon means that fewer sugars are consumed for cell growth and relatively more sugars remain available for *P. stipitis* to produce ethanol. Glucose was exhausted after 49 hours of low agitated-incubation and the highest ethanol concentration achieved was 8.314 g/L with a total ethanol production rate of 0.20 g ethanol/L-h. Since glucose consumption was more pronounced than xylose fermentation, the total substrate consumption rate was 0.63 g glucose/L-h, which is very close to the values reported in literature under similar fermentation conditions [15].

The last system to be discussed is glucose fermentation with *S. cerevisiae*. This one is probably one of the most widely studied and best understood fermentation processes, because of its well-known desirable properties. One of its advantages is, unlike *P. stipitis*, which requires small quantities of oxygen, that *S. cerevisiae* is an efficient ethanol producer under strictly anaerobic or microaerobic conditions. This makes it feasible for the co-culture scheme as described in next chapter. Besides the remarkably high growth rate attainable by this yeast at very low levels of dissolved oxygen and its efficient transformation of glucose to ethanol, it makes it so attractive for alcohol production [16]. This high growth was briefly observed in Figure 4.2 with a value for μ just smaller than those reported previously in one of the first attempts to study the oxygen requirements for *S. cerevisiae* with glucose as a carbon source for ethanol production [18]. However, the complete profile concentration is shown in Figure 4.8 where it is observed that after 7 hours of fermentation, glucose was completely exhausted, from an initial concentration of 25 g/L. This rapid glucose abatement occurred with a total substrate consumption of 3.93 g glucose/L-h, a value which is five-fold greater than those reported by previous research works [8]. The total ethanol production rate was 1.19 g/L-h, which is at the same time a large value if compared to those typically found in literature, reflecting the higher growth efficiency of this particular strain. Unlike fermentations carried

out with *P. stipitis* this system does not reveal the slight post-exponential linear cell growth observed in xylose-fermenting yeast strains, proving again that *S. cerevisiae* is able to produce ethanol efficiently under total oxygen absence or under oxygen-limited conditions.

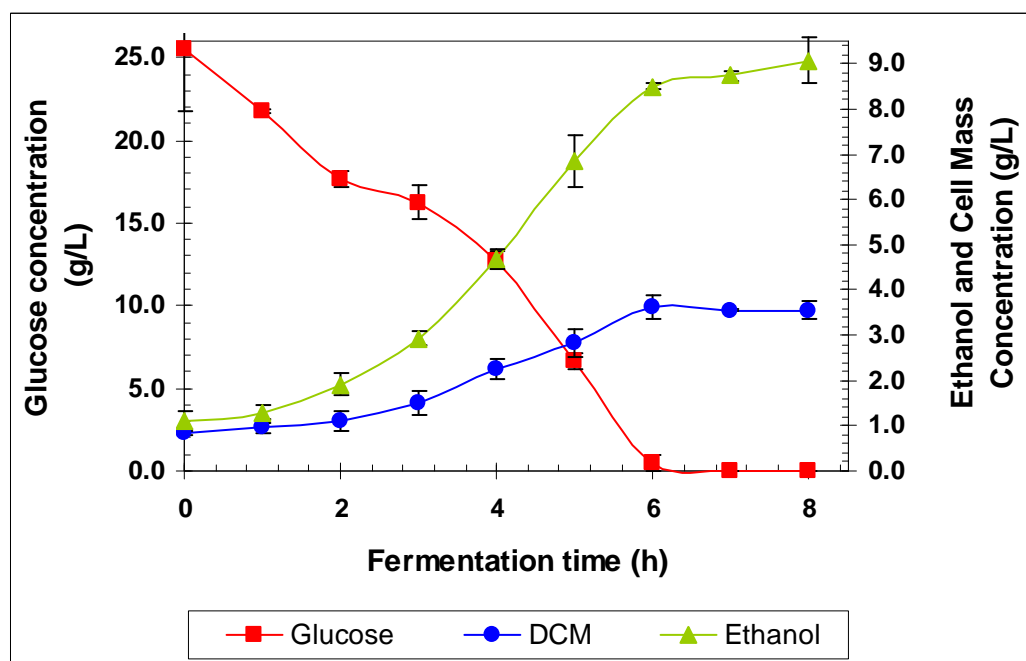


Figure 4.8 – Experimental profile concentration for glucose fermentation with *S. cerevisiae*. Error bars are ± 1 standard deviation of 3 replicates.

A graphic comparison among the total volumetric rates of substrate consumption and ethanol production of the systems analyzed before was made, as shown in Figures 4.9 and 4.10. In those figures it is also indicated the procedure followed for the calculation of the volumetric coefficients, which is based in linear regression along the fermentation time for each system, but not limited to the exponential cell growth rate. The linear regression method for the calculation of volumetric rates has been successfully used by other researchers in ethanol batch fermentations as indicative of process productivity [18, 19]. These volumetric rates denote one more time the predominant fast kinetics of glucose over xylose, and the ability efficiency of *S. cerevisiae* to utilize the carbon source to produce biomass and ethanol

over *P. stipitis*. Further in this chapter it will be demonstrated that consumption rates by themselves are not enough to describe overall efficiency in fermentation experiments, and they must be supported by yield coefficients.

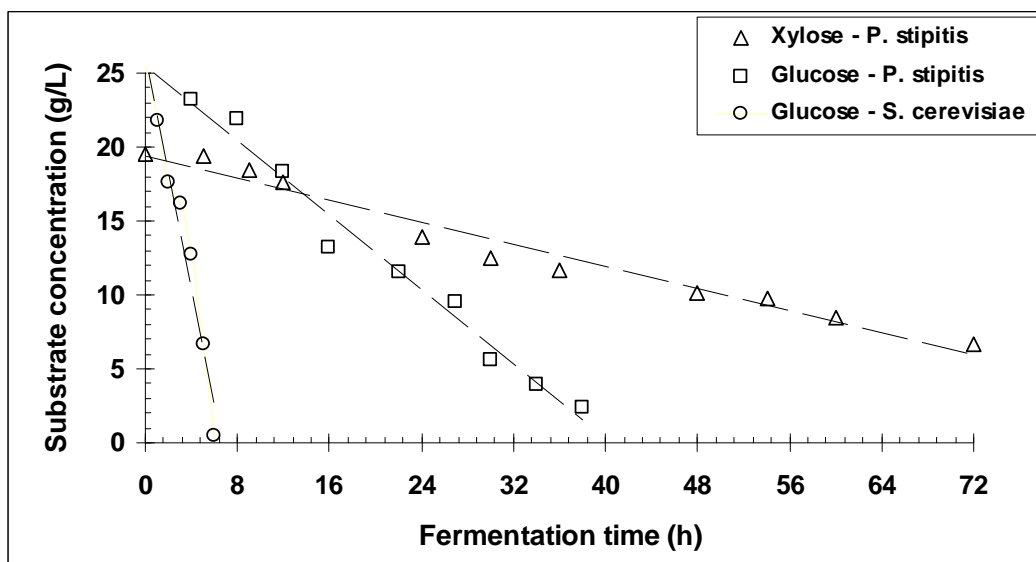


Figure 4.9 – Total substrate consumption rates for single substrate fermentations, Q_s .
Xyl - *P. stipitis*: 0.19 g/L-h; Glu - *P. stipitis*: 0.63 g/L-h; Glu - *S. cerevisiae*: 3.93 g/L-h.

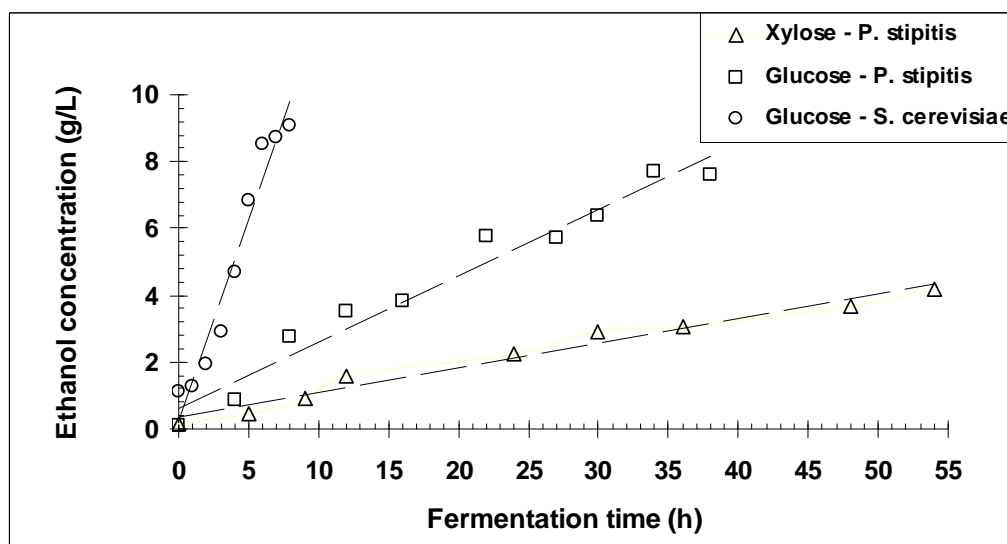


Figure 4.10 – Total ethanol production rates for single substrate fermentations, Q_p .
Xyl - *P. stipitis*: 0.07 g/L-h; Glu - *P. stipitis*: 0.20 g/L-h; Glu - *S. cerevisiae*: 1.19 g/L-h.

4.2. Fermentation yields

Yields in a fermentation process have significant implications on several aspects of processing but the most relevant issues are those concerning attainable productivity and operating costs. This is the reason why efficiency in a fermentation process is usually measured by means of yield coefficients, the ones that have their basis on the proportionality relationship existing between cells, substrates and products, i.e. the assumption that total amount of cell mass obtained by growth is proportional to the mass of substrate. This is most utilized mathematical definition of the coefficient $Y_{X/S}$ [20]. The methods used for the calculation of apparent yield coefficients were described in Chapter 3, being the result of matching concentrations of cells, substrates and products, for the same instant of time; however other methods have been successfully used for yield coefficient estimation based on stoichiometry, carbon balances and ATP mole balances with a high degree of accuracy [21].

4.2.1. Experimental yield of biomass on substrate

The yield of biomass produced with respect to substrate consumed for the three fermentation systems analyzed is shown in Figure 4.11. Fermentation runs carried out in this work were performed under hypoxic conditions, therefore $Y_{X/S}$ values are smaller than those achieved when growing cells under aerobic conditions. This difference lies in ATP yield; when working under aerobic conditions the value of ATP yield tends to be greater than 25 g cell/mol ATP (i.e. glucose with *S. cerevisiae*), as long as yields of ATP under anaerobic conditions have a value nearly constant of 10.5 ± 2 g cell/mol ATP; the higher yields of ATP the larger values in $Y_{X/S}$ [23]. Yield of *S. cerevisiae* on glucose was the highest of the three fermentations with a value of 0.1184 g cell/g glucose, representing a 97.93% of the theoretical value, which is 0.116 g cell/g glucose. This high efficiency means that sugar uptake was fast and the cell utilized the carbon source and the other nutrients for a rapid growth, being this the

reason why the exponential phase was steep and the fermentation time was noticeably shorter than those reported in literature [17, 23-24]. Again, *S. cerevisiae* proved its superiority to grow either under aerobic or anaerobic conditions. However, even a high biomass yield does not guarantee a successfully overall fermentative process, because it is important to find a balance between the cell growth and the formation of ethanol.

The system glucose – *P. stipitis* achieved a biomass yield of 0.0941 g cell/g glucose, which represents the 81.12% of the theoretical yield, being a little lower than those values found in literature [8,15,17,24]. In those research works the values of $Y_{X/S}$ are also lower when compared with the yields obtained with *S. cerevisiae*. Although biomass yield was not as high as in the previous system, it is well known that *P. stipitis* kinetics is slower because of transport issues involving sugar uptake into the cytoplasm, and the cell likely utilizes its resources more in accumulation of extracellular products than for budding, and this could increase product yields, but this product formation can even involve the accumulation of intermediate metabolites from glycolysis, reducing the yield of the main product. However, despite the attempt to achieve some HPLC peak quantification for these metabolites, no measurable quantity was determined for some possible biochemical compounds such as acetic acid, glycerol, lactic acid, and others [25].

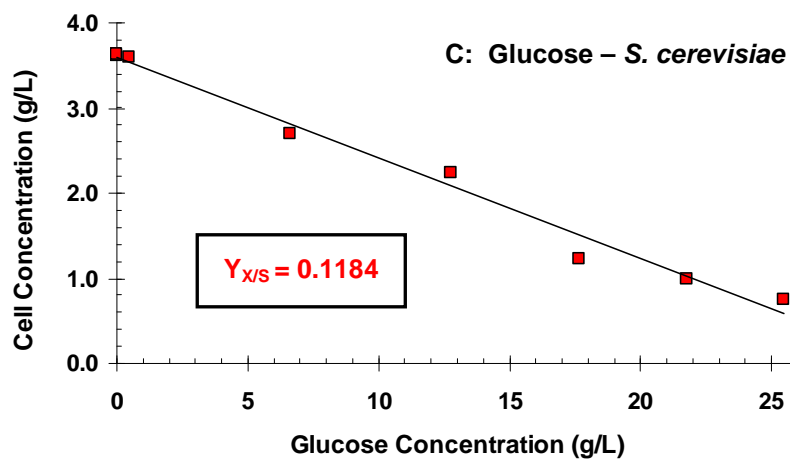
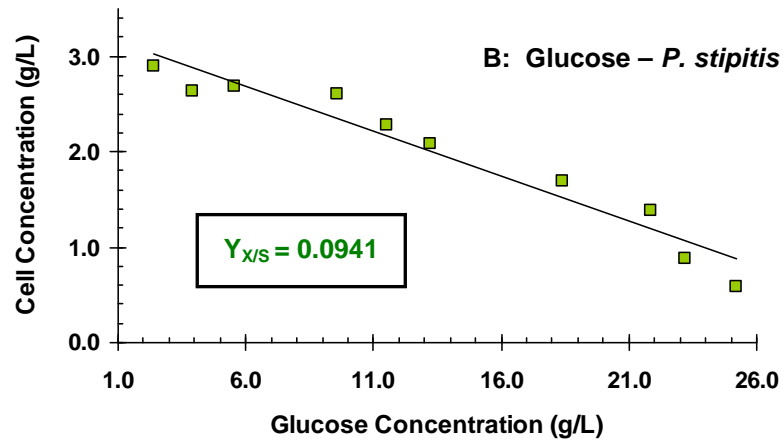
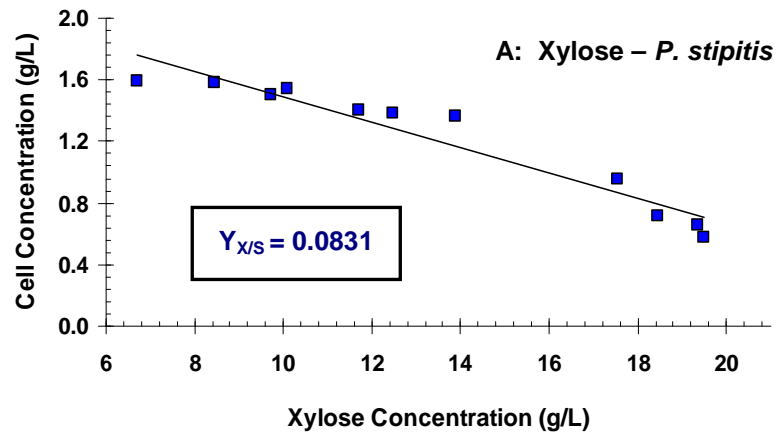


Figure 4.11 – Determination of biomass yield on substrate, $Y_{X/S}$.

The system xylose – *P. stipitis* yielded 0.0831 g cell/g xylose which is a 71.64% of the theoretical yield, showing a decrease if compared to the systems discussed above. Other authors present similar results to those obtained in this work, even there was a $Y_{X/S}$ value exceeding the 100% of the theoretical value for a different yeast strain [24]. *P. stipitis* revealed in both substrates this trend of not producing the maximum of cell growth, based on stoichiometric calculations to obtain the theoretical values of $Y_{X/S}$. Ethanol production from glucose yields 2 moles of ATP per mole of glucose, and each mole of xylose promotes the formation of ~1.67 moles of ATP [22]. As a concluding remark, it is assumed that *P. stipitis* invests its resources equitable between cell growth and the formation of extracellular products, as discussed later in the section of ethanol yield, which is supported by special features attributed to this yeast strain, and discussed by Hahn-Hägerdal and co-workers [26].

4.2.2. Experimental yield of ethanol on substrate

The amount of product accumulated from a given amount of substrate is a stoichiometric proportion which allows to know the yield in a fermentative process. Although substrates are also utilized for cellular growth as discussed in previous section through the coefficient $Y_{X/S}$, yield of extracellular product has stronger implications since it is a key factor for process economy, hence the need to achieve high values for these yields, near the theoretical ones. Since the yield coefficient, $Y_{P/S}$ for ethanol fermentation is obtained using the molar proportion between sugars and ethanol, which is 1:2 ratio for glucose and 3:5 for xylose, according to equations 2.2 and 2.3 of this document, there is a maximum achievable value for $Y_{P/S}$, which is 0.51 g ethanol/g sugar, for both glucose and xylose, being this the theoretical yield used to compare yields obtained experimentally. The vast majority of ethanol fermentations hardly reach $Y_{P/S}$ with 100% of efficiency (0.51 g/g), and the xylose-fermenting yeast strains have this condition more marked if compared to those hexose-

fermenting ones, (i.e., *S. cerevisiae*), being a challenge for all the pentose-fermenting wild-type microorganisms [16] and this is one of the main reasons supporting the use of genetically engineered microbes. However $Y_{P/S}$ does not depend only on the type of microorganism but operation conditions, such as temperature, pH, oxygen levels and initial cell concentration, therefore several studies have focused on establishing optimal operation conditions to gradually improve ethanol yield [26, 27].

Correlations used to determine $Y_{P/S}$ are shown in Figure 4.12 along with the numerical values for each system. Starting with *P. stipitis*, it was observed that ethanol yield was higher with xylose than with glucose, but the difference between both sugars is minimal. $Y_{P/S}$ with xylose as a carbon source was 0.3529 g ethanol/g xylose, this is 69.20% of the theoretical value, being pretty close to yields reported by du Preez [2] and Sánchez [8], and a little lower than the other studies [7,17,24]. Among all those previous works, the highest $Y_{P/S}$ obtained was 0.47 g/g, although higher values, near the theoretical have been reported when using recombinant strains of *S. cerevisiae* encoding genes of *P. stipitis*.

Ethanol yield with xylose – *P. stipitis* system was the highest of the three systems, although its cell yield was the lowest because of *P. stipitis* utilizes efficiently its carbon source to promote a balanced cell growth, the one that stimulates sugar degradation into ethanol production. Small amounts of xylitol were observed during the last hours of fermentation, which is completely normal since xylitol is a strong and stable intermediate in early xylose degradation, before entering the glycolysis pathway, and this has been also observed for all the xylose-fermenting yeast strains (*P. stipitis*, *C. shehatae*, *P. tannophilus*), but the amount of xylitol accumulated varied from one study to another. Xylitol production does not occur with glucose as a carbon source, since it is not an intermediate metabolite in the pathway followed by glucose to produce ethanol.

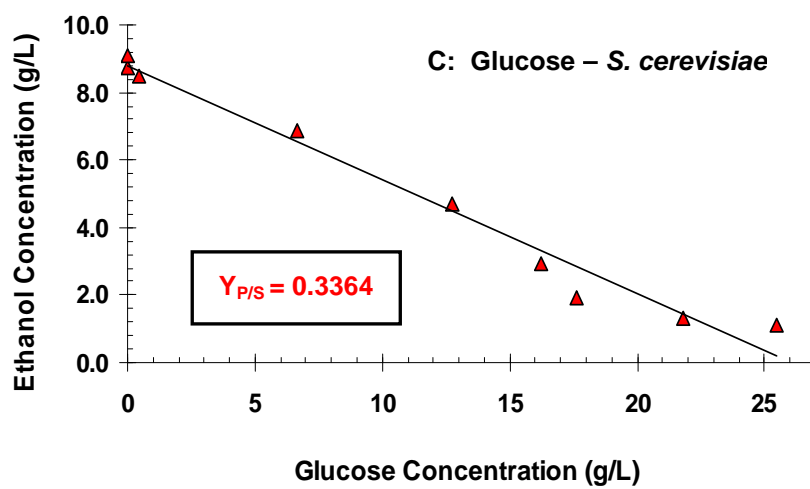
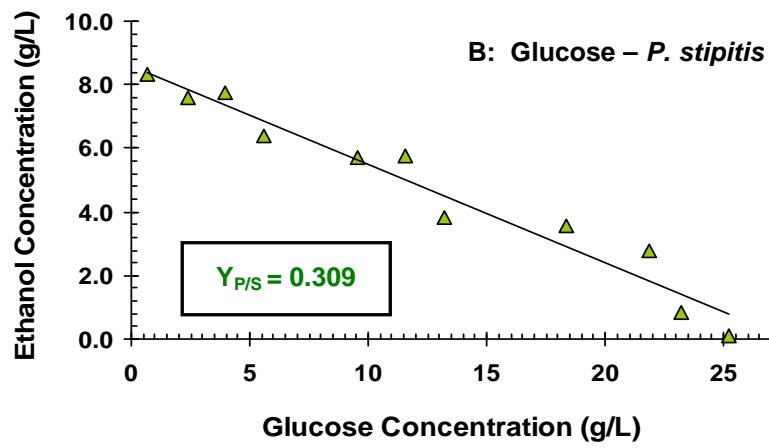
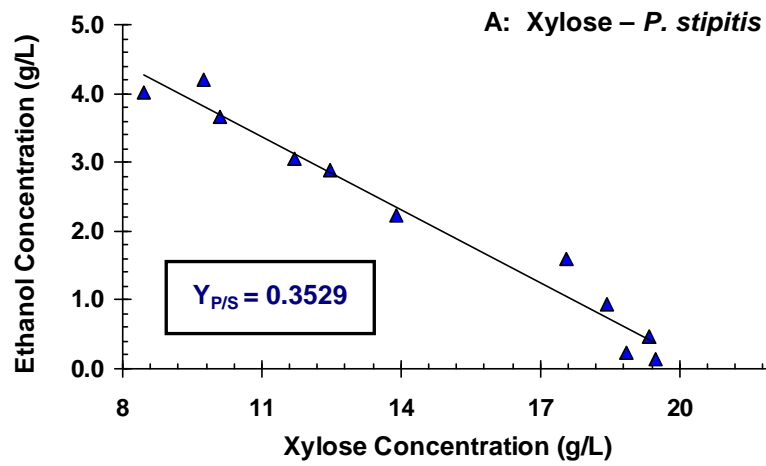


Figure 4.12 – Determination of ethanol yield on substrate, $Y_{P/S}$.

The system glucose – *P. stipitis* yielded a $Y_{P/S}$ of 0.309 g ethanol/g glucose with a 60.59% of the theoretical yield, which is lower if compared with xylose. This was observed and discussed by Lightelm and co-workers [17], for both anaerobic and hypoxic conditions, suggesting yield diminishing as an effect of ribitol accumulation, however for this work we were unable to have an adequate ribitol determination, since the HPLC column used does not detect this compound. Ribitol accumulation is not a common event in this type of fermentations, and so far the work developed by Lightelm is the only one found in literature that discusses ribitol production.

S. cerevisiae produced an $Y_{P/S} = 0.3364$ g ethanol/g glucose, similar and a little lower to those reported previously, with 65.96% of theoretical yield. Despite the high $Y_{X/S}$ for this system and the fast sugar consumption, the yield of ethanol on substrate was not that high since substrate was used more efficiently for cell growth than for ethanol production, as will be discussed in the next section, even when the final ethanol concentration was good. One alternative to improve ethanol yield would be to perform this fermentation under strictly anaerobic conditions, since it was carried out hypoxically. However, Laplace and co-workers have demonstrated that fermentative behavior was not modified with respect to the anaerobic culture, and this may be due to the fact that, as performed in this work, inoculum was pre-cultured under strong aerobic conditions and the cells may have found enough oxygen necessary for the synthesis of key compounds [23].

4.2.3. Experimental yield of ethanol on biomass

Yields discussed above can be complemented through the yield of ethanol on biomass $Y_{P/X}$ and its determination and values are shown in Figure 4.13. This parameter is interesting because it allows quantifying how much ethanol can be produced as compared to biomass that is being simultaneously produced from the substrate, explaining if substrate consumption has

been balanced or if it has favored cell growth or ethanol production. The theoretical value for this yield is 4.38 g ethanol/g cells, and the higher its value, the better ethanol production, being favored this pathway rather than cell production. This is the case of xylose – *P. stipitis*, with an $Y_{P/S} = 3.59$ g ethanol/g cells which confirms the discussion above regarding that this was the system presenting the best balance between cell and ethanol production. The system glucose – *P. stipitis* yielded 3.21 g ethanol/g cells, which is a little lower than that for xylose, suggesting once again that performance of this yeast strain is more efficient with xylose. A lower value was the one obtained for the system glucose – *S. cerevisiae* with $Y_{P/X}$ of 2.81 g ethanol/g cells, it was expected to happen this way since the value for $Y_{X/S}$ was the highest, suggesting that cell growth was favored rather than ethanol production, even when the amount of ethanol produced was significant. As an alternative, fermentation can be carried out with a higher initial cell concentration to promote less cell proliferation during exponential growth, attenuating substrate consumption for cell growth since the number of cells present in culture media at the beginning of experiment is large enough to stimulate ethanol production.

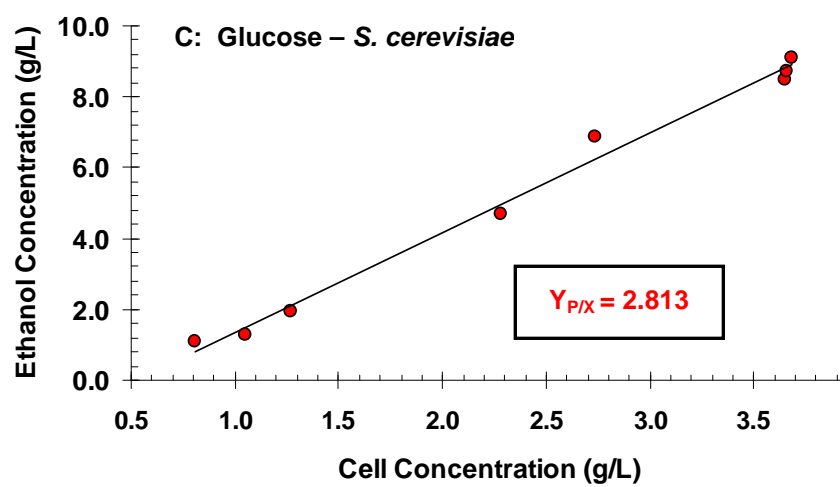
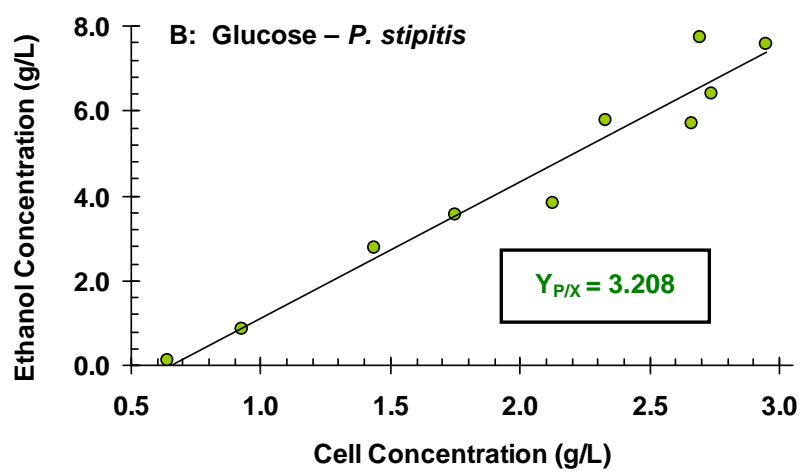
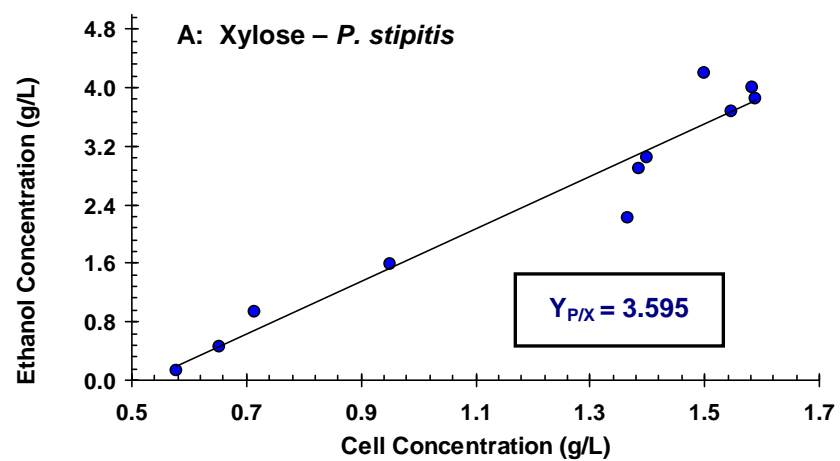


Figure 4.13 – Determination of ethanol yield on biomass, $Y_{P/X}$.

Two additional parameters supporting yield coefficients are the specific substrate consumption rate, q_s , and the specific ethanol production rate, q_p . These specific rates are useful because they relate the amounts of substrate consumed and ethanol accumulated, specifically in grams, with respect to one single gram of biomass produced. Unlike total volumetric rates discussed in section 4.1, the ones that describe the rates with respect to the fermentation time without relating the consumption or production to any other quantity, the specific rates are always related to biomass, therefore they support and help to better explain yield coefficients. Specific rates are summarized in Table 4.1, along with the apparent yield coefficients previously discussed, and Table 4.2 shows the maximum yield coefficients for each fermentation system. The maximum achievable values for the yield coefficients were obtained following the procedure suggested by Shuler and Kargi [22] and they were also compared to their apparent values. This comparison was made by means of the relative error respect of the maximum yield coefficient for each fermentation system. The values of relative error fell below 11.5% showing that the apparent yield coefficients were very close to their maximum values, which confirms the assumption of balanced cell growth for all the experiments. However, a more accurate determination of maximum yield coefficients can be achieved using experiments in a continuous culture to test the effects of energy maintenance when balanced growth does not take place for the most of the fermentation time [20].

Regarding the specific substrate consumption rates, the glucose – *S. cerevisiae* system was the system having the highest q_s , with 2.19 g glucose/g cell-h. This value was 2.5-fold the q_s for the glucose – *P. stipitis* system, and 4.5-fold for the q_s for the xylose – *P. stipitis*. For *P. stipitis*, specific consumption rates were lower and higher, respectively, to those reported by Sánchez and co-workers [8], however, that study concluded that *P. stipitis* with xylose was the fastest kinetics, which is the opposite to the present work.

Specific ethanol production rates followed the same pattern of substrate consumption. The values for q_p , as shown in Table 4.1 are high for glucose – *S. cerevisiae* with 0.73 g ethanol/g cells-h, decreasing for *P. stipitis* with glucose and xylose, with 0.302 and 0.148 g ethanol/g cells-h, respectively. Some other research works have obtained values of q_p very close to the ones obtained in the present work, such as the work of Laplace and co-workers [23] for the system xylose – *P. stipitis* and the results of Ligthelm and co-workers [17] for glucose – *P. stipitis*.

Table 4.1 – Summary of the apparent yield coefficients and specific rates.

Fermentation system	$Y_{X/S}$ (g/g)	$Y_{P/S}$ (g/g)	$Y_{P/X}$ (g/g)	q_s (g/g-h)	q_p (g/g-h)
Xylose – <i>P. stipitis</i>	0.0831	0.3529	3.5945	0.496	0.148
Glucose – <i>P. stipitis</i>	0.0941	0.3090	3.2080	0.846	0.302
Glucose – <i>S. cerevisiae</i>	0.1184	0.3364	2.8131	2.190	0.730

Table 4.2 – Maximum yield coefficients.

Fermentation System	$Y_{X/S}^M$ (g/g)	$Y_{P/S}^M$ (g/g)	$Y_{P/X}^M$ (g/g)
Xylose – <i>P. stipitis</i>	0.0809	0.3173	3.9232
Glucose – <i>P. stipitis</i>	0.1013	0.3345	3.5515
Glucose – <i>S. cerevisiae</i>	0.1131	0.3136	2.7731

4.3. Unstructured kinetic modeling

Once the kinetic information for each of the individual fermentative systems with their corresponding yields were determined, all of the required parameters are available for the construction of models describing cell growth, substrate consumption and product accumulation, based on a simple Monod model. As mentioned earlier in this chapter, the simple Monod model was used since inhibition phenomena for both substrates and product are not likely to occur in any of the fermentations carried out in this research project, because of the low initial sugar concentrations utilized and the low ethanol concentrations achieved from their corresponding substrates. All of these concentrations are therefore, out of the limits established by several studies developed in the subject of inhibition [2-5]. Using equations 2.12 – 2.14 presented in Chapter 2, and coupling the kinetic parameters and yield coefficients, differential equations were solved numerically through a fourth order Runge-Kutta method, as described in Chapter 3. The optimization criteria used was the minimization of the error generated by differences between experimental and predicted data, which is described by the objective function (Eq. 3.1), thus obtaining the best fitting and optimization of the Monod model parameters μ_{\max} and K_s . Error minimization was based on least squares associated with the maximum experimental values for biomass, sugars and ethanol achieved in the fermentation [28]. Profile concentrations are shown in Figures 4.14 – 4.16, depicting the fitting of predicted values from simulations to those obtained experimentally. Statistical validation of simulations was made taking into account three statistic parameters: Mean Squared Error (MSE), Linear Correlation Coefficient (LCC) and Residual Standard Deviation (RSD) expressed as a percentage of the average of experimental data, the ones that have been used in previous studies of kinetic modeling and parameter estimation [28, 29]. In the next figures, solid symbols were used to depict experimental data, and the entire set of simulated values is depicted by means of continuous lines. Model predicting substrate consumption for

the system xylose – *P. stipitis* is shown in Figure 4.14, displaying a slow descending ramp with an almost linear trend, fitting very well experimental data for more than half of the total fermentation time, but it deviated towards the end of the experiment, having an LCC of 0.965. For glucose fermentations, sugar consumption was noticeably a little more abrupt, and the models presented a soft curve that fits well the experimental trend of sugar consumption in these systems. Agbogbo and co-workers [29] developed a mathematical modeling for xylose with *P. stipitis* using a two-parameter method for biomass prediction, varying initial cell concentrations, and the Leudeking-Piret equation to describe substrate consumption and ethanol production, achieving a good fitting for all the simulations. However, they did not use the concept of μ to describe cell growth rate and did not use yield coefficients or optimization criteria for parameter estimation. For glucose – *P. stipitis* the model suggests that sugar should have a faster uptake, and as shown in Figure 4.15, simulation of glucose consumption was totally consumed almost ten hours before it occurred experimentally; some authors have also reported this situation for fructose with *S. cerevisiae*, using the Monod model with Moser and Luong kinetic model for μ to take into account substrate and product inhibition [30] and also for glucose fermentation with *S. cerevisiae* using the logistic model [31]. According to LCC, better substrate consumption simulations were achieved for the system glucose – *S. cerevisiae*, with 0.981 of linear correlation between simulated and experimental data. For this system the simulation model suggests that glucose should have a little lower consumption rate, but by the time at which sugar is completely exhausted it becomes identical to that observed experimentally, as shown in Figure 4.16. The percentage of RSD remained in the range [3.3% - 6.4%], a similar range has been reported in literature for glucose [28]. In bioprocess engineering, it is better to analyze RSD written as a percentage of the average of the experimental values, because the simple RSD will vary depending on the

magnitude of the variable to be predicted. Thus, the values of RSD (%) below 10% can be considered acceptable [32].

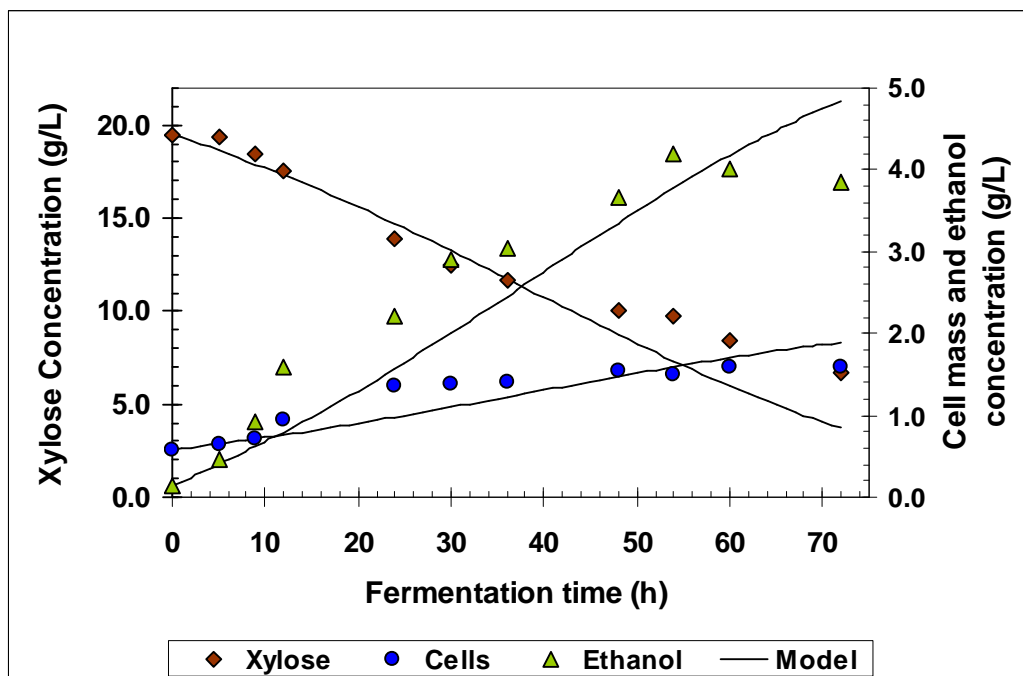


Figure 4.14 – Comparison of the experimental data and predicted kinetics using the simple Monod model in xylose fermentation with *P. stipitis*.

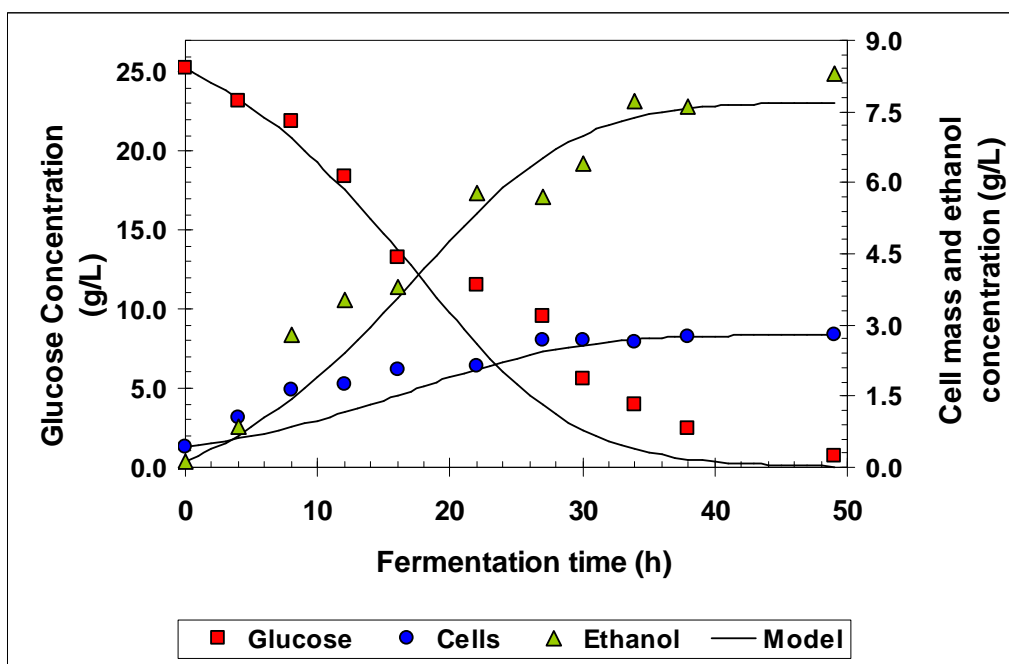


Figure 4.15 – Comparison of the experimental data and predicted kinetics using the simple Monod model in glucose fermentation with *P. stipitis*.

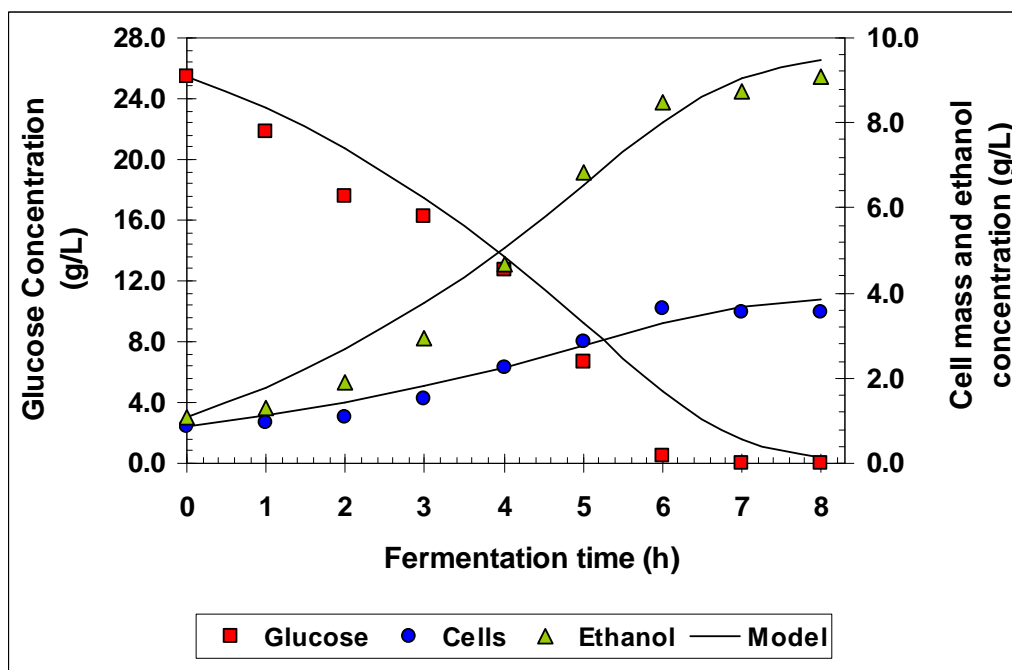


Figure 4.16 – Comparison of the experimental data and predicted kinetics using the simple Monod model in glucose fermentation with *S. cerevisiae*.

Table 4.3 – Optimized kinetic parameters used in Monod model.

Fermentation system	μ_{\max} (h ⁻¹)	K _s (g/L)
Xylose – <i>P. stipitis</i>	0.054	25.00
Glucose – <i>P. stipitis</i>	0.1766	25.00
Glucose – <i>S. cerevisiae</i>	0.3095	5.487

Regarding biomass production, the best fits were obtained in fermentation systems using glucose as a carbon source. The highest LCC, 0.9711 was achieved for the system glucose – *S. cerevisiae*, and it appears to be the higher fit for biomass, although the MSE value for xylose – *P. stipitis* was the lowest value for the three systems, with 0.038. However, making a comparison between the two values of MSE, the difference is small, and such comparison is possible since both concentrations are in the same scale. Arellano-Plaza and co-workers [29] have reported some inaccuracy in the fittings for biomass when working at high and low substrate concentrations (i.e. 30 g/L of glucose present at $t = 0$), but this situation has been attributed to the assumption that yield coefficients are constant for different initial substrate concentrations [29]. RSD percentages, in average, were lower for biomass simulations than those for substrate and ethanol, thus according to this statistical parameter, biomass was the component best fitted by an unstructured model. However, for systems using xylose as the carbon source, the model was not able to efficiently capture the exponential growth phase.

Regarding ethanol production, a good fit was obtained in the system glucose – *S. cerevisiae* with a LCC of 0.9837, which was the highest value for all the components in all the fermentation systems, unlike the case of xylose – *P. stipitis*, which had a fit that was less accurate, presenting the highest RSD of all the fermentation systems, with a value of 7.018%.

This situation can be justified since the trend followed by ethanol production in this last fermentation system did not have a constant upward pattern. Instead, it fluctuated having ups and downs throughout the fermentation time. Also, the maximum ethanol concentration achieved was not that value at the end of the fermentation as in the glucose systems, and therefore the value used in the objective function for the optimization of the differential equations system was not the last one at $t = 72$; this may have caused that model simulation for ethanol production soared upwards along the last experimental ethanol concentrations. However, the equation for the objective function requires the maximal values obtained in the experiment [32], even when that maximum value does not match the last concentration measured.

Of the three statistical parameters used to test the fitting of the models to the experimental data for the unstructured model, the one that gives more reliable and objective information is RSD expressed as percentage, because it takes into account the differences between experimental and simulated data by means of least squares analysis but also relates these square differences to the average experimental value for each component, which diminishes the effect introduced by the difference in magnitude, even when the concentrations units are the same; it is pretty different to work with biomass concentrations ranging between 0 and 4 g/L than substrate concentrations ranging between 0 and 25 g/L. Therefore, the magnitude of all concentrations is equated, being more appropriate to make a comparison among components whether if they have concentration ranges similar or different.

Table 4.4 summarizes the statistical parameters utilized to validate the sensitivity of the unstructured model to predict the behavior of the experimental concentrations. Furthermore, the consistency and agreement between predicted and experimental concentrations was successfully evaluated and validated by means of Figures A.1 – A.3 presented in Appendix A. The small biases of the matched concentrations from the 45°

diagonal line is a good indication of the consistency between the simulations and the experimental profile concentrations. Appendix B includes a graphic analysis of the residuals of the fermentation modeling, showing if the compared pairs of data (experimental and predicted) follow a statistical normal distribution. In all the cases, the normality criterion was demonstrated since the residuals seem to fit a straight line.

Table 4.4 – Statistical analysis for kinetic modeling with the simple Monod model. Units: MSE [(g/L)²]; LCC [%]; RSD [%].

Fermentation system	Statistical parameter	Cells (X)	Sugar (S)	Ethanol (P)
Xylose – <i>Pichia stipitis</i>	MSE	0.0381	2.2573	0.3263
	LCC	0.8188	0.9650	0.8982
	RSD	4.8770	3.3688	7.0184
Glucose – <i>Pichia stipitis</i>	MSE	0.1382	6.3951	0.4472
	LCC	0.9119	0.9693	0.9535
	RSD	5.4670	6.1866	4.2199
Glucose – <i>Saccharomyces cerevisiae</i>	MSE	0.0454	4.6790	0.2483
	LCC	0.9711	0.9810	0.9837
	RSD	3.1570	6.4260	3.3137

Overall, the proposed unstructured model based on simple Monod kinetics, describes satisfactorily and with a good degree of accuracy, the trend that biomass, substrates and product follow in a batch fermentation to produce ethanol, under hypoxic conditions. The relevance of optimizing the kinetic parameters, along with the determination of yield coefficients, is reflected on the utilization of all the information procured on the single

substrate experiments to construct the structured model, as will be discussed in Chapter 5. Likewise, since the results of the unstructured mathematical model describing single substrate fermentations are accurate, the model becomes a very useful tool for design and process control of fuel ethanol production and can be utilized for scale-up in this and other type of bioprocess engineering.

4.4. References cited

- [1] Govinddaswamy, S.; Vane, L.M. (2007). Kinetics of growth and ethanol production on different carbon substrates using genetically engineered xylose-fermenting yeast. *Bioresource Technology*. **98**:677-685.
- [2] Du Preez, J.C.; van Driessel, B.; Prior, B.A. (1989). Ethanol tolerance of *Pichia stipitis* and *Candida shehatae* strains in fed-batch cultures at controlled low dissolved oxygen levels. *Appl. Microb. Biotechnol.* **30**(1):53-58.
- [3] Slininger, P.J.; Branstrator, L.E.; Bothast, R.J.; Okos, M.R.; Ladisch, M.R. (2004). Growth, death, and oxygen uptake kinetics of *Pichia stipitis* on xylose. *Biotechnol. Bioeng.* **37**(10):973-980.
- [4] Thatipamala, R.; Rohani, S.; Hill, G.A. (1992). Effects of high product and substrate inhibitions on the kinetics and biomass and product yields during ethanol batch fermentation. *Biotechnol. Bioeng.* **40**:289-297.
- [5] Luong, J.H.T. (1985). Kinetics of ethanol inhibition in alcohol fermentation. *Biotechnol. Bioeng.* **27**:280-285.
- [6] Jeffries, T.W. (2006). Engineering yeasts for xylose metabolism. *Current opinion in Biotechnology*. **17**:320-326.
- [7] Hamidimotlagh, Agbogbo, Meyrial, V.; Delgenes, J.P.; Romieu, C.; Moletta, R.; Gounot, A.M. (1995). Ethanol tolerance and activity of plasma membrane ATPase in *Pichia stipitis* grown on D-xylose or on D-glucose. *Enzyme Microb. Technol.* **17**:535-540.
- [8] Sánchez, S.; Bravo, V.; Castro, E.; Moya, A.J.; Camacho, F. (2002). The fermentation of mixtures of D-glucose and D-xylose by *Candida shehatae*, *Pichia stipitis* or *Pachysolen tannophilus* to produce ethanol. *Journal of Chem. Technol. and Biotechnol.* **77**:641-648.
- [9] Kim, I.S.; Barrow, K.D.; Rogers, P.L. (2000). Kinetic and nuclear magnetic resonance studies of xylose metabolism by recombinant *Zymomonas mobilis* ZM4(pZB5). *Appl. Environm. Microb.* **66**(1):186-193.

- [10] Attfield, P.V.; Bell, P.J. (2006). Use of population genetics to derive nonrecombinant *Saccharomyces cerevisiae* strains that grow using xylose as a sole carbon source. *FEMS Yeast Res.* **6**:862-868.
- [11] Matsuchika, A.; Watanabe, S.; Kodaki, T.; Makino, K.; Sawayama, S. (2008). Bioethanol production from xylose by recombinant *Saccharomyces cerevisiae* expressing xylose reductase NADP⁺-dependent xylitol dehydrogenase, and xylulokinase. *Journal of Bioscience and Bioengineering.* **105**(3):296-299.
- [12] Does, A.L.; Bisson, L.F. (1989). Characterization of xylose uptake in yeasts *Pichia heedii* and *Pichia stipitis*. *Appl. Environ. Microb.* **55**(1):159-164.
- [13] Saez-Miranda, J.C. (2006). Kinetic, intracellular ATP growth and maintenance studies, and modeling of metabolically engineered *Zymomonas mobilis* fermenting glucose and xylose mixtures. Ph.D. thesis, University of Puerto Rico, Mayagüez Campus.
- [14] Busturia, A.; Lagunas, R. (1986). Catabolite inactivation of the glucose transport system in *Saccharomyces cerevisiae*. *J. Gen. Microbiol.* **132**:379-385.
- [15] Agbogbo, F.K.; Coward-Kelly, G.; Torry-Smith, M.; Wenger, K.S. (2006). Fermentation of glucose/xylose mixtures using *Pichia stipitis*. *Process Biochemistry.* **41**:2333-2336.
- [16] Mousdale, D.M. (2008). Biotechnology of bioethanol production from lignocellulosic feedstocks. *Biofuels: Biotechnology, Chemistry and Sustainable Development*. First Edition. CRC Press, Taylor & Francis Group. **Chapter 3**:95-142.
- [17] Ligthelm, M.E.; Prior, B.A.; du Preez, J.C. (1988). The oxygen requirements of yeasts for the fermentation of D-xylose and D-glucose to ethanol. *Appl. Microb. Biotechnol.* **28**:63-68.
- [18] Onsoy, T.; Thanonkeo, P.; Thanonkeo, S.; Yamada, M. (2007). Ethanol production from Jerusalem Artichoke by *Zymomonas mobilis* in batch fermentation. *Sci. Tech. Journal.* **7**(S1):55-60.
- [19] Görgens, J.F.; Van Zyl, W.H.; Knoetze, H. (2005). Reliability of methods for the determination of specific substrate consumption rates in batch culture. *Biochem. Eng. Journal.* **25**:109-112.
- [20] Bailey, J.E.; Ollis, D.F. (1986). Metabolic stoichiometry and energetics. *Biochemical Engineering Fundamentals*. Second Edition. McGraw-Hill, Inc. **Chapter 5**:279-300.
- [21] Slininger, P.J.; Branstrator, L.E.; Dien, B.S.; Okos, M.R.; Ladisch, M.R.; Bothast, R.J. (2006). Stoichiometry and kinetics of xylose fermentation by *Pichia stipitis*. *Annals of the New York Academy of Sciences.* **589**(Biochemical Engineering):25-40.
- [22] Shuler, M.L.; Kargi, F. (2002). Stoichiometry of microbial growth and product formation. *Bioprocess Engineering – Basic Concepts*. Second Edition. Prentice Hall. **Chapter 5**: 227-238.

- [23] Laplace, J.M.; Delgenes, J.P.; Moletta, R.; Navarro, J.M. (1991). Alcoholic fermentation of glucose and xylose by *Pichia stipitis*, *Candida shehatae*, *Saccharomyces cerevisiae* and *Zymomonas mobilis*: oxygen requirement as a key factor. *Appl. Microbiol. Biotechnol.* **36**:158-162.
- [24] Hamidimotlagh, R.; Iraj, N.; Giti, E.; Sorah, A. (2007). Mixed sugar fermentation by *Pichia stipitis*, *Saccharomyces cerevisiae*, and an isolated xylose-fermenting *Kluyveromyces marxianus* and their cocultures. *African Journal of Biotechnology.* **6**(9):1110-114.
- [25] Nelson, D.L.; Cox, M.M. (2005). Glycolysis, Gluconeogenesis, and the Pentose Phosphate Pathway. *Lehninger Principles of Biochemistry*. Fourth edition. Freeman. **Chapter 14**:521-555.
- [26] Slininger, P.J.; Bothast, R.J.; Ladisch, M.R.; Okos, M.R. (1990). Optimum pH and temperature conditions for xylose fermentation by *Pichia stipitis*. *Biotechnol. Bioeng.* **35**:727-731.
- [27] Skoog, K.; Hahn-Hägerdal, B. (1990). Effect of oxygenation on xylose fermentation by *Pichia stipitis*. *Appl. Environ. Microbiol.* **56**:3389.
- [28] Ccopa Rivera, E.; Costa, A.C.; Atala, D.I.P.; Maugeri, F.; Wolf Maciel, M.R.; Maciel Filho, R. (2006). Evaluation of optimization techniques for parameter estimation: Application to ethanol fermentation considering the effect of temperature. *Process Biochemistry.* **41**:1682-1687.
- [29] Agbogbo, F.; Coward-Kelly, G.; Torry-Smith, M.; Wenger, K.; Jeffries, T.W. (2007). The effect of initial cell concentration on xylose fermentation by *Pichia stipitis*. *Appl. Biochem. Biotechnol.* **136-140**:653-662.
- [30] Arellano-Plaza, J.; Herrera-López, E.J.; Díaz-Maldonado, D.M.; Moran, A.; Ramírez-Córdova, J.J. (2007). Unstructured kinetic model for tequila batch fermentation. *Int. Journal of Mathematics and Computers in Simulation.* **1**(1):1-6.
- [31] Wang, D.; Xu, Y.; Hu, J.; Zhao, G. (2004). Fermentation kinetics of different sugars by apple wine yeast *Saccharomyces cerevisiae*. *Journal of the Institute of Brewing.* **110**(4):340-346.
- [32] Atala, D.I.P.; Costa, A.C.; Maciel, R.; Maugeri, F. (2001). Kinetics of ethanol fermentation with high biomass concentration considering the effect of temperature. *Appl. Biochem. Biotechnol.* **91-93**(1-9):353-366.

5. MIXED SUBSTRATE FERMENTATIONS

This Chapter presents the results and analysis of the structured modeling of glucose-xylose mixtures using the suspended co-culture of the two yeast strains used separately in single substrate fermentations. The results of the experimental runs carried out to validate the simulations are also presented, along with the analysis of the specific enzyme levels for the consumption glucose and xylose.

5.1. Construction of the structured cybernetic model

The cybernetic modeling framework developed by Kompala and Ramkrishna [1] previously introduced in Chapter 2, builds upon the idea that an organism's nutritional goals are carried out entirely within the domain of chemical kinetics through judicious utilization of metabolic capabilities. The sum of all the chemical transformations taking place in a cell or organism, occurs through a series of enzyme-catalyzed reactions that constitute metabolic pathways and the cybernetic perspective of microbial growth has reported that the metabolic regulation of biochemical process can be controlled by enzyme synthesis (cybernetic variable u) and enzyme activity (cybernetic variable v).

As mentioned earlier, equations 2.17 and 2.18 are modifications to the unstructured Monod rate expressions, taking into account the cybernetic perspective which suggests including the effect of key enzymes synthesis for the metabolism of two or more different substrates. Those equations contain the subscript i which specifies the synthesis of the i th set of enzymes for the i th substrate to produce both biomass and the particular extracellular product, in this case ethanol. Since the present work requires mathematical expressions for a binary mixture of carbohydrates using a co-culture of two yeast strains, the cybernetic framework was extended not only to identify two different carbohydrates but to make a distinction between two different strains of cells (biomass) growing from each carbon source.

Therefore, since numbers are traditionally used in the nomenclature to represent the substrates, the subsequent equations contain numerical subscripts identifying: (1) glucose and (2) xylose, while alphanumeric subscripts were assigned to the yeast strains: (a) *S. cerevisiae* and (b) *P. stipitis*. Now, equations 2.17 and 2.18 with the cybernetic approach become:

$$r_{B,i,k} = \frac{\mu_{i,k} e_{i,k} [S_i] X_k}{K_{i,k} + [S_i]} \quad (5.1)$$

$$r_{E,i,k} = \frac{\alpha [S_i] X_k}{K_{i,k} + [S_i]} \quad (5.2)$$

where i represents the i th substrate (from 1 to 2), and k represents the k th yeast strain (from a to b). Subscript B represents the biomass growth rate and subscript E denotes the corresponding enzyme synthesis rate, having four mathematical expressions for each combination of substrate-strain. The experimental methodology applied to this work did not include measurements for enzymatic levels, thus the parameter $e_{i,k}$, the specific level of key enzymes, were estimated following the same criteria utilized in previous work [2], suggesting the replacement of the traditional specific growth rate expression $\mu_{i,k}$ by the following equation:

$$\mu_{i,k} = \frac{\mu_{\max,i,k} (\mu_{\max,i,k} + \beta)}{\alpha} \quad (5.3)$$

where α and β are the protein decay and the enzyme synthesis rate constants, respectively, and their values were assigned as described afterwards in this same section to bring out the influence of specific enzyme levels on the growth kinetics. Mathematical representation of

the specific enzyme level e_i is used instead $e_{i,max}$ since this value is not as important as the relative level $e_i/e_{i,max}$. Similarly, prior the discussion of the expanded equations system, it is necessary to emphasize the adaptation of the equations 2.23 and 2.24 to the cybernetic framework with two microbial species. Both equations must include now the subscript k to differentiate between the two strains. This modification yields the following equations for the cybernetic variables:

$$u_{i,k,j} = \frac{r_{i,k}}{\sum_{j,k} r_{j,k}} \quad (5.4)$$

$$v_{i,k} = \frac{r_{i,k}}{\max_{j,k}(r_{j,k})} \quad (5.5)$$

where the subscript j joined with the subscript k keeps representing the rate of any of the two substrates, but specifying the metabolism of that same substrate with one particular yeast strain (equation 5.4) or the rate of any of the substrate-strain systems having the maximum value in any given instant (equation 5.5). These equations are the heart of the cybernetic perspective, based exclusively on the matching and proportional laws, which are heuristic control policies serving as optimization surrogates for predicting the response of metabolic control circuits that modulate enzyme levels and activities [3]. The cybernetic variable u accounts for the regulatory control inputs enacted at the transcriptional and translational levels that determine the enzyme synthesis rates. High values for u suggest the induction of enzyme synthesis while low values denote its repression; if $u=0$ the polymerase does not transcribe the gene for the enzyme of E_i and if $u=1$ then obviously only E_i is induced. The cybernetic variable v represents the mechanisms of catabolite inhibition and activation controlling the

activity of the existing enzymes. If $v=1$, the enzyme is activated and reaction proceeds to metabolize the first available carbohydrate while enzyme for metabolism of the second carbohydrate is inhibited, and therefore the rate of substrate consumption of the first sugar is higher than the rate of the second; otherwise, v is close to zero suggesting that the enzyme previously inhibited is now activated.

According to equation 2.19, the formation of biomass now is represented by two different equations: one for the growth of *S. cerevisiae* (a) and the other one for the growth of *P. stipitis* (b), from both substrates: glucose (1) and xylose (2), as follows:

$$\frac{dX_a}{dt} = X_a \left[\frac{\mu_{\max,1,a} e_{1,a} [S_1] v_{1,a}}{K_{1,a} + [S_1]} + \frac{\mu_{\max,2,a} e_{2,a} [S_2] v_{2,a}}{K_{2,a} + [S_2]} \right] \quad (5.6)$$

$$\frac{dX_b}{dt} = X_b \left[\frac{\mu_{\max,1,b} e_{1,b} [S_1] v_{1,b}}{K_{1,b} + [S_1]} + \frac{\mu_{\max,2,b} e_{2,b} [S_2] v_{2,b}}{K_{2,b} + [S_2]} \right] \quad (5.7)$$

The second term of equation 5.6 can be neglected because $\mu_{\max,2,a}$ and $K_{2,a}$ are zero; there is no growth of *S. cerevisiae* due to xylose consumption, therefore this term becomes zero. In fact, all the parameters and expressions with the subscript $2,a$ can be deleted from all of the equations of this model since they belong to the sugar-strain system indicated above. Nevertheless, the subsequent equations will include those parameters for a better understanding of the effect that both substrates have in the development of the complete model.

Substrate consumption also has to be divided in two different equations to denote the utilization of each carbohydrate by each of the yeast strains. While equations describing cell growth include terms on both sides of the sum to stand for the contribution of the two

carbohydrates, the following equations also display this sum but representing the contribution of the two yeast strains:

$$\frac{dS_1}{dt} = -X_a \left[\frac{1}{Y_{X/S,1,a}} + Y_{P/X,1,a} \right] \frac{\mu_{\max,1,a} e_{1,a} [S_1] \nu_{1,a}}{K_{1,a} + [S_1]} - X_b \left[\frac{1}{Y_{X/S,1,b}} + Y_{P/X,1,b} \right] \frac{\mu_{\max,1,b} e_{1,b} [S_1] \nu_{1,b}}{K_{1,b} + [S_1]} \quad (5.8)$$

$$\frac{dS_2}{dt} = -X_a \left[\frac{1}{Y_{X/S,2,a}} + Y_{P/X,2,a} \right] \frac{\mu_{\max,2,a} e_{2,a} [S_2] \nu_{2,a}}{K_{2,a} + [S_2]} - X_b \left[\frac{1}{Y_{X/S,2,b}} + Y_{P/X,2,b} \right] \frac{\mu_{\max,2,b} e_{2,b} [S_2] \nu_{2,b}}{K_{2,b} + [S_2]} \quad (5.9)$$

Ethanol production is the result of sequential consumption of both substrates, and therefore the equation 2.21 describing the accumulation of ethanol is the sum of the two yeast strains metabolisms multiplied by their own yield coefficient, adopts the following form:

$$\begin{aligned} \frac{dP}{dt} = & X_a \left[Y_{P/X,1,a} \frac{\mu_{\max,1,a} e_{1,a} [S_1] \nu_{1,a}}{K_{1,a} + [S_1]} + Y_{P/X,2,a} \frac{\mu_{\max,2,a} e_{2,a} [S_2] \nu_{2,a}}{K_{2,a} + [S_2]} \right] + \\ & X_b \left[Y_{P/X,1,b} \frac{\mu_{\max,1,b} e_{1,b} [S_1] \nu_{1,b}}{K_{1,b} + [S_1]} + Y_{P/X,2,b} \frac{\mu_{\max,2,b} e_{2,b} [S_2] \nu_{2,b}}{K_{2,b} + [S_2]} \right] \end{aligned} \quad (5.10)$$

Enzyme synthesis mass balance described by equation 2.22 is now applied for each particular combination of substrate-strain, and since this intracellular synthesis is performed by different metabolic pathways between the two strains, four equations illustrate mathematically, the synthesis of the key enzymes necessary to initiate the complexity of steps involved in the metabolic pathways, already described in section 2.3. The equations are the following:

$$\frac{de_{1,a}}{dt} = \frac{\alpha[S_1]u_{1,a}}{K_{1,a} + [S_1]} - \beta e_{1,a} - e_{1,a} \frac{dLnX_a}{dt} \quad (5.11)$$

$$\frac{de_{2,a}}{dt} = \frac{\alpha[S_2]u_{2,a}}{K_{2,a} + [S_2]} - \beta e_{2,a} - e_{2,a} \frac{dLnX_a}{dt} \quad (5.12)$$

$$\frac{de_{1,b}}{dt} = \frac{\alpha[S_1]u_{1,b}}{K_{1,b} + [S_1]} - \beta e_{1,b} - e_{1,b} \frac{dLnX_b}{dt} \quad (5.13)$$

$$\frac{de_{2,b}}{dt} = \frac{\alpha[S_2]u_{2,b}}{K_{2,b} + [S_2]} - \beta e_{2,b} - e_{2,b} \frac{dLnX_b}{dt} \quad (5.14)$$

The values for the enzyme synthesis rate constant α is a numeric estimation for the maximum specific level of a single enzyme, which in average, is of the order of 10^{-3} g enzyme/g cell, and that value can be fixed for an average enzyme E_i . The first-order degenerative loss of the active enzyme E_i is described by the constant β , which value has been fixed at 0.05 h^{-1} for all enzymes E_i 's, and it was estimated from studies made on protein decay, showing a slow rate and reaching its maximum rate of 5%/h under non-growth conditions. The values for these two parameters were assumed to be the same for all key enzymes in the present work, and the same values have been successfully used in other simulations found in the literature [2, 4-5].

Equations 5.6 – 5.14 are therefore the final expressions of the complete cybernetic model developed for this work, including the kinetic parameters and yield coefficients determined in single substrate experiments as discussed in Chapter 4. Solving this complex non-linear ordinary differential system, including the criterion of resources optimization denoted by cybernetic variable v simultaneously for each yeast strain, was possible using the

same 4th order Runge-Kutta method included in the MATLAB command ODE45. The model was first constructed for each of the yeast strains, in efforts to model single substrate-single strain fermentations and to compare the unstructured Monod model with the structured cybernetic perspective. Also, mathematical projections were made for sugar mixtures with a single yeast strain, attempting to analyze the individual performance of *S. cerevisiae* and *P. stipitis* in a mixed substrate environment. However, these simulations, presented in the next section, are just a complementary vision of the modeling work to evaluate the behavior of these co-fermentation systems but no statistical comparison or validation was possible since experiments for these schemes were not part of the specific objectives and therefore were not included in the methodology of this work.

Additional approaches have been proposed and used in other studies to optimize the mathematical description of the cellular metabolism such as the precursor perspective developed by the same authors of the cybernetic framework, which involves the formation of biosynthetic constituents of a lumped precursor pool along with the production of energy in the form of reduced pyridine nucleotides (e.g. NADH and ATP) [6].

5.2. Simulation of glucose-xylose mixtures using one single yeast strain

Fermentation of mixtures of glucose-xylose to produce ethanol using one single microbial strain have been lately studied using either wild-type or genetically engineered strains in order to improve the efficiency of the fermentative process and ethanol yield, as well. The approach of the majority of these studies focuses on kinetic parameter estimation and yields determination, but other authors have also worked with both unstructured and structured mathematical models. However, very few attempts have been made using the cybernetic perspective, as discussed later in this section. Cybernetic modeling applied to systems comprising only one substrate is not that relevant in the sense that cellular resources

optimization to synthesize more than one carbon source does not occur, but it is important to demonstrate some theoretical aspects between unstructured and structured models. For instance, the equation of maximum specific growth rate for the single substrate present in culture media also involves the maximum specific enzyme level because during balanced growth the specific enzyme level remains at its maximum value. For that reason, cybernetic model in this case reduces to the simple Monod model, as described in the next figures where the single substrate fermentations from Chapter 4 are analyzed again to make a comparison with respect to the experimental data, but this time contrasting both the Monod and cybernetic model. After this comparison, simulations of glucose-xylose mixtures are analyzed prior the discussion of co-fermentations that were carried out with a co-culture of yeast strains. Equations 5.5 – 5.14 were used but taking only the terms of each equation (or the entire equation) corresponding to any given strain (e.g., half the equations comprising the subscripts a for *S. cerevisiae*) and using only one equation for microbial growth.

Figure 5.1 shows the comparison explained above, with dotted lines representing the Monod model and solid lines representing the cybernetic model. It is evident that both mathematical projections overlap, proving actually that the equations of the cybernetic perspective are reduced to the Monod model equations for single substrate systems, the ones that are identified as: glucose – *S. cerevisiae* (A), glucose – *P. stipitis* (B) and xylose – *P. stipitis* (C). When the cybernetic model reduces to the simple Monod model, the value for the cybernetic variable v is 1 throughout the whole fermentation time, and this occurs because the predominant rate is that existing for the only substrate that is being metabolized. Using this same analysis for the cybernetic variable u , we can easily determine that its value is also one. Mathematically, the main difference between the two models is the contribution of e , but for these single substrate systems it has no effect the specific level of the key enzymes responsible for substrate degradation are all the time at their maximum value.

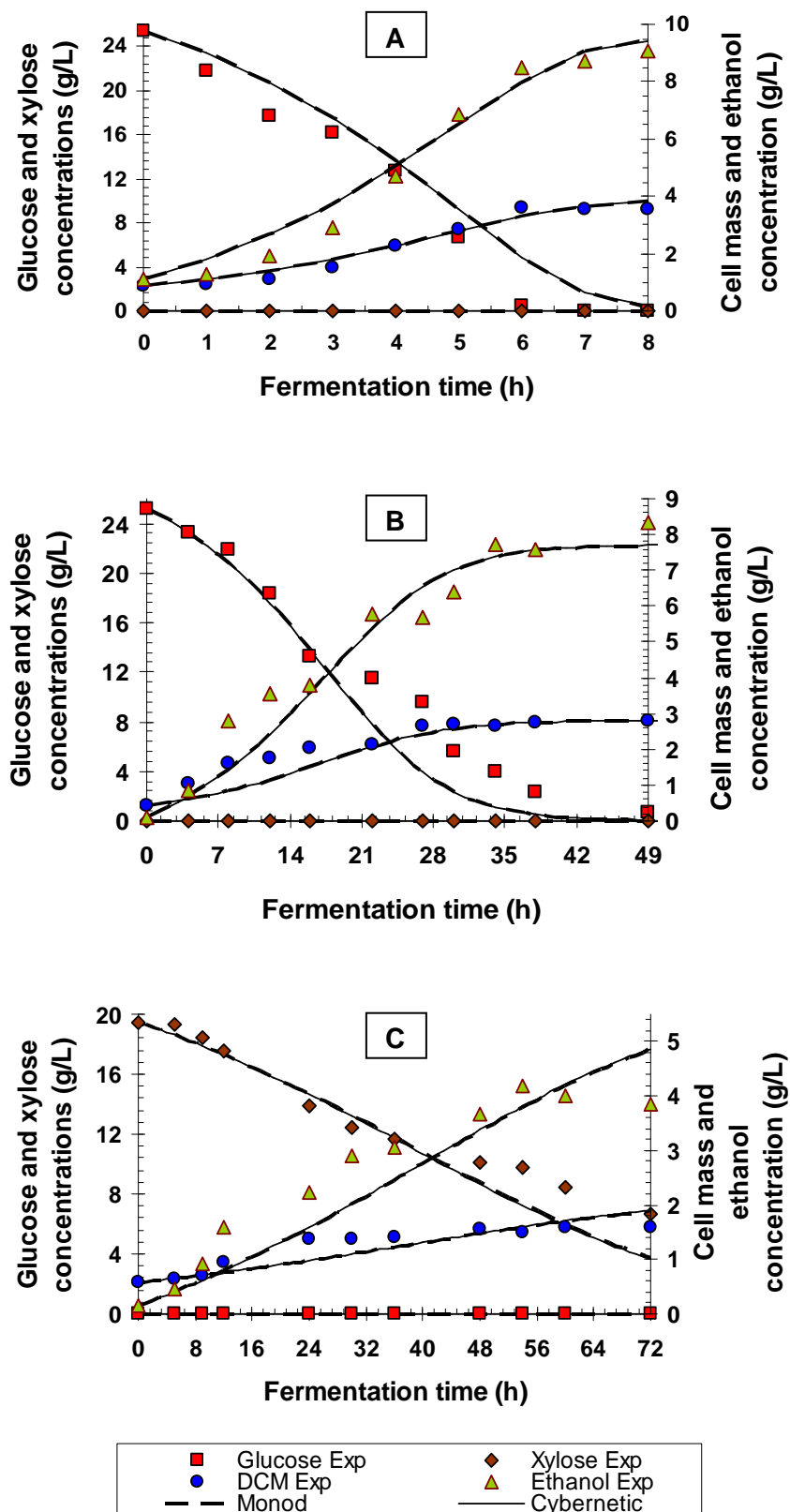


Figure 5.1 – Comparison of the Monod model to the cybernetic perspective for single substrate fermentations. A: Glucose – *S. cerevisiae*; B: Glucose – *P. stipitis*; C: Xylose – *P. stipitis*.

As mentioned before, the model developed now is applied to simulate mixtures of glucose-xylose separately for each yeast strain, as shown in Figure 5.2. The percentages of glucose/xylose utilized are 75/25 (mixture A), 50/50 (mixture B) and 25/75 (mixture C) g/L, in a basis of 25 g/L of total sugar concentration initially present in the culture media. These simulations have been made as an introduction to the analysis of utilization of two substrates, including graphic representations of specific enzyme levels e , necessary for the well understanding of the cybernetic perspective, and using information provided in previous studies where monoculture was utilized (mainly *P. stipitis*) to relate those experimental results to the ones obtained by simulation in this work.

Beginning with the mixtures using *S. cerevisiae* as the sole fermenting yeast strain, Figure 5.2 shows the simulation for mixtures A, B and C, with cellular and ethanol initial concentrations of 0.85 and 0.50 g/L, respectively; those values are an average of the ones that were used as initial conditions in single substrate fermentations, varying only the initial proportions of carbohydrates. For the three mixtures, xylose concentration remained virtually unchanged throughout the total fermentation time, having a very slight consumption of approximately 0.25 g/L in average for the three analyzed systems, which has been also reported in literature [7]. As discussed earlier in this document, although *S. cerevisiae* naturally does harbor genes for xylose utilization, these are expressed at such low levels that they do not support growth on xylose, therefore at least a very small amount of this carbohydrate is utilized by cells attempting to metabolize it but without success because they are not able to put it into the metabolic pathway to produce ethanol [8]. Glucose consumption occurs similarly to the system when xylose is not present, and its exhaustion depends on the initial proportion of glucose; the higher the proportion of sugar the faster the glucose exhaustion, showing a steep reduction because there is more biomass growing and hence the sugar transports rapidly across the cell membrane.

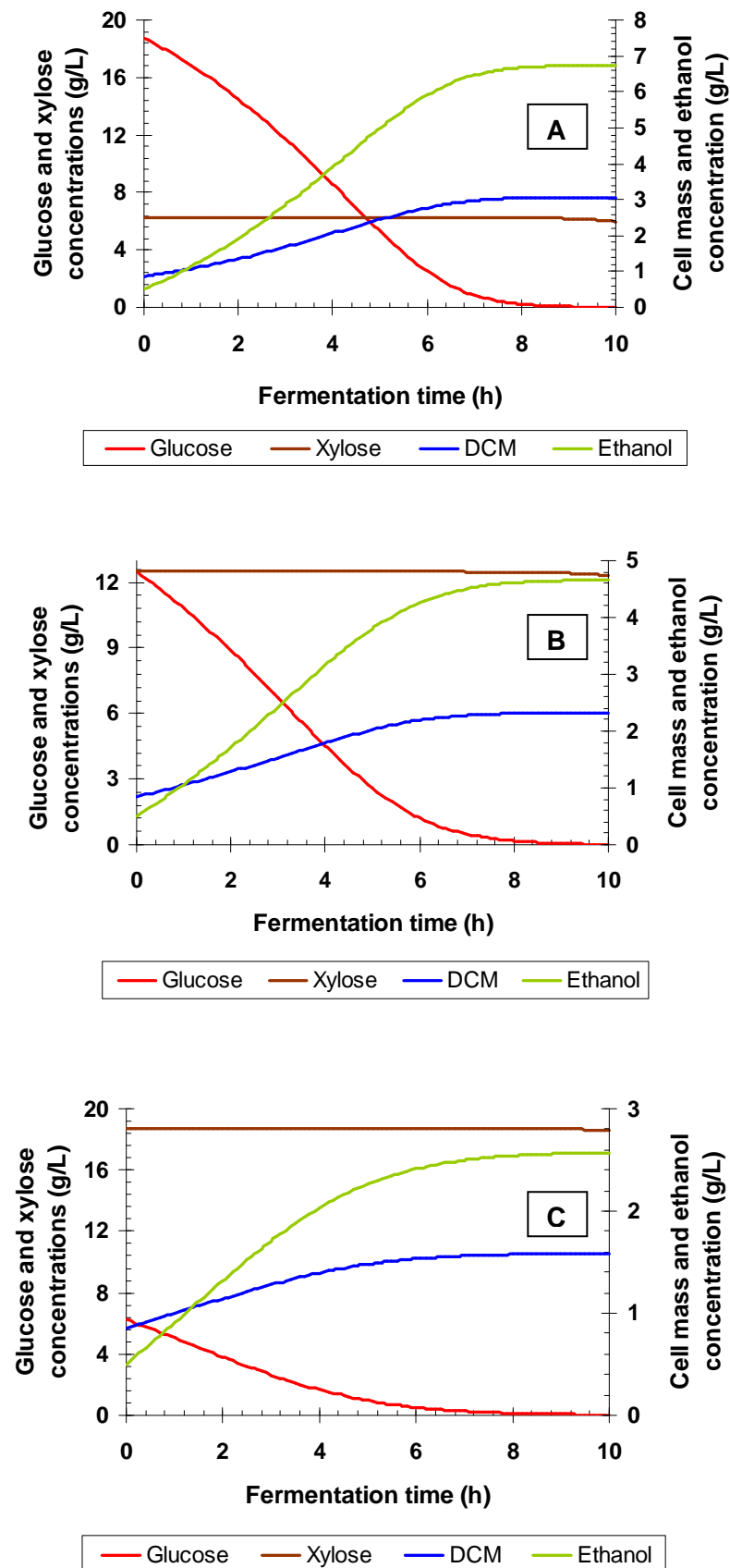


Figure 5.2 – Simulations of glucose-xylose fermentation mixtures with *S. cerevisiae*. A: 75% Glu – 25% Xyl; B: 50% Glu – 50% Xyl; C: 25% Glu – 75% Xyl.

Since glucose is the only carbon source utilized by *S. cerevisiae* in this fermentative system, it is expected that both cell growth and ethanol production will be less efficient in mixtures with low glucose fractions, if compared to other systems where both substrates are consumed. These simulations were then useful to prove that the cybernetic model is able to predict the null xylose metabolism by *S. cerevisiae*, no matter how high or low is the concentration of this sugar in the mixture. Besides, glucose consumption is not affected by the presence of xylose, but when the xylose proportion is very high then the system resembles a pure xylose fermentation, which does not make any sense when using a wild-type strain of *S. cerevisiae*. Moreover, the existence of fermentation systems in bioethanol production where xylose concentration is very high when compared to glucose concentration in the same culture broth is not the usual, since the majority of hydrolyzed fractions from pre-treated lignocellulosic biomass have higher or equal proportion of glucose, nevertheless this depends on the type of feedstock [9].

Figure 5.3 shows the evolution of the specific levels of key enzymes for substrate degradation, glucose in this case. Since inocula for the three mixtures were pre-cultured in pure glucose, the initial value for e for glucose consumption is assumed to be approximately 90% of the maximum specific enzyme level [2], while 0% was assumed for e in xylose because, despite the existence of genes for xylose metabolism in *S. cerevisiae*, the cells did not have even minimum levels for xylose degradation since inoculum was cultured using pure glucose. Therefore, the change in specific level of enzyme for glucose (e_1) displays a slow increase, reaching its maximum value towards the fourth hour of fermentation, and this proves the assumption made for the initial value. In the other hand, the values for specific levels of enzyme for xylose (e_2) remained virtually close to zero. It was expected that while the glucose proportion decreases, its enzyme level decreases because the cell spends less resources in synthesizing that particular enzyme if availability of sugar is poor.

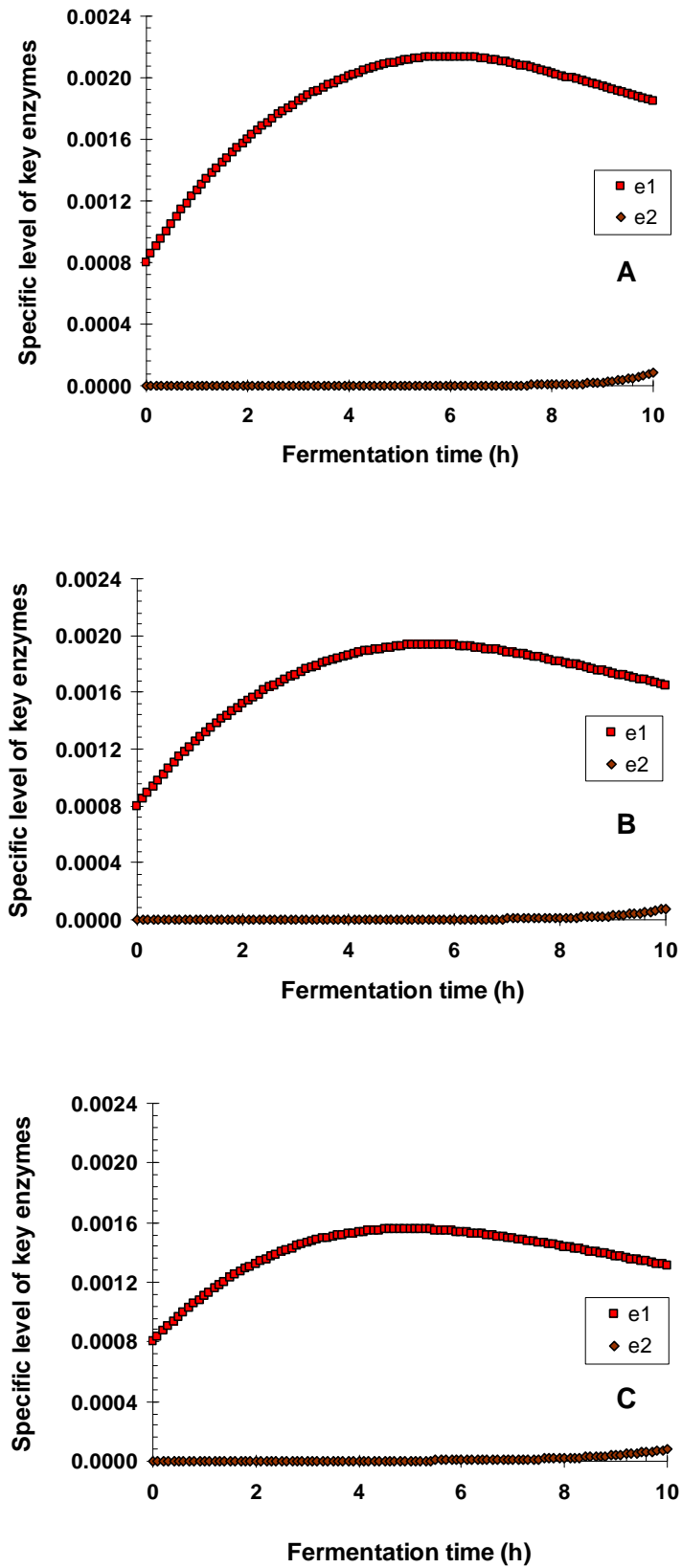


Figure 5.3 – Simulation of enzyme levels in glucose-xylose fermentation with *S. cerevisiae*.
A: 75% Glu – 25% Xyl; B: 50% Glu – 50% Xyl; C: 25% Glu – 75% Xyl.

The performance of *P. stipitis* was also evaluated creating simulations for the same mixtures used in the *S. cerevisiae* simulations. The predictions suggest sequential carbohydrate consumption for all of the mixtures but having this effect noticeably in mixtures A and B; glucose was first consumed while xylose concentration remained virtually constant or decreased slightly until glucose concentration was low enough to allow faster xylose consumption. Simulations are shown in Figure 5.4 and the initial values for cell and ethanol concentrations were the same for the three mixtures, with 0.4 and 0.1 g/L, respectively, but in practice these values can be different depending on the history of the inoculum which can be cultured either on pure glucose, pure xylose, or a mixture of both sugars. For the present simulation it was assumed that the *P. stipitis* inoculum was grown on pure xylose, but sometimes working with inocula grown on mixtures of each sugar helps to standardize all the possible results that can be achieved through experimental work [10].

Simulations indicate that glucose consumption should be faster for those mixtures with high glucose fractions, because it is the preferred substrate for *P. stipitis*, but when glucose concentration is low cells experiment a decrease in their growth due to the limited glucose present and they start to consume xylose, especially when inoculum has been grown on pure xylose or a mixture of glucose xylose; when this occurs the small fraction of available glucose is consumed slowly. This is the reason why xylose consumption for mixture C begins even when glucose is not completely exhausted, and similar observations have been reported in the literature [11], with inocula also grown in pure xylose. These studies have also reported that, the high xylose fractions have had also a slightly higher ethanol yield. Of course this also depends on the yeast strain utilized because some of these strains, like *Pichia stipitis* CBS 5773, display less ability to synthesize the inducible enzyme necessary for degrading xylose, which is the result of the strong catabolite repression caused by glucose [12].

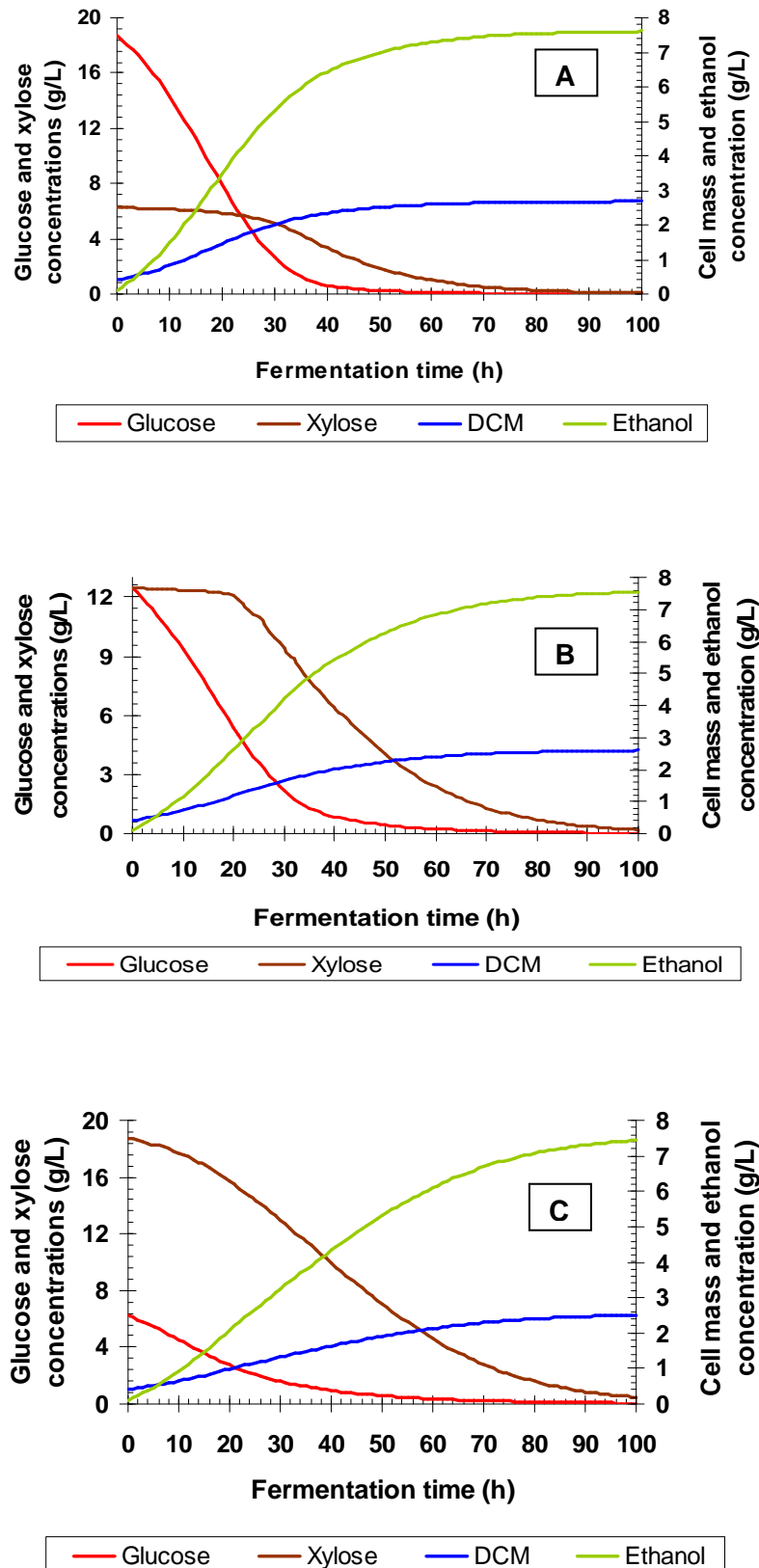


Figure 5.4 – Simulations of glucose-xylose fermentation mixtures with *P. stipitis*. A: 75% Glu – 25% Xyl; B: 50% Glu – 50% Xyl; C: 25% Glu – 75% Xyl.

Despite *P. stipitis* yield on xylose is slightly lower than that on glucose, for the previous simulations it was assumed that inoculum has been grown on pure xylose because this allows the xylose degrading enzymes to achieve levels at the beginning of fermentation, and although at this time, enzymatic synthesis is fully repressed by the presence of the preferred substrate, when glucose is almost completely exhausted the polymerase will not spend much time transcribing again the gene for xylose degrading enzymes, and hence enzyme activation will be much faster if compared to the scenario when enzymes are not originally present in the cell (i.e. when inoculum has been grown on pure glucose). Additionally, when growing inoculum in the less preferred substrate a marked reduction in the intermediate lag phase (diauxic lag) is achieved, and this is a desirable situation for time optimization in fermentation processes [2].

Figure 5.5 shows the evolution of the specific enzyme levels for glucose (e_1) and xylose (e_2) consumption in simulations previously described, for the same mixtures A, B and C. The initial values for e_1 and e_2 were chosen following the analysis of specific and relative enzyme levels found in literature [2] being 3×10^{-4} and 6×10^{-4} , respectively. Since inoculum was cultured on xylose, the initial levels of enzymes for xylose degradation are higher than that for glucose, but when working high glucose fractions (mixture A) e_2 is strongly repressed and it tends to decrease while glucose is being consumed because already existing enzymes are inhibited; activation occurs after e_1 has reached its maximum value. Unlike mixture A, the other mixtures show a faster e_2 activation even before e_1 is decreasing for mixture B and even high values before e_1 reaches its maximum value for mixture C; this last situation causes that xylose consumption occurs before glucose concentration drops to zero, which has been reported by Agbogbo and co-workers for the same mixture but with a little lower xylose consumption rate [13] and also for the same mixtures using *Zymomonas mobilis* [10].

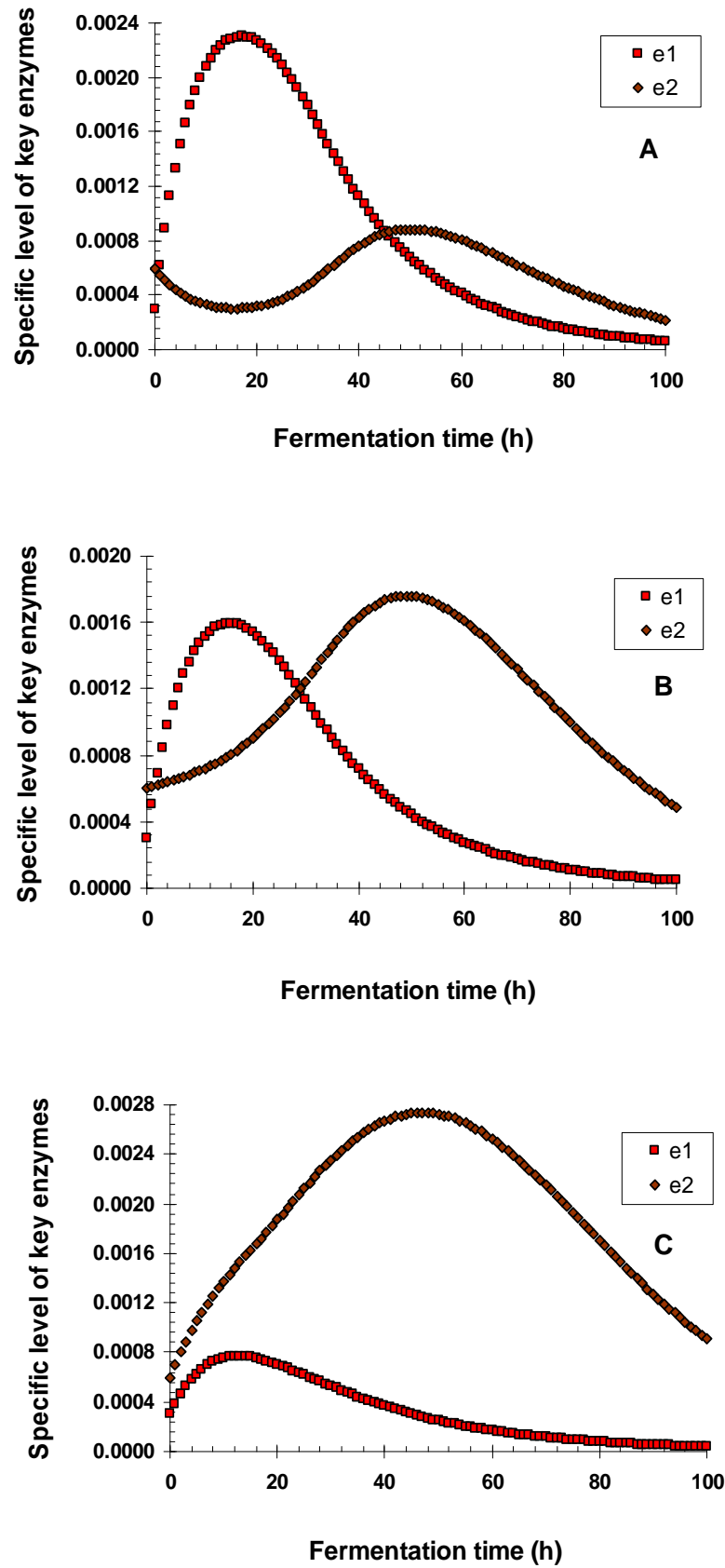


Figure 5.5 – Simulation of enzyme levels in glucose-xylose fermentation with *P. stipitis*. A: 75% Glu – 25% Xyl; B: 50% Glu – 50% Xyl; C: 25% Glu – 75% Xyl.

5.3. Experimental profiles and fermentation yields

The same mixtures considered previously for simulations of glucose and xylose using a single yeast strain were carried out experimentally to study the performance of *S. cerevisiae* and *P. stipitis* co-cultured for ethanol production, then the same nomenclature is kept (A, B and C) and will be also utilized to make reference to each mixture from now on. Using the observations made in single substrate fermentations, there was a modification in the procedure for the cultivation of inoculum, to achieve a high cell concentration, as described in Chapter 3. Each yeast strain was grown in its respective high-performance carbohydrate (i.e. *S. cerevisiae* on glucose and *P. stipitis* on xylose) to promote the induction of necessary enzymes for the degradation of both sugars in each strain, and thus reducing or eliminating the intermediate lag phase, as it was first made in fermentation of glucose-xylose mixtures with *Klesbiella oxytoca* [2].

Figure 5.6 shows the evolution of cell growth for each mixture, the ones that display clearly the distinction of two phases: the first one is the growth under glucose, which took place rapidly in the first then hours of fermentation, and the second one is the growth phase under xylose, which was prolonged towards the end of fermentation time. Glucose consumption occurred mainly under the action of *S. cerevisiae*, because although the proportion of cell concentrations from each strain in the inocula was fairly similar, kinetics of *P. stipitis* on glucose is markedly low as a result of the reduced affinity for the transport of this carbohydrate into the cytoplasm when compared to *S. cerevisiae* [14]. Therefore, after the promoter was activated with the exhaustion of glucose, the inducible enzyme was produced, causing the degradation of xylose by *P. stipitis*, less rapidly and with smaller proportion than on the glucose growth phase.

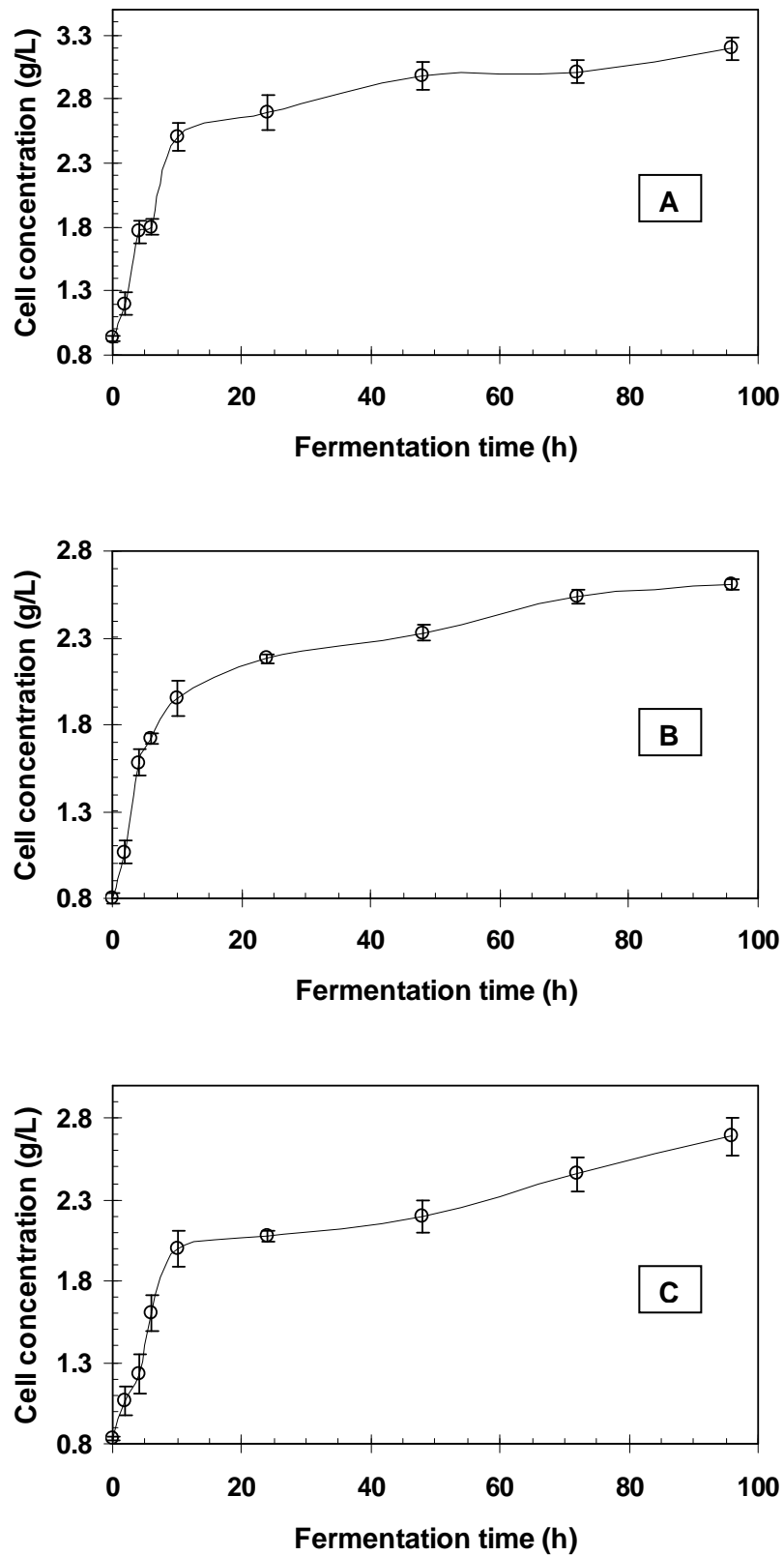


Figure 5.6 – Cell growth curves for glucose-xylose mixtures with yeast co-culture. A: 75% Glu – 25% Xyl; B: 50% Glu – 50% Xyl; C: 25% Glu – 75% Xyl. Error bars are ± 1 standard deviation of 3 replicates.

Mixture A was the only one that displayed clearly a short intermediate lag phase between the fourth and sixth hours of fermentation. The high glucose proportion caused a stronger xylose repression, promoting a cell growth cessation while enzymes for xylose degradation are synthesized, therefore transition from glucose to xylose consumption was able to be observed unlike mixtures B and C; the first one had an almost imperceptible intermediate lag phase, and the last one did not exhibit this phase. Similar results were found in literature for glucose-xylose mixtures with proportions 67% – 33%, respectively [12]. In general, between 50 and 65% of total cell production was obtained by glucose degradation, even in mixture C that had only 5.3 g/L of glucose initially present.

Cell growth inhibition in suspended co-cultures by any of the microbial strains is one limiting step in the development of efficient choices for mixed cultures, especially between *S. cerevisiae* and xylose-fermenting yeast strains. However, the work developed by Laplace and co-workers [15] supports the use of these two particular yeast strains, since their compatibility was tested using a special technique involving mitochondrial inhibitors, in which no growth inhibition occurred from *S. cerevisiae* to *P. stipitis* and vice versa. Accordingly, no growth inhibition phenomena were observed between the two yeast strains utilized in the co-culture process for this work. The relationship existing between them is neutralism since there was no appreciable change in growth rate of any of them, and the pure-culture behavior of both species was very close to their behavior in mixed culture, with high growth rates for *S. cerevisiae* and a low growth rates for *P. stipitis*, but showing an excellent compatibility and performance for ethanol production, as discussed later on this section.

Experimental profiles are now analyzed for the three mixtures, showing the monitored concentrations of total cell mass, glucose, xylose and ethanol throughout 100 hours of hypoxic fermentation. Each mixture was performed by triplicate, and each replicate was cultured using the same initial cell and sugar concentrations, thus the mean value of replicates

is displayed in the next profiles, with error bars corresponding to \pm one standard deviation for each concentration.

Profile concentrations are depicted in Figure 5.7. In general, the three mixtures show fast glucose consumption in less than ten hours of batch fermentation, which promoted both cell growth and ethanol production at high rates due to degradation of this carbohydrate. Xylose consumption remained virtually unchanged along this short time, mainly for mixtures A and B, showing an average xylose decline of 0.5 g/L, and approximately 0.75 g/L for mixture C, until complete glucose exhaustion. Also, the three mixtures revealed the same pattern of incomplete xylose utilization at the end of fermentation because of the severe inhibition by glucose on the xylose conversion, causing that the xylose conversion rate be significantly lower than the glucose conversion rate, which has been also reported in the literature [7,15], but xylose remaining concentrations in those studies have been considerably higher. However, making a comparison of the three mixtures in Figure 5.7, the curve of xylose consumption shows a steep descent when the xylose concentration is high, indicating that as the initial lower glucose concentration is low, the faster turns out to be the xylose consumption, as shown later in Table 5.1. There, the total substrate consumption rates are compiled; these were calculated in basis of the time required for the consumption of each substrate, similar to the method used in Chapter 4. Mixture C presents the highest xylose consumption rate (0.185 g/L-h) and the lowest glucose consumption rate (0.838 g/L-h) of the three mixtures, which was previously predicted in the simulation of this mixture using only *P. stipitis*. Despite the increase in xylose consumption rate in mixture C, the remaining xylose concentration was the highest, suggesting probably a larger time of fermentation in order to further evaluate if complete xylose degradation is possible.

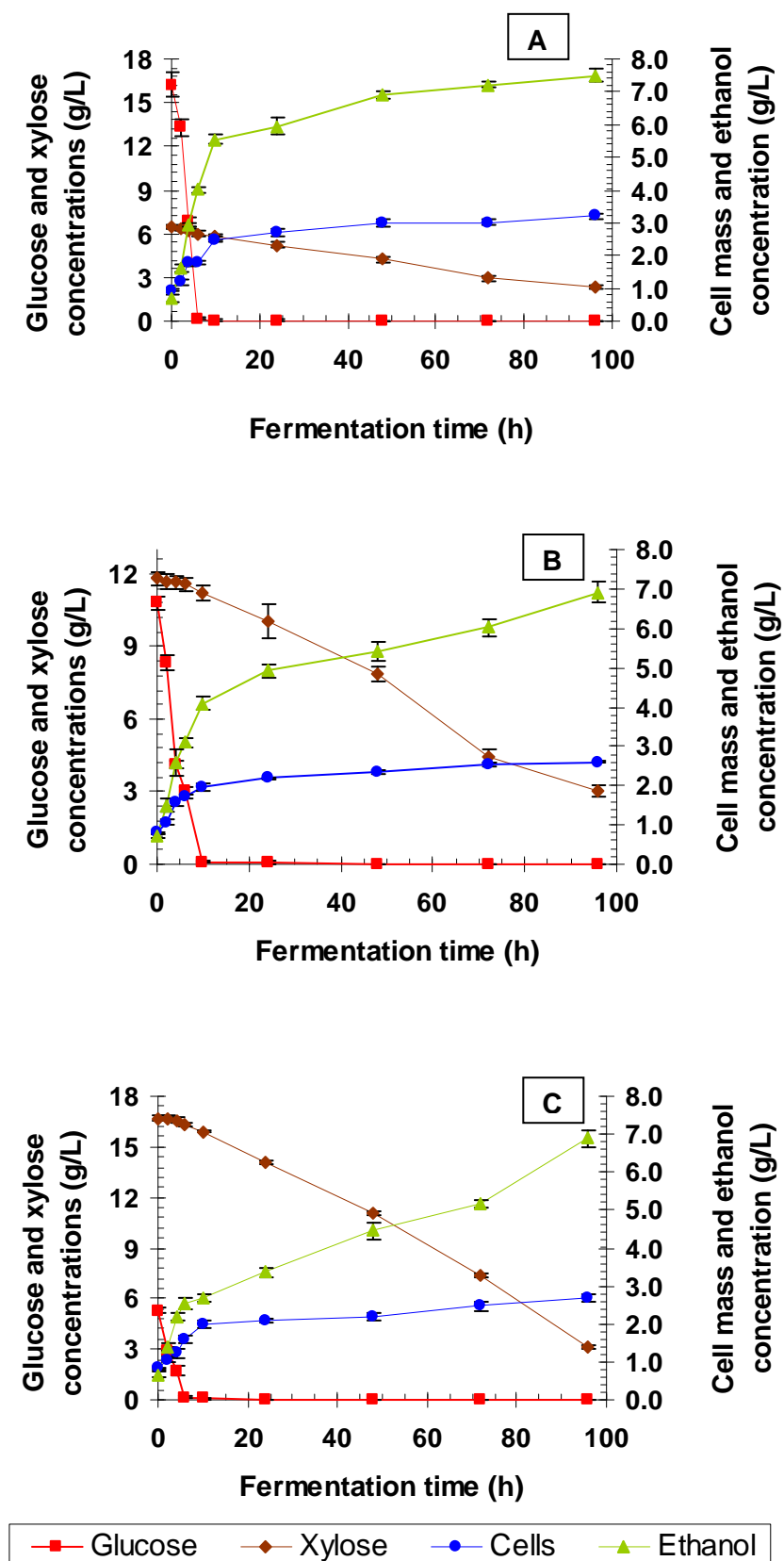


Figure 5.7 – Experimental profiles for glucose-xylose fermentations using suspended co-culture of *S. cerevisiae* and *P. stipitis*. A: 75% Glu – 25% Xyl; B: 50% Glu – 50% Xyl; C: 25% Glu – 75% Xyl. Error bars are ± 1 standard deviation of 3 replicates.

Table 5.1 – Substrate and ethanol volumetric rates from each sugar in the fermentation mixtures with the yeast co-culture.

Sugar Mixtures (% Glucose - % Xylose)	Glucose		Xylose	
	Q _s (g/L-h)	Q _p (g/L-h)	Q _s (g/L-h)	Q _p (g/L-h)
A (75 – 25)	2.729	0.565	0.042	0.023
B (50 – 50)	1.375	0.414	0.099	0.030
C (25 – 75)	0.838	0.319	0.185	0.047

In the other hand, other alternatives such as immobilization of *P. stipitis* in combination with suspended *S. cerevisiae* or using a respiratory deficient mutant yeasts of *S. cerevisiae* have been proposed as an alternative to improve xylose utilization, but results obtained by some authors still report incomplete xylose utilization [15,16].

Competition between the two yeast strains for oxygen in the culture media is also a parameter having a great significance in mixed culture fermentations, especially when working with xylose-fermenting strains because of their well known requirements for low oxygen levels. Since batch co-fermentations were carried out under hypoxic conditions, competition for oxygen availability was not likely to occur, and this assumption is valid since both yeast strains had a level of growth pretty close to the single substrate experiments for each substrate. Otherwise, all the available oxygen would be used by *S. cerevisiae* to grow aerobically, producing a large number of cells and thus reducing ethanol production. The ethanol consumption rates shown in Table 5.1, and the ethanol concentrations achieved from glucose consumption proved that oxygen concentrations were adequate for both yeast strains. Nonetheless, remaining xylose concentrations at the end of fermentation for each mixture were substantially lower than those reported in the literature when using the same co-culture and also for *S. cerevisiae* co-cultured with *Candida shehatae* [17].

Regarding ethanol production, it was observed that the maximum concentration achieved was 7.486 g/L in mixture A, while mixtures B and C reported 6.919 and 6.906 g/L, respectively. It is worthy to note that, although the difference in ethanol produced among the three mixtures is small, ethanol produced in mixture A was higher than the other two mixtures not because of the high glucose concentration but because of xylose utilization, which was better utilized in mixture A. In fact, percentages of total ethanol produced from glucose were decreasing from mixture A to C, from 54% to 64%, and ethanol produced from xylose increased from 46% in mixture A to 64% in mixture C, proving that despite the fast cell growth and rapid ethanol produced with glucose, both sugars had their respective contribution for total ethanol production.

Ethanol yield on substrate was slightly higher in mixture A, but yield coefficients for the three mixtures are very close to each other, and at the same time are very similar to those obtained in single substrate experiments, which means that the co-fermentation process is efficient because ethanol yields were not lower than any of those achieved in fermentations comprising only one substrate and only one yeast strain. All $Y_{P/S}$ coefficients were greater than 0.32 g ethanol/g sugar, very close to those values obtained by Ballesteros and co-workers for the suspended co-culture of *S. cerevisiae* with *C. shehatae* [18], however better yields and better xylose utilization, as mentioned before, can be achieved using coimmobilization with high initial concentrations of *P. stipitis*, since the glucose concentration in the center of the beads will be almost zero, which makes xylose conversion possible [19].

Similar to the yields of ethanol on biomass obtained in Chapter 4 for xylose fermentation with *P. stipitis*, the mixtures comprising the same or higher proportion of xylose yielded larger $Y_{P/X}$ coefficients than those on mixture A, and at the same time, this mixture exhibits the highest $Y_{X/S}$ coefficient, meaning that sugar uptake in *P. stipitis* is more efficient for ethanol production rather than for cell growth. However, all the yield coefficients in the

mixtures, shown in Table 5.2, have a short variability when comparing the different mixtures and demonstrates that the three systems are good alternatives for ethanol production using the suspended co-culture. Although the initial cell concentrations utilized were high enough to reduce lag time and to promote high cell density in the culture medium, higher values should be used in future experiments, in order to improve yields and to have a total xylose consumption, which will also increase $Y_{P/S}$ coefficients.

Table 5.2 – Summary of yield coefficients for glucose-xylose fermentations with the yeast co-culture.

Sugar Mixtures (% Glucose - % Xylose)	$Y_{P/S}$ (g/g)	$Y_{P/X}$ (g/g)	$Y_{X/S}$ (g/g)
A (75 – 25)	0.336	3.003	0.111
B (50 – 50)	0.3169	3.429	0.092
C (25 – 75)	0.3313	3.363	0.098

Fermentation byproducts were monitored with the analytical determination of sugars and ethanol by means of HPLC analyses. Very small amounts of glycerol, acetic acid and lactic acid were detected, especially in mixture A, but the quantification was not necessary since the peaks only were visible when the scale of chromatograms was amplified. Another byproduct of particular interest in xylose fermentations is xylitol, which has been reported to affect ethanol yields in fermentative systems comprising both xylose alone and mixtures of glucose-xylose [17, 20]. Xylitol accumulation was observed in mixture C and in less proportion in mixture B, but likewise the other byproducts, the amounts produced were very small and this did not affect significantly ethanol yields. In fact, one of the main advantages offered by fermentation of mixtures of glucose and xylose is a reduction in xylitol accumulation, because under these conditions the rate of xylose utilization is increased, as

shown in Table 5.1, suggesting that xylitol formation is a consequence of insufficient xylose flux [22].

5.4. Structured modeling glucose-xylose mixtures using

Once the kinetic parameters were estimated and further optimized by means of the Monod unstructured model, according to the results discussed in Chapter 4, and having the complete set of equations developed in section 5.1, the aim and main objective of this work is the kinetic modeling of the glucose-xylose fermentation mixtures, using the yeast co-culture, by means of one adequate structured model that takes into account the instantaneous cellular optimization occurring in a multisubstrate environment: the cybernetic framework. This last section displays the results obtained when modeling the same mixtures so far discussed, evaluating the quality of the model and its application to real fermentation systems for process optimization and scaling-up for industrial applications.

Using equations 5.6 – 5.14 with the inclusion of kinetic and yield parameters from single substrate experiments, the non-linear differential system was solved in MATLAB as described in Figure 3.18 with the constraint for rate maximization described by the cybernetic variable v , in each step of the Runge-Kutta method; before solving numerically the system for each instant of time t , the rate of the uppermost limiting substrate was computed and included in the denominator of equation 5.5, thus the cellular resources optimization was represented mathematically at the start of every iteration. This procedure has been utilized in the programming of Runge-Kutta methods for the growth a co-culture of *Kluyveromyces marxianus* and *Candida utilis* [22]. However, it is worthy to note that the simulations obtained in the present work were not subject of further optimizations for error minimization, therefore the proposed models were directly compared to the results obtained experimentally, and statistically validated by means of the same parameters used for the validation of

unstructured models: Linear Correlation Coefficient (LCC), Mean Squared Error (MSE) and Residual Standard Deviation expressed as a percentage of average of experimental values (%RSD), the ones that will be later summarized.

The model obtained for mixture A is depicted in Figure 5.8, and it shows a very good concordance between simulated and experimental data, especially for the prediction of cell and ethanol concentrations since there were the lowest values for both MSE and RSD%. Ethanol appears to be the best fitted parameter, with an LCC of 99.38%, since the predicted model captures the stages of ethanol production in the mixture: the first one very fast and accelerated which corresponds to glucose consumption and the second one corresponding to xylose consumption. The maximum cell mass and ethanol concentrations achieved are very well predicted by the model. Xylose consumption prediction by the model is slightly less accurate, even though it is statistically supported with RSD% of 4.60 and 98.83% of LCC, showing some differences mainly at the end of the fermentation, since the model predicts a higher sugar degradation which may be due to the lack of adequate oxygen levels at the end of fermentation or the requirements of higher initial concentration of *P. stipitis*, which has been previously studied by means of experiments varying the initial concentrations of *P. stipitis* [23].

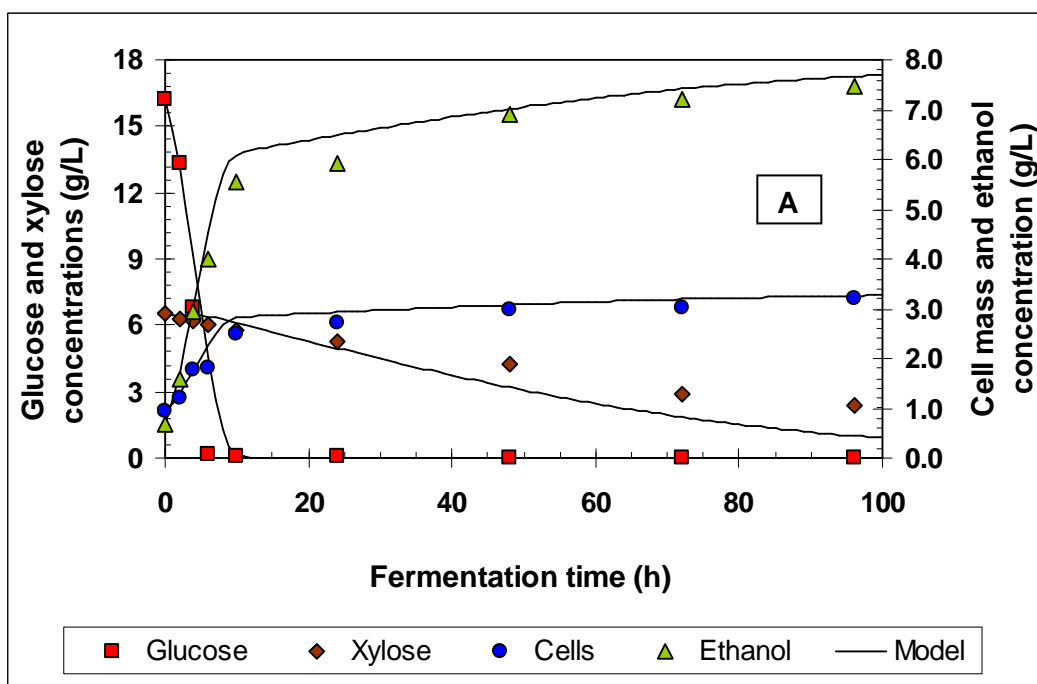


Figure 5.8 – Comparison of the experimental data and predicted kinetics of the mixture A, with 75% of glucose and 25% of xylose using a suspended co-culture of *S. cerevisiae* and *P. stipitis*.

Glucose consumption is predicted to be a little less fast than that measured experimentally, showing a noticeable difference between experimental and predicted concentrations in the sixth hour of fermentation causing that both MSE and RSD% to be large when compared to the other parameters. Experimental values are very similar to those obtained in the single substrate system glucose – *S. cerevisiae*, since glucose is completely exhausted between the six and eight hours, but model simulation somehow predicts the consumption of this sugar more slowly. This situation depends exclusively on the rate maximization responsible for the values of the cybernetic variable v , and this at the same time is a direct consequence of the initial values chosen for the specific levels of key enzymes, the ones that are based on the history of inocula. For this simulation, the initial value for e_1 was 8×10^{-4} since *S. cerevisiae* was pre-cultured on glucose, however other values in the range

suggested by Ramkrishna and Kompala [2] can be chosen in order to improve the fitting of simulations for substrate consumption. Despite the difference explained above, the RSD% calculated was 10.636, barely above of the 10% which is the limit considered statistically acceptable for bioprocess engineering [24]. Overall, this mixture provides an average LCC of 0.9727 for prediction of cells, substrates and ethanol profiles.

The mixture B involving the same proportion of sugars was also simulated by means of the cybernetic model, as shown in Figure 5.8. This shows in the first place, a better prediction of both glucose and xylose consumptions when compared to the mixture A, with LCC of 0.9867 and 0.9954, respectively. Simulation of xylose profile concentration was the parameter best fitted in this mixture, with RSD% lower than 1 and MSE of 0.055; very accurate prediction of the final xylose concentration was also achieved which is an important tool to foresee the proper fermentation time in further fermentation experiments.

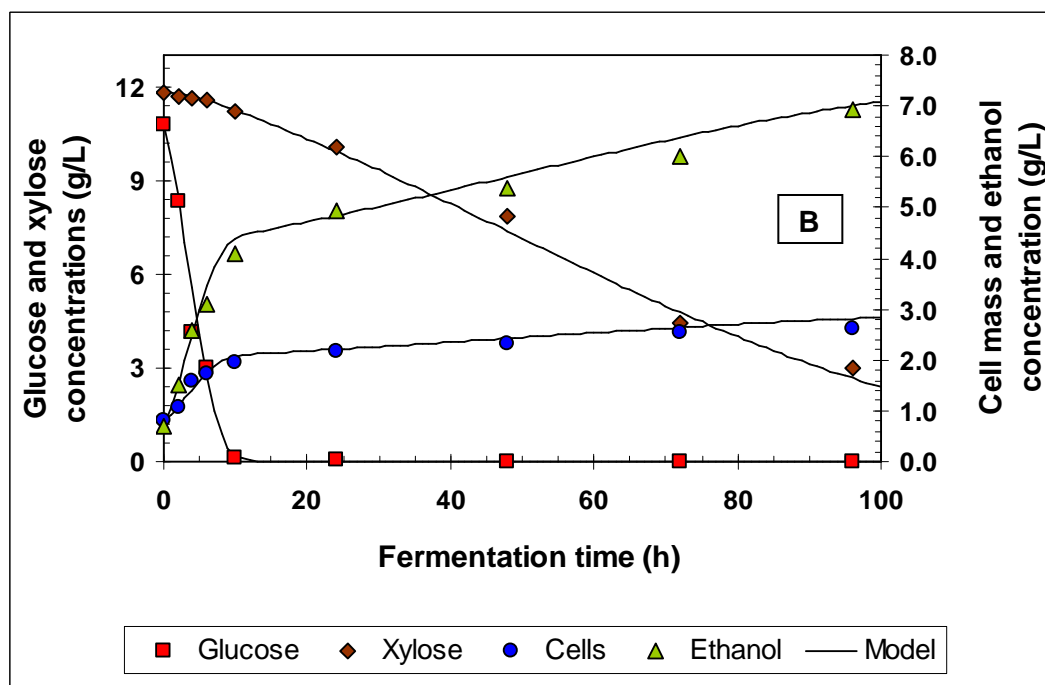


Figure 5.9 – Comparison of the experimental data and predicted kinetics of the mixture B, with 50% of glucose and 50% of xylose using a suspended co-culture of *S. cerevisiae* and *P. stipitis*.

Ethanol production and cell growth simulations also showed excellent convergence for this co-fermentation, with both production stages (corresponding to glucose and xylose degradation, respectively) well defined and in good agreement with experimental data. Unlike mixture A where the model simulation for cell growth did not account for of the intermediate lag phase efficiently, the growth rate was very well predicted in this mixture capturing the right moment where *S. cerevisiae* stopped its growth, leading *P. stipitis* growth in the culture medium. The RSD% for cell growth was 1.956 and 1.811 for ethanol production, and these values are a good indicative of high accuracy in the prediction of the trends followed in this fermentation mixture. These results are very similar to those reported by Leksawasdi and co-workers [10] in glucose-xylose mixtures using recombinant *Zymomonas mobilis* with 50/50 sugar proportion. By analyzing the statistical information extracted from the model simulations, it can be demonstrated that mixture B had the better overall prediction by cybernetic model since it reports the lowest average RSD% and the highest average LCC with values 2.214 and 0.9906, respectively. This high accuracy may be attributed because at the beginning of fermentation, the amount of both sugars in the culture medium was the same, and the proportion in total cell concentration was approximately 60% for *S. cerevisiae*; this cell proportion fermented rapidly all the glucose available in solution, while *P. stipitis* had just began to consume this sugar but at this moment it was almost completely exhausted, which caused the enzyme induction for xylose and therefore, the slight diauxie existing in cell growth between the consumption of both sugars was perfectly captured by the model, which originally was created to describe the diauxic nature of multiple substrate environments. This did not occur in mixture A, because it had a higher amount of glucose and probably it was necessary to set a lower initial concentration of *P. stipitis* as an initial condition for the simulation, however if this had been done also experimentally the remaining amount of xylose without consumption would have been likely greater.

Unfortunately, at the moment when this document was written we were unable to make comparisons to other co-fermentations using the same suspended co-culture, since this scheme was not found in literature, having only results of experiments performed with immobilization and co-immobilization techniques, but lacking models attempting to simulate the fermentation kinetics.

Simulation of mixture C, with 25% glucose/75% xylose, depicted in Figure 5.9, which reveals a slight consumption of xylose from the beginning of the fermentation, in the same manner that it was observed experimentally. This consumption which took place even before glucose exhaustion, and it was also captured by the cybernetic model, suggests the high potential of *Pichia stipitis* NRRL-Y11545 to be considered in other processes configurations, either suspended or immobilized, involving hydrolysates from high hemicellulose fractions.

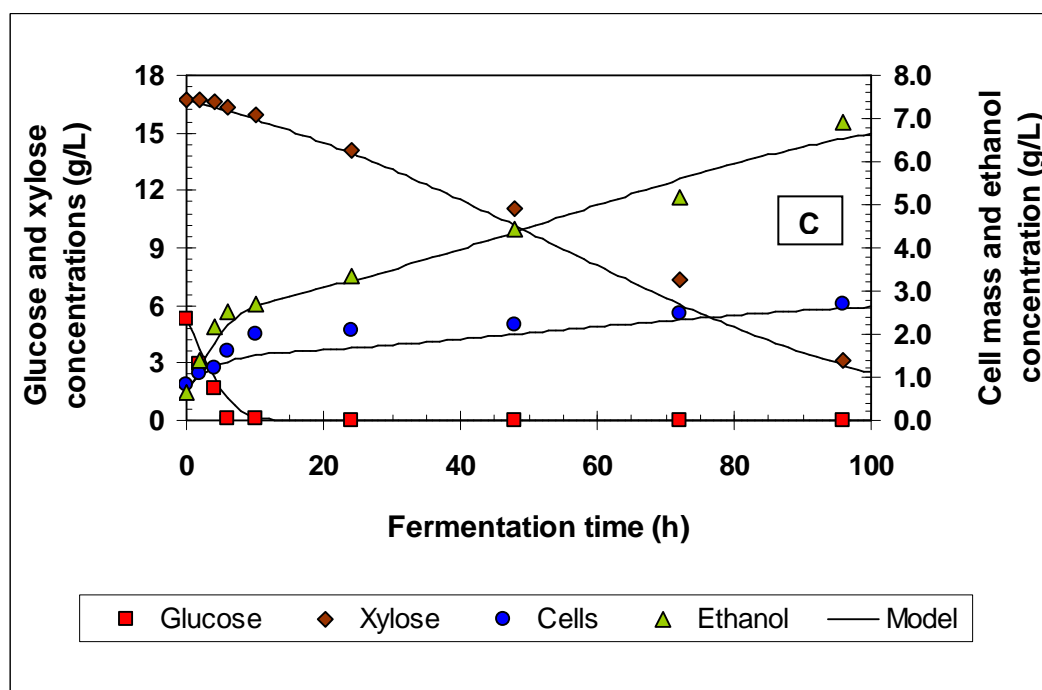


Figure 5.10 – Comparison of the experimental data and predicted kinetics of the mixture C, with 25% of glucose and 75% of xylose using a suspended co-culture of *S. cerevisiae* and *P. stipitis*.

The sensitivity of the model to predict xylose consumption is such that it was the parameter better predicted, involving the lowest RSD% and the higher LCC with values of 1.134 and 0.9953, respectively. Regarding cell growth, the model was not able to capture properly the amount of cells grown from glucose consumption. In this case, similar to the explanation for mixture A, higher initial concentrations of *S. cerevisiae* as initial condition for solving the non-linear differential system would probably fall into a better prediction of cell growth, especially in the moment where *P. stipitis* starts to grow as a consequence of xylose degradation. This situation is feasible since a little increase in concentration of *S. cerevisiae* will cause that, when glucose depletion is imminent, *P. stipitis* will consume xylose by itself while *S. cerevisiae* will not grow any longer. This is a good alternative to improve the discrepancies between the model simulation and the experimental values for cell growth. However, RSD% for this prediction is under 10%. With an increase in the accuracy to simulate cell growth will be also improved the accuracy for glucose consumption, which reached the highest RSD% for this mixture. Prediction of ethanol production was also in good agreement with the experimental values, especially for the stage when ethanol is produced from xylose consumption. RSD% for ethanol simulation in this mixture was 1.811.

Table 5.3 – Statistical analysis for kinetic modeling using cybernetic model. Units: MSE [(g/L)²]; LCC [%]; RSD [%].

Fermentation mixture	Statistical parameter	Cells	Glucose	Xylose	Ethanol
A 75% glucose – 25% xylose	MSE	0.047	2.7786	0.487	0.108
	LCC	0.9675	0.9411	0.9883	0.9938
	RSD	3.252	10.636	4.600	2.329
B 50% glucose – 50% xylose	MSE	0.012	0.2314	0.055	0.045
	LCC	0.9865	0.9867	0.9954	0.9938
	RSD	1.956	4.245	0.846	1.811
C 25% glucose – 75% xylose	MSE	0.058	0.2274	0.300	0.073
	LCC	0.9310	0.9570	0.9953	0.9842
	RSD	4.483	9.434	1.394	2.754

In general, the results obtained and discussed from simulations of glucose-xylose mixtures, allow to postulate that the model utilized has been successfully validated by means of fermentation runs, and the fitting of predicted values to the experimental profiles is statistically consistent, based on information presented in Table 5.3, having small deviations commonly found in one system which has not been object of further error minimizations, and these deviations fall in a range considered as adequate. As mentioned before, the values obtained in the average of RSD% for substrates, cells and ethanol, the mixture exhibiting the best fitting by cybernetic model was that having equal proportion of glucose-xylose (mixture B) with an average RSD of 2.214%; followed by mixture C and mixture A with RSD values of 4.516% and 5.204%, respectively. Similarly to Chapter 4, a qualitative analysis of the consistency and agreement between the predicted and experimental concentrations was carried out for total cell growth, glucose, xylose and ethanol concentrations, respectively.

Therefore, figures A.4 – A.7 in Appendix A support the statistical criteria used to evaluate the sensitivity of the models in the mixed substrate – mixed strain fermentations.

The performance of the cybernetic model can be also analyzed using the profiles followed by the specific level of key enzymes, responsible for consumption of any given substrate, by each of the yeast strains present in the culture media. These profiles are shown in Figure 5.10 indicating that in mixture A the enzyme levels for glucose degradation for both yeast strains (e_1 and e_3) prevail and predominate during the first then hours of fermentation. From those levels, the ones exhibited by *S. cerevisiae* are almost twofold those levels present in *P. stipitis*, which is a valid argument to prove that the majority of glucose degradation was carried out by means of *S. cerevisiae* metabolism, while contribution of *P. stipitis* in this degradation was minimum. Levels of e_2 , key enzymes for xylose degradation by *S. cerevisiae* will be always close to zero because of the null xylose consumption existing in this yeast strain. Also, the strong catabolite repression caused by glucose consumption can be observed in the slight reduction of e_4 initially present in *P. stipitis*, and product of pre-culturing its inoculum on pure xylose [2, 3]. As soon as glucose was exhausted, enzymes initially present in *P. stipitis* were induced and xylose degradation proceeds showing the obvious increase in e_4 .

The argument explained previously about setting higher or lower initial concentrations for any of the two yeast strains for simulations purposes only in a mixture, has a great effect in the enzyme levels profiles currently analyzed because of according to the basic postulates of the cybernetic model, the parameter e is included in the biomass rate, and at the same time all the e 's also include the terms for biomass rate; all the equations of the model are dependent of each other which increases the non-linearity and therefore, any change or modification in cell concentrations, even at the beginning, returns that effect on the specific enzyme level profiles.

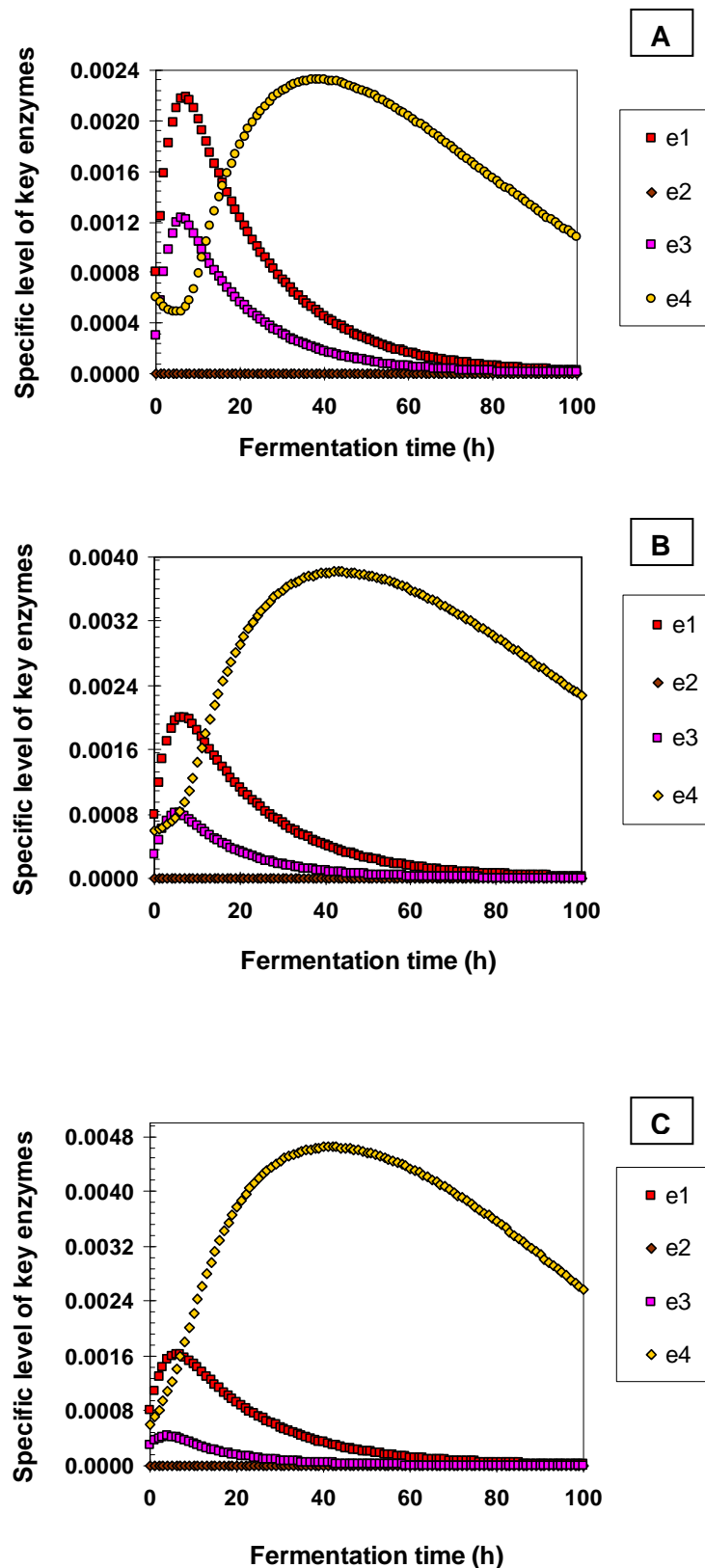


Figure 5.11 – Simulation of enzyme levels in glucose-xylose fermentation with *S. cerevisiae*: e_1 and e_2 , and *P. stipitis*: e_3 and e_4 A: 75% Glu – 25% Xyl; B: 50% Glu – 50% Xyl; C: 25% Glu – 75% Xyl.

In mixture B, a decrease in e_1 and e_3 as a result of the lower amount of glucose present in culture medium caused the more anticipated increase in e_4 as compared to mixture A. Likewise, repression caused by glucose is barely observable and the specific level for xylose consumption by *P. stipitis*, e_4 is now higher than e_1 . It is important to note that the narrowest the maximum specific enzyme level curve, the faster the consumption of substrate, hence the curve for e_4 for mixtures B and C is very similar because xylose consumption was slower; the difference is the maximum level achieved.

Finally, mixture C suggests that the amount of e_1 to degrade the small amount of glucose is just a little higher than the initial level that was attained from pre-culturing the inoculum of *S. cerevisiae* on pure glucose. Besides, e_3 did not have a significant increase, falling below e_4 , which is a new indicative to prove again the predicted earlier in this chapter regarding the no contribution of *P. stipitis* for glucose consumption in this mixture, since activation of the enzyme levels for xylose degradation, achieved at the same time in its respective inoculum, was immediate at the beginning of fermentation. This is the reason why xylose consumption took place even slightly simultaneously with glucose consumption, due to the small amount of glucose initially present and the high rate of consumption that was not enough to repress e_4 .

Based on the results already discussed, the proposed structured model to predict the behavior of glucose-xylose mixtures using the cybernetic framework, has fulfilled the main objective of this research work, and the corresponding conclusions and improvements to the methodology used in this project will be expanded in Chapter 6. Because of the excellent accuracy between the model and experimental data, this model can be utilized not only for the scale-up of batch fermentation, but also for trying other configurations such as fed-batch and continuous culture, in order to chose that scheme which provides the best yields in ethanol production. Furthermore, the model can be applied to other process entailing suspended co-

cultures, such as the production of antibiotics in the pharmaceutical industry, the production of probiotic yogurts from mixtures of *Lactobacillus* strains, and other applications in the vast knowledge area of bioprocess engineering.

5.5. References cited

- [1] Kompala, D.S.; Ramkrishna, D.; Tsao, G.T. (1984). Cybernetic modeling of microbial growth on multiple substrates. *Biotechnol. Bioeng.* **26**:1272-1281.
- [2] Kompala, D.S.; Ramkrishna, D. (1986). Investigation of bacterial growth on mixed substrates: Experimental evaluation of cybernetic models. *Biotechnol. Bioeng.* **28**:1044-1055.
- [3] Young, J.D.; Ramkrishna, D. (2007). On the matching and proportional laws of cybernetic models. *Biotechnol. Prog.* **23**:83-89.
- [4] Narang, A.; Konopka, A.; Ramkrishna, D. (1996). Dynamic analysis of the cybernetic model for diauxic growth. *Chem. Eng. Science.* **52**(15):2567-2578.
- [5] Narang, A.; Konopka, A.; Ramkrishna, D. (1997). The dynamics of microbial growth on mixtures of substrates in batch reactors. *J. theor. Biol.* **184**:201-317.
- [6] Ramkrishna, R.; Ramkrishna, D. (1996). Cybernetic modeling of growth in mixed, substitutable substrate environments: Preferential and simultaneous utilization. *Biotechnol. Bioeng.* **52**:141-151.
- [7] Rouhollah, H.; Iraj, N.; Giti, E.; Sorah, A. (2007). Mixed sugar fermentation by *Pichia stipitis*, *Saccharomyces cerevisiae*, and an isolated xylose-fermenting *Kluyveromyces marxianus* and their co-cultures. *African Journal of Biotechnology.* **6**(9): 1110-1114.
- [8] Hahn-Hägerdal, B.; Karhumaa, K.; Fonseca, C.; Spencer-Martins, I.; Gorwa-Grauslund, M.F. (2007). Towards industrial pentose-fermenting yeast strains. *Appl. Microbiol. Biotechnol.* **74**:937-953.
- [9] Mousdale, D.M. (2008). Chemistry, Biochemistry and Microbiology of lignocellulosic biomass. *Biofuels: Biotechnology, Chemistry and Sustainable Development.* First Edition. CRC Press, Taylor & Francis Group. **Chapter 2**:49-86.
- [10] Leksawasdi, N; Joachimsthal, E. L.; Rogers, P. L. (2001). Mathematical modeling of ethanol production from glucose/xylose mixtures by recombinant *Zymomonas mobilis*. *Biotechnol. Letters.* **23**:1087-1093.

- [11] Agbogbo, F.K.; Coward-Kelly, G.; Torry-Smith, M.; Wenger, K.S. (2006). Fermentation of glucose/xylose mixtures using *Pichia stipitis*. *Process Biochemistry*. **41**:2333-2336.
- [12] Nakamura, Y.; Sawada, T.; Inoue, E. (2001). Mathematical model for ethanol production from mixed sugars by *Pichia stipitis*. *Journal of Chem. Technol Biotechnol*. **76**:586-592.
- [13] Agbogbo, F.K.; Coward-Kelly, G.; Torry-Smith, M.; Wenger, K.S. (2006). Fermentation of glucose/xylose mixtures using *Pichia stipitis*. *Process Biochemistry*. **41**:2333-2336.
- [14] Busturia, A.; Lagunas, R. (1986). Catabolite inactivation of the glucose transport system in *Saccharomyces cerevisiae*. *J. Gen. Microbiol*. **132**:379-385.
- [15] Taniguchi, M.; Tohma, T.; Itaya, T.; Fujii, M. (1997). Ethanol production from a mixture of glucose and xylose by co-culture of *Pichia stipitis* and a respiratory-deficient mutant of *Saccharomyces cerevisiae*. *Journal of Fermentation and Biotechnology*. **83**(4):364-370.
- [16] Laplace, J.M.; Delgenes, J.P.; Moletta, R. (1992). Alcoholic glucose and xylose fermentations by the coculture process: compatibility and typing of associated strains. *Can. J. Microbiol*. **38**:654-658.
- [17] Lebeau, T.; Jouenne, T.; Junter, G.A. (2007). Long-term incomplete xylose fermentation, after glucose exhaustion, with *Candida shehatae* co-immobilized with *Saccharomyces cerevisiae*. *Microbiological Research*. **162**:211-218.
- [18] Ballesteros, M.; Ballesteros, I.; Olivia, J.M.; Cabanas, A.; Saez, F.; Carrasco, J. (1991). Comparative study of different fermentation schemes to produce ethanol from lignocellulosic sugar components. In: Grassi G, Collina A, Zibetta H (eds) Proceedings of the 6th European Conference on Biomass for Energy, Industry and Environment. 21-27 April, Athens. Elsevier Applied Science, London and New York, Pp. 536-540.
- [19] Grootjen, D.R.J.; Meijlink, L.H.H.M.; Vleesenbeek, R. van der Lans, R.G.J.M.; Luyben, K.Ch.A.M. (1991). Cofermentation of glucose and xylose with immobilized *Pichia stipitis* in combination with *Saccharomyces cerevisiae*. *Enzyme Microb. Technol*. **13**:530-536.
- [20] Sánchez, S.; Bravo, V.; Castro, E.; Moya, A.J.; Camacho, F. (2002). The fermentation of mixtures of D-glucose and D-xylose by *Candida shehatae*, *Pichia stipitis* or *Pachysolen tannophilus* to produce ethanol. *Journal of Chem. Technol. and Biotechnol*. **77**:641-648.
- [21] Hahn-Hägerdal, B.; Karhumaa, K.; Fonseca, C.; Spencer-Martins, I.; Gorwa-Grauslund, M.F. (2007). Towards industrial pentose-fermenting yeast strains. *Appl. Microbiol. Biotechnol*. **74**:937-953.

- [22] Saliceti-Piazza, L. (1994). Aerobic co-cultures of *Kluyveromyces marxianus* and *Candida utilis* utilizing multiple substrates from whey bioconversion waste streams. PhD Thesis, Purdue University.
- [23] Laplace, J.M.; Delgenes, J.P.; Moletta, R.; Navarro, J.M. (1993). Ethanol production from glucose and xylose by separated and co-culture processes using high cell density systems. *Process Biochemistry*. **28**:519-525.
- [24] Atala, D.I.P.; Costa, A.C.; Maciel, R.; Maugeri, F. (2001). Kinetics of ethanol fermentation with high biomass concentration considering the effect of temperature. *Appl. Biochem. Biotechnol.* **91-93**(1-9):353-366.

6. CONCLUSIONS AND RECOMMENDATIONS

6.1. Single substrate fermentations

Overall, the work developed in Chapter 4 provided a better understanding of the properties and performance of *Saccharomyces cerevisiae* and *Pichia stipitis* as efficient fermenting yeast strains for bioethanol production from glucose and xylose, respectively. The detailed analysis of these single substrate experiments separately allowed the determination of kinetic parameters and yield coefficients, which at the same time were the key parameters to determine aspects such as the performance of the fermentation process, the unstructured modeling of each individual fermentative system and the source of all the parameters necessary for the modeling of mixed substrate fermentations. Therefore, reliable kinetic information was estimated from these experiments and the quality of the Monod model to predict profile concentrations was successfully demonstrated.

6.1.1. Conclusions on single substrate fermentations

The yield of ethanol on substrate was found to be higher in xylose fermentations with *P. stipitis* ($Y_{P/S} = 0.35$ g/g), which represents almost a 70% of the theoretical yield based on stoichiometric calculations, thus it is considered an acceptable value when compared to those yields reported in the literature for other non-engineered xylose-fermenting yeast strains. Even when the yield of biomass on substrate was higher for glucose fermentation with *S. cerevisiae* it is concluded that *P. stipitis* utilized xylose efficiently to promote a balanced cell growth that channeled sugar degradation into ethanol production. This situation was confirmed with the yield of ethanol on biomass, which was higher for the system xylose – *P. stipitis* ($Y_{P/X} = 3.59$ g/g) and the nearest to the theoretical value, supporting the conclusion that this yeast strain degrades xylose preferentially for ethanol production rather than cell growth.

The quality of the proposed model to predict the profile concentrations behavior in the different fermentation systems was very good, which proves that the utilization of the simple Monod model to describe and quantify cell growth and its further incorporation in the mass balances for the batch fermentation process, was suitable and provides excellent kinetic information which can be used as a tool for optimization, scaling-up and the development of other process configurations such as fed-batch and continuous culture, in order to improve the yields in the production of ethanol from lignocellulosic feedstock.

Since the initial concentration of substrates utilized for each experiment and the maximum ethanol concentrations achieved did not exceed the limits to take into account both substrate and product inhibition, the combination of the kinetic models proposed by Moser and Luong, successfully used in batch fermentation experiments carried out by other researchers, were assayed by modifying the Monod equation with the corresponding inhibition terms and constants, but it was demonstrated that these mathematical expressions representing the inhibition phenomena were reduced to the unity, which at the same time reduced the equation to that represented by the simple Monod model, supporting the use of this substrate-limiting model to mathematically represent cell growth in this work.

In order to estimate the sensitivity of the model to choose the system best fitted based on R^2 and RSD for the average of cell mass, substrate and ethanol concentrations, it is concluded that such system is glucose – *S. cerevisiae* with $R^2 = 0.98$ and $RSD = 4.30\%$, being these the highest and lowest values of the three systems, respectively. However, none of the other fermentative systems yielded average RSD values higher than 7.5%, which demonstrates that all the models predict the experimental profile concentrations with statistical consistency, and therefore the obtained and optimized kinetic parameters were suitable to be used in the structured model developed to describe the behavior of glucose-xylose mixtures.

6.1.2. Recommendations on single substrate fermentations

Even when the model obtained to predict the behavior of profile concentrations in single substrate fermentations was accurate, the yields of ethanol produced from glucose and xylose using the two yeast strains were acceptable, and the optimization of kinetic parameters provided the minimization of error when comparing the simulated values to those obtained experimentally, it is necessary to stress about complementary work and techniques that certainly will help to enhance the results already obtained, expanding them to study other factors and configuration processes.

It would be interesting to quantify the specific cell growth rate from either various batch experiments varying the initial concentration of substrate for each experiment, or similarly, conducting continuous culture experiments to maintain control of the specific growth rates. In this manner, the maximum specific growth rate (μ_{\max}) and the Monod saturation constant (K_s) would be determined more accurately using any of the linearized forms of the Monod equation (e.g. Lineweaver-Burk, Eadie-Hoffstee or Hanes-Woolf plots, or continuous culture graphical analysis). Some of these plots were used in this work to determine the Monod saturation constant, but using the finite differences technique with cell and substrate concentrations in order to construct one set of different substrate concentrations. This method provided the “initial guess” value for K_s , which was further optimized with the values of μ_{\max} when solving the differential system by means of the Runge-Kutta method.

Although it was demonstrated that inhibition effects did not impact neither growth kinetics nor ethanol production, it is recommended to study and evaluate the applicability of other growth models such as the logistic and the Malthus rate equations, the ones that have been utilized with great results by other authors in fermentation of various carbon sources to produce ethanol. In case that these models provide great results with high accuracy to describe fermentation kinetics, even more interesting it would be the utilization of them to

construct the structured platform, coupling the enzyme synthesis rate and the instantaneous cellular optimization. This approach would be challenging for the fermentation modeling area since the process control and optimization in bioprocess engineering increasingly demands the use of robust models involving different perspectives to represent cell growth. This is a critical factor in the nature of these bioprocesses, therefore finding a model that optimally predicts the behavior of cell growth will allow to design the best and most successful operation.

It is also recommended to perform each one of the single substrate experiments using a continuous culture in order to have a complete characterization of kinetic parameters and yield coefficients. This scheme is a powerful experimental tool since it allows the variation of the specific growth rate as an independent parameter (dilution rate) in order to better estimate K_s , μ_{\max} and the maximum yield coefficients.

6.2. Mixed substrate and mixed strain fermentations

Through the work described in Chapter 5, a solid and complete structured model with the cybernetic perspective was developed for a binary mixture of substrates, biocatalyzed by the co-culture of two yeast strains. Likewise, a better understanding on the behavior of the experimental profiles of these mixtures, and the prediction of trends followed by these profiles from data collected in single substrate fermentations, was accomplished. Very good ethanol yields were attained by co-culturing the two yeast strains with the sugar mixtures, being in the same order of magnitude to those obtained in single substrate experiments, which means that the two strains had an excellent role in the consumption of both carbohydrates. All these insights are very promising in the lignocellulosic biomass-to-ethanol growing industry, and the results obtained in this work when the model was evaluated have greatly fulfilled the objectives settled at the beginning of the project.

6.2.1. Conclusions on mixed substrate and mixed strain fermentations

A non-linear ordinary differential equation system comprising of nine equations was constructed by applying the basic equations and postulates of the cybernetic model to a mixture of two carbohydrates with two yeast strains. Unlike other cybernetic platforms proposed previously in the literature, the actual system involves two different equations to separately represent the growth of the two yeast strains interacting in the culture medium, and each of those equations accounts for the consumption of the two limiting substrates. Therefore, a system of m different microbial strains growing on an environment where n substrates limit their growth, the structured model constructed under the cybernetic perspective will have $m \times n$ combination of equations for microbial growth and substrate consumption, respectively. Even when the quantification of total cell mass is good enough to test the models predicted, the mathematical distinction between the two yeast strains is desirable in order to evaluate their corresponding growth patterns. Ultimately, the total number of equations included in the cybernetic model in a system comprising of $m \times n$ combination of strains-substrates will be $2(m \times n) + p$, where the number 2 expands two-fold the combination of strains and substrates to take into account their respective equations describing the specific levels of key enzymes, and p represents the number of extracellular products of interest in the fermentative process.

From experimental profile concentrations it is concluded that the three mixtures analyzed provide very good ethanol yields on substrate, being these values very similar to each other. However, in mixtures comprising of same or higher xylose proportions, *P. stipitis* showed a slightly higher efficiency for ethanol production rather than for cell growth, and this behavior is very similar to that obtained when culturing this yeast strain on pure xylose as a carbon source, already discussed in the previous section.

Overall, the results obtained from the simulations applied to mixtures of glucose-xylose using the co-culture scheme suggest that the proposed unstructured model fits accurately experimental data, being statistically consistent according to the averaged values of R^2 coefficients and RSD. The sensitivity of the model increased for the majority of the profiles among substrates, cell mass and ethanol, when compared to those analyzed in single substrate experiments, and in average, the mixture better predicted is that comprising of the same proportion of both glucose and xylose sugars, 50% glucose-50% xylose, with $R^2 = 0.9906$ and $RSD = 2.214\%$, followed the mixture comprising of 75% xylose-25% glucose with $RSD = 4.516\%$, and finally the mixture comprising of 75% glucose-25% xylose with $RSD = 5.204\%$, with R^2 for these latter mixtures above 0.97. It is worthy to note that the predictions achieved have successfully fulfilled the main goal of this To work, since the models were obtained only utilizing data collected from single substrate fermentations, and they were not subject of subsequent error minimization, therefore the prediction made by the structured model in this work, when applied to the fermentation mixtures with the co-culture of yeast strains represents a meaningful contribution to the fermentation modeling area since it is one of the few works developed in course where cybernetic modeling is also applied for a mixed microbial population.

6.2.2. Recommendations on mixed substrate and mixed strain fermentations.

As discussed in Chapter 5, the consumption of glucose in the fermentation mixtures was carried out mainly by *S. cerevisiae* with a little low contribution of *P. stipitis*, but when the xylose proportion in the mixture increased the contribution of *P. stipitis* was not significant, reason why the consumption of xylose started even when glucose was not completely exhausted for the high xylose fractions. Even when the two yeast strains demonstrated their performance to degrade both glucose and xylose, it would be interesting to study the effect of immobilization and coimmobilization techniques in cell growth to promote

higher concentrations of *P. stipitis* and hence, a higher xylose conversion which will also improve the ethanol yields, as proposed by other authors. Working with immobilized cells changes substantially the equations used to describe the growth rate, because it is necessary to account for the transport of substrates into the immobilized bead and the conversion of those substrates inside the bead, therefore the development of a complete structured model with either immobilized or coimmobilized scheme is an interesting option to be considered in the future.

Because of the accuracy achieved with the model developed in this work, the extension of the same model can be done to other process configurations such as fed-batch and continuous culture, pursuing the evaluation of the option showing an optimum balance between ethanol yield, substrate conversion and the minimization of secondary metabolites. Also, as mentioned at the end of Chapter 5, the actual model can be utilized not only at bioethanol industry levels, but to processes related to pharmaceutical and food industry; the production of antibiotics from complex fermentation broths, the processing of probiotic yogurts, and bioremediation processes carried out in wastewater and soil, are examples of industrial processing where microbial mixed cultures are utilized, thus the use of a robust model able to describe efficiently cell growth would be strongly recommended.

The use of controlled sequential addition of biomass to the culture media along the fermentation time may be useful, starting the batch process with the mixture of glucose and xylose but only with *S. cerevisiae*. Later on, when glucose has been completely exhausted, the aseptic inoculation of *P. stipitis* could be carried out in order to lead the consumption of xylose. This complementary process configuration entails some difficulties to consider, such as the oxygen availability in culture medium after the growth of *S. cerevisiae*, the adaptation of *P. stipitis* to an environment having a dense concentration of biomass, and the high initial concentration of *P. stipitis* necessary to avoid a prolonged lag phase. Additionally, the

mathematical model used to simulate the fermentation kinetics should be subject to the corresponding modification to describe the incorporation of the new microbial strain, and the right time when this inoculation can take place. Particularly, this scheme for the sequential addition of biomass it would be useful especially when the strain of *P. stipitis* utilized causes an inhibitory effect over *S. cerevisiae*, or when catabolic repression of glucose consumption over xylose utilization is too strong that intermediate lag phase is very large. Therefore, the study of this scheme could be certainly analyzed in a future research project.

Regarding the experimental measurement of cell concentration, even when the quantification of total cell mass is good enough to estimate both biomass proliferation and adequacy of the structured kinetic model, it may be also useful the distinction between the two yeast strains by means of an appropriate method like replica plating, based in the inability of *S. cerevisiae* to grow on xylose. This distinction will provide the experimental profiles for each strain, the ones that could be compared to those obtained from simulations, which will lead to a better understanding of the relationships existing in the mixed culture. Measurement of enzymatic levels can be also performed experimentally to validate the simulated trends obtained by means of the cybernetic model. Furthermore, both experimental and simulated specific enzyme level trends can be compared with those reported in the literature of xylose fermentation.

Ultimately, it is also recommended for both single substrate and mixed substrate – mixed strain fermentations the use of a continuous stirred-tank reactor (CSTR bioreactor) in order to have a better control of the critical process parameters such as temperature, agitation, pH, and dissolved oxygen. Likewise, the measurement of these parameters can be optimized by the implementation of Process Analytical Technologies (PAT) using essential tools such as Near Infrared and Raman Spectroscopy, biosensors and multivariate data acquisition for the accurate determination of experimental concentrations of cells, sugars and ethanol.

APPENDICES

APPENDIX A: CONSISTENCY OF THE PROPOSED MODELS

In order to support the statistical analysis made in Chapters 4 and 5 and to evaluate the sensitivity of the proposed models, this appendix includes a qualitative analysis of error to better understand the capability to predict the experimental trends followed in all the experiments. The consistency between the concentrations is evaluated by means of a 45° diagonal line that represents the perfect agreement between predicted and experimental concentrations. In all the cases the solid symbols represent the different fermentation systems as follows: squares: Xylose – *P. stipitis*, triangles: Glucose – *P. stipitis*, diamonds: Glucose – *S. cerevisiae*.

A.1 Single substrate fermentations

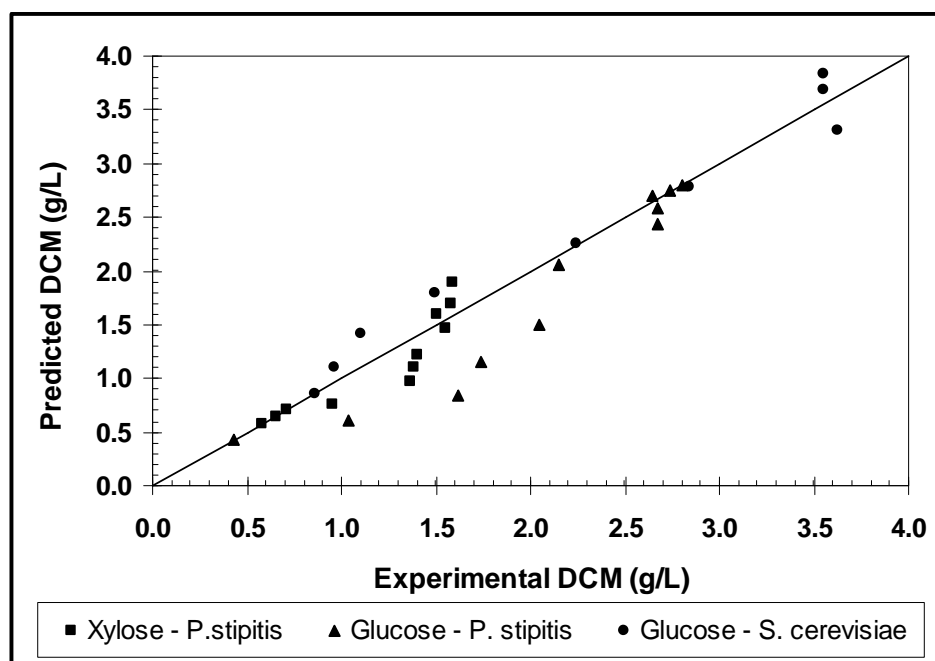


Figure A.1 – Comparison of the consistency between predicted and experimental cell concentrations.

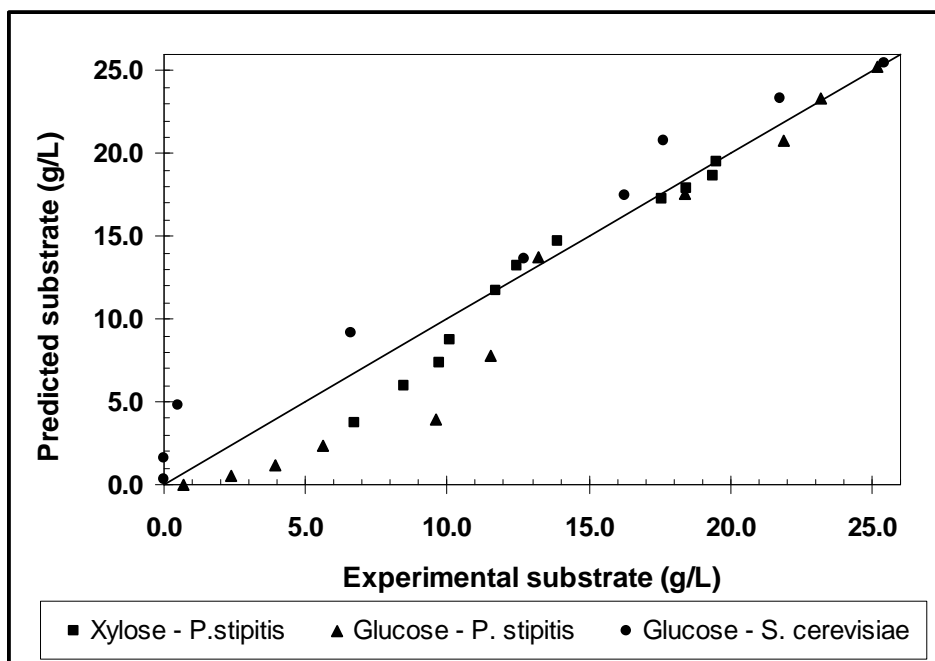


Figure A.2 – Comparison of the consistency between predicted and experimental substrate concentrations.

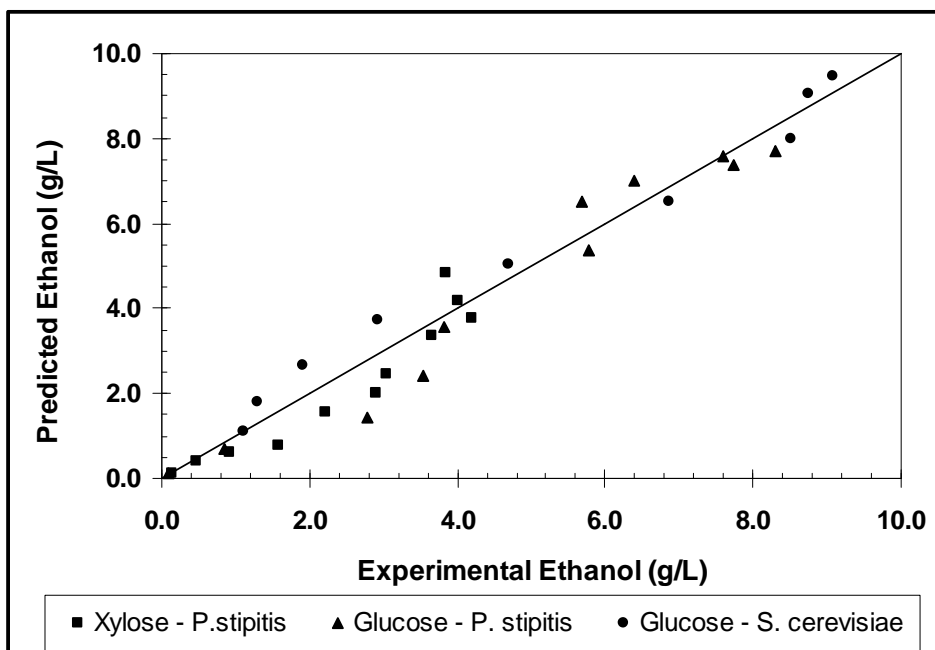


Figure A.3 – Comparison of the consistency between predicted and experimental ethanol concentrations.

A.2 Mixed substrate – mixed strain fermentations

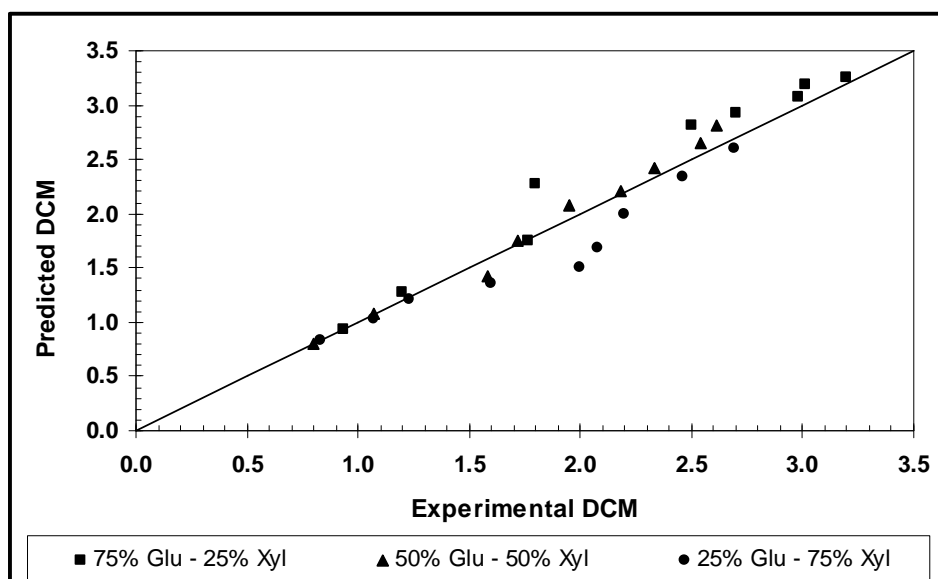


Figure A.4 – Comparison of the consistency between predicted and experimental total cell concentrations.

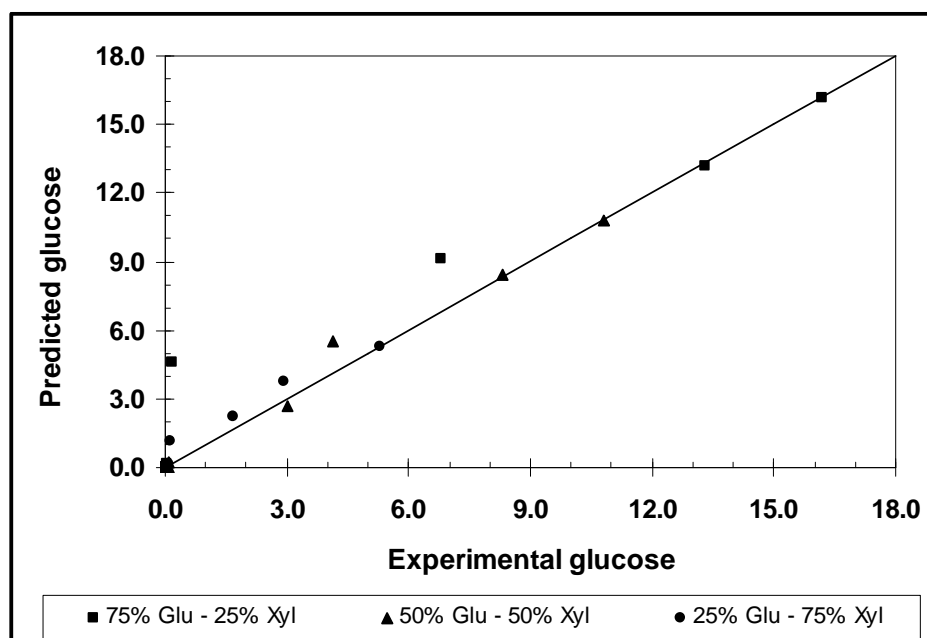


Figure A.5 – Comparison of the consistency between predicted and experimental glucose concentrations.

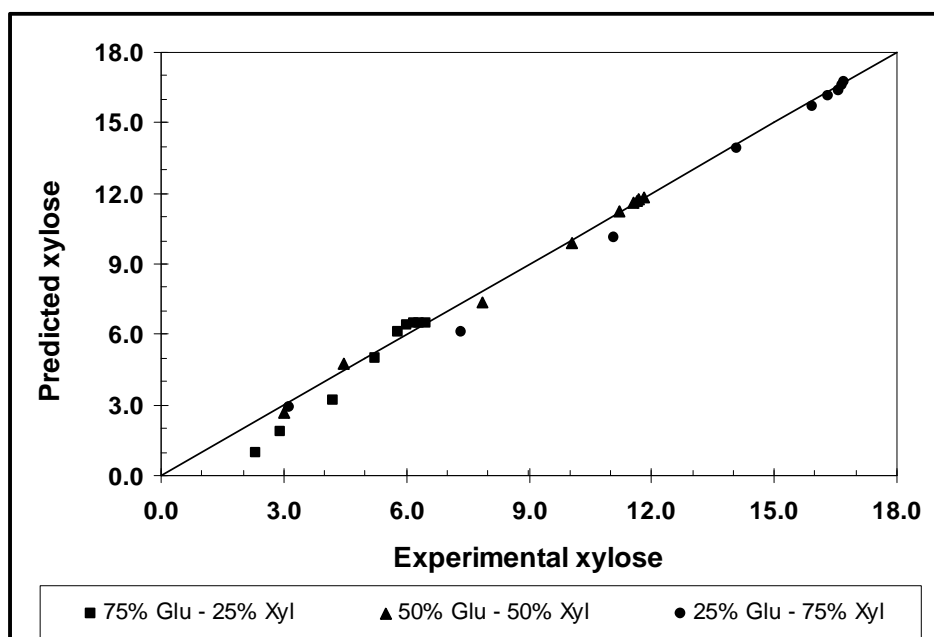


Figure A.6 – Comparison of the consistency between predicted and experimental xylose concentrations.

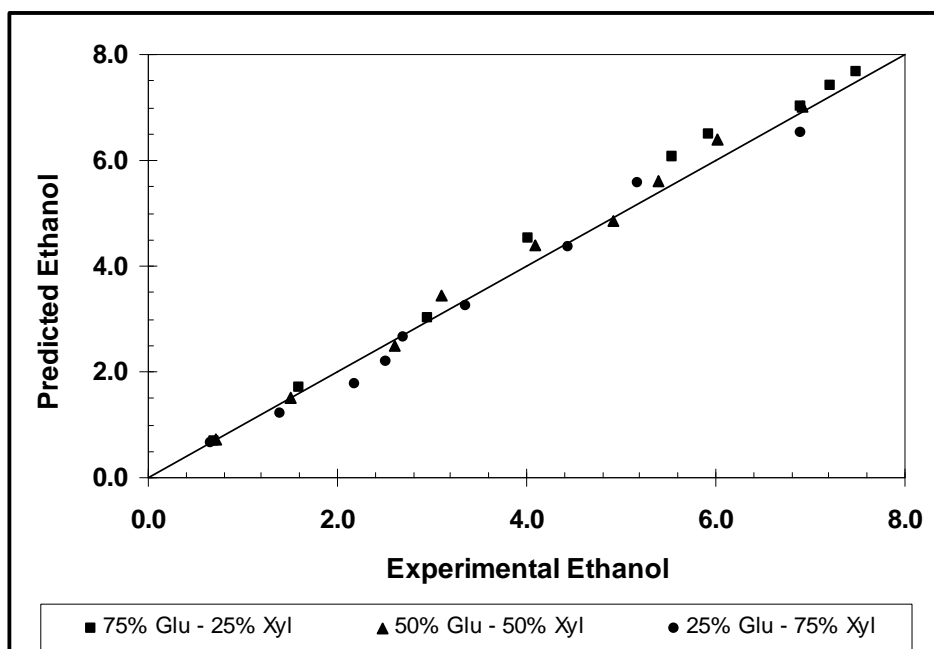


Figure A.7 – Comparison of the consistency between predicted and experimental ethanol concentrations.

APPENDIX B: ANALYSIS OF RESIDUALS

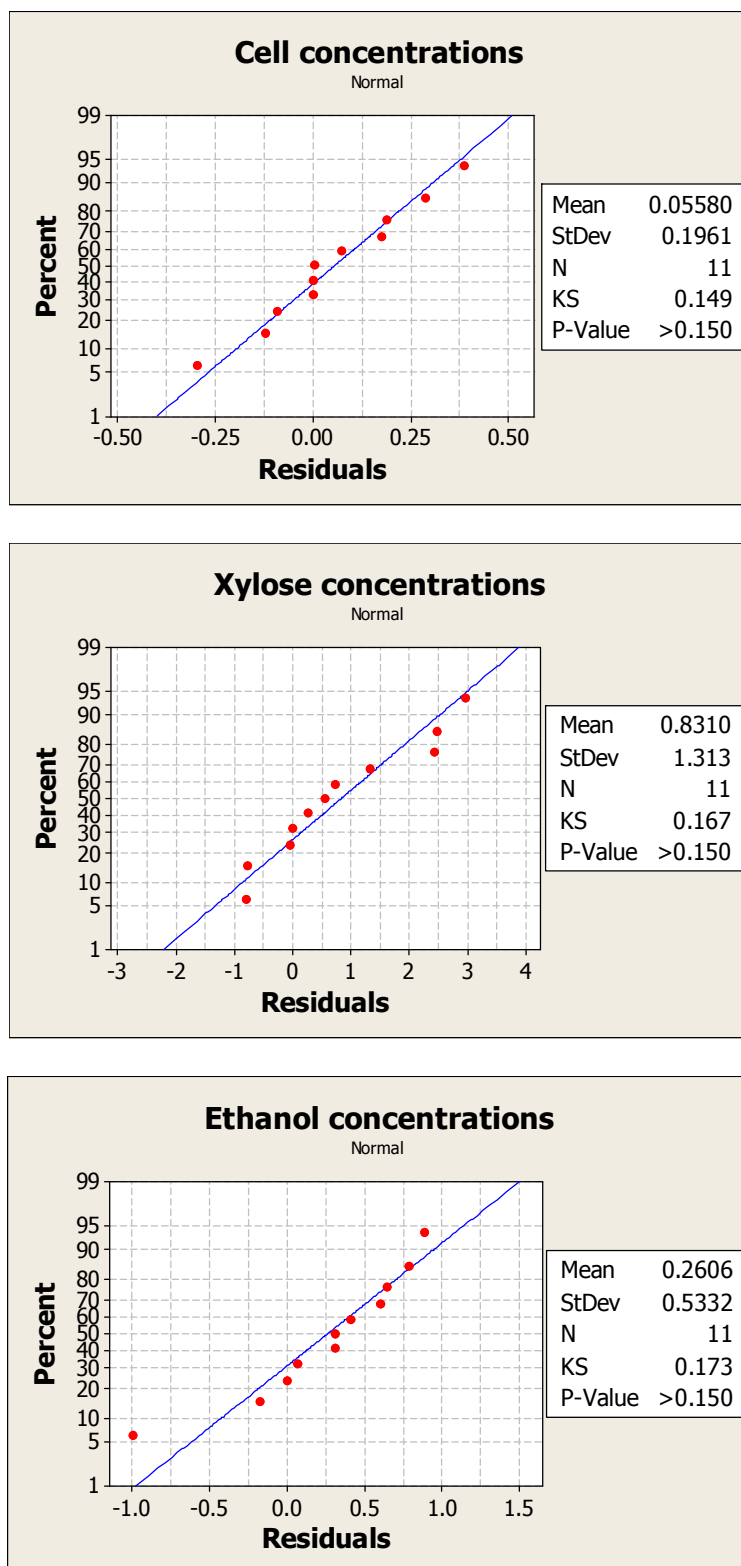


Figure B.1 – Residual probability plots for the system xylose – *P. stipitis*.

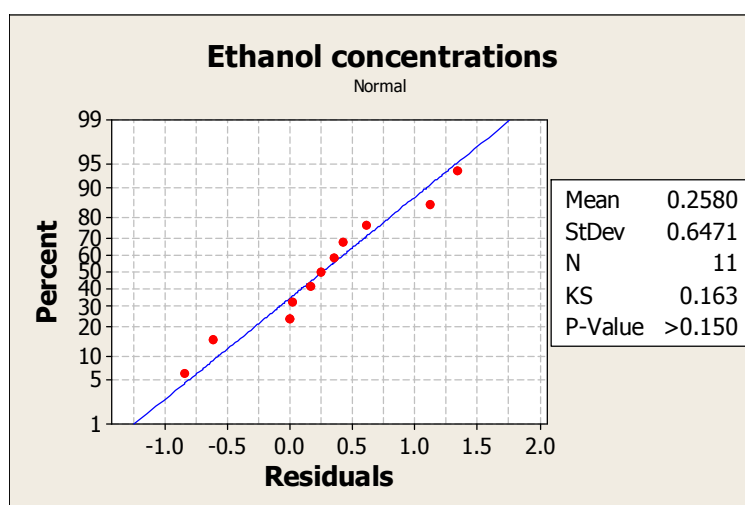
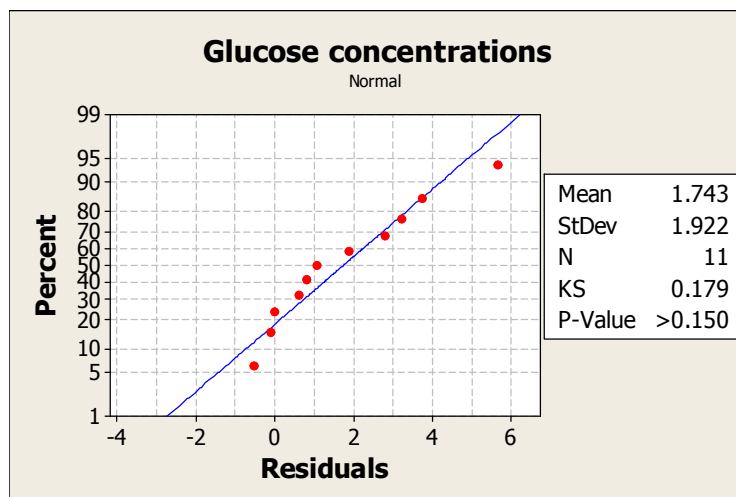
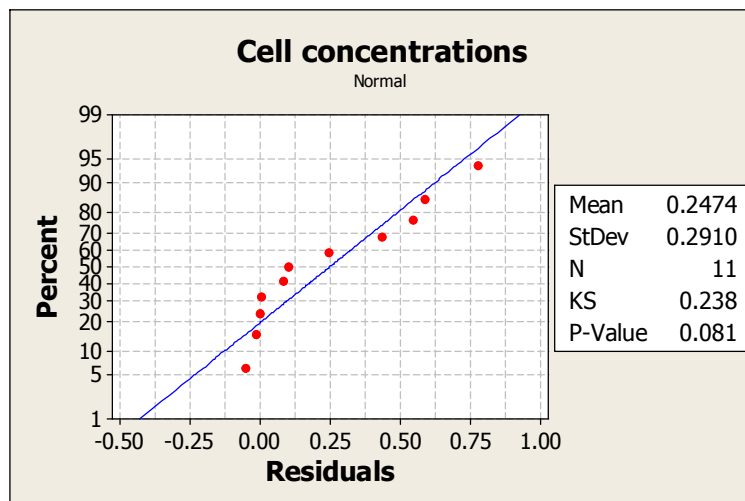


Figure B.2 – Probability plots of residuals for the system glucose – *P. stipitis*.

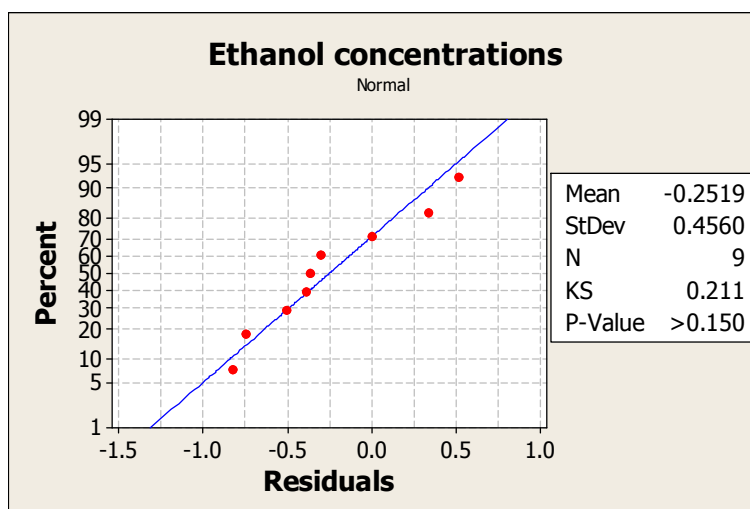
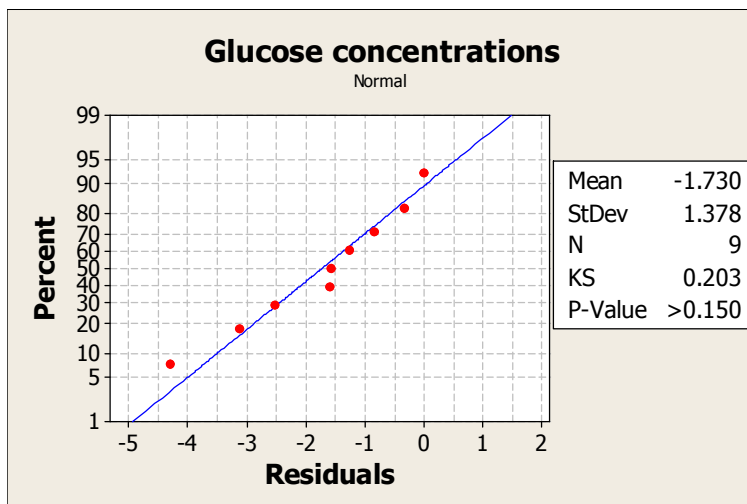
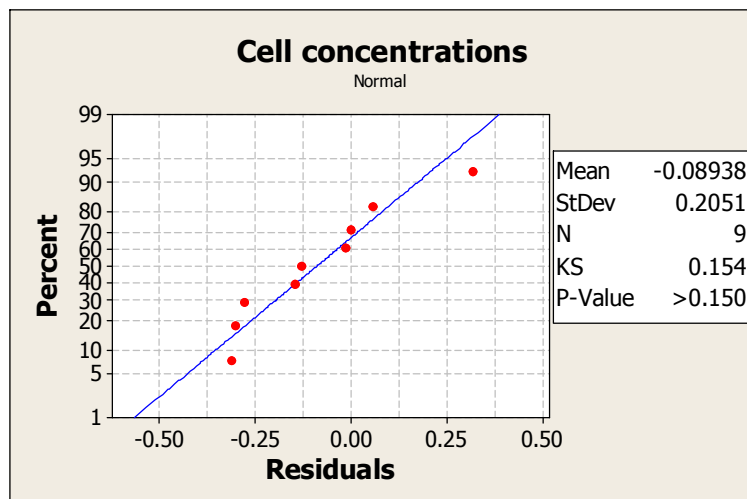


Figure B.3 – Probability plots of residuals for the system glucose – *S. cerevisiae*.

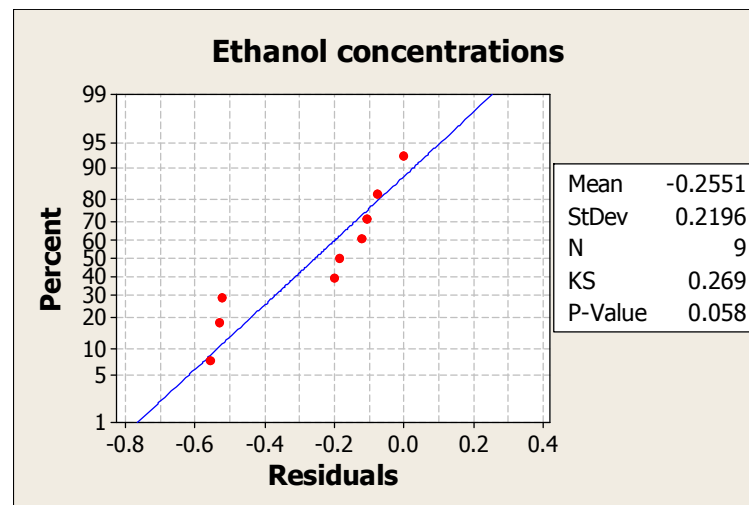
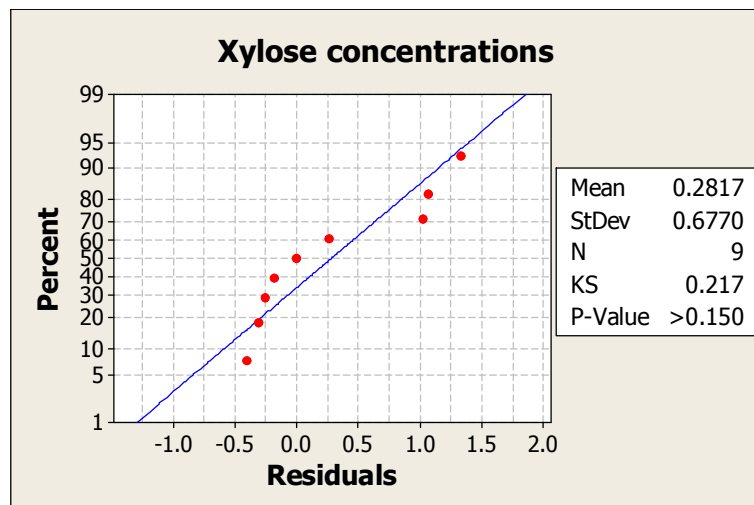
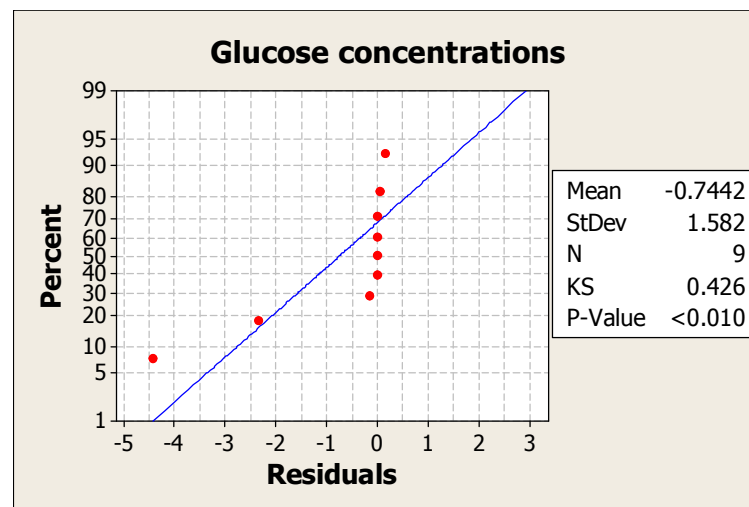
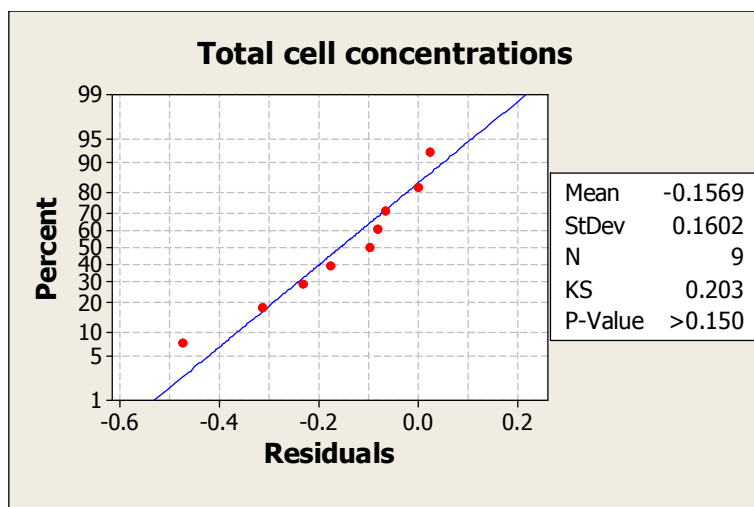


Figure B.4 – Probability plots of residuals for the mixture of 75% glucose and 25% xylose.

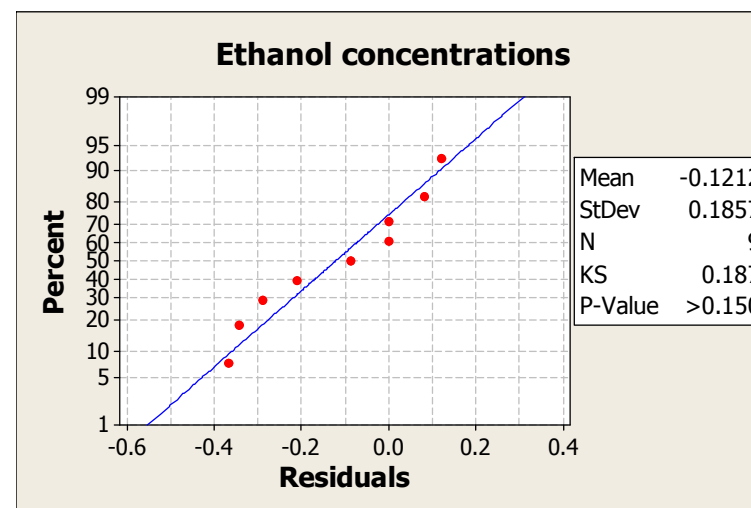
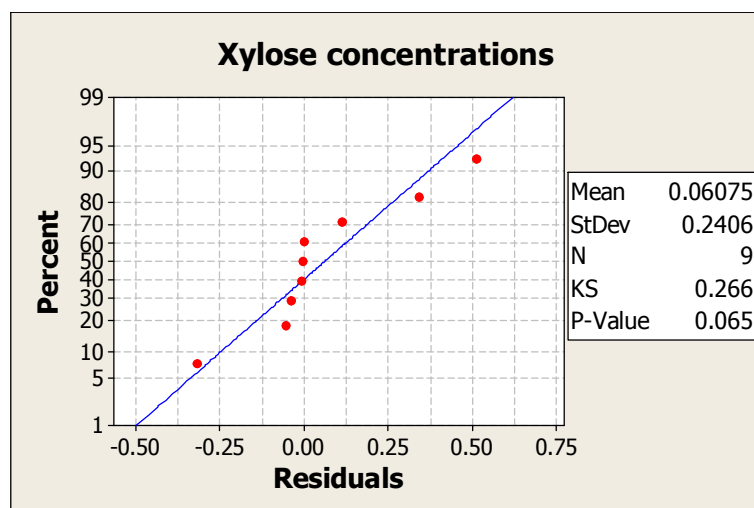
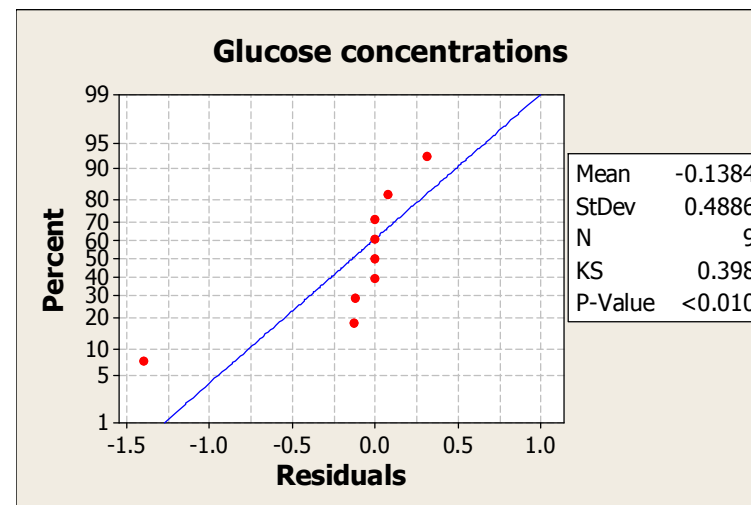
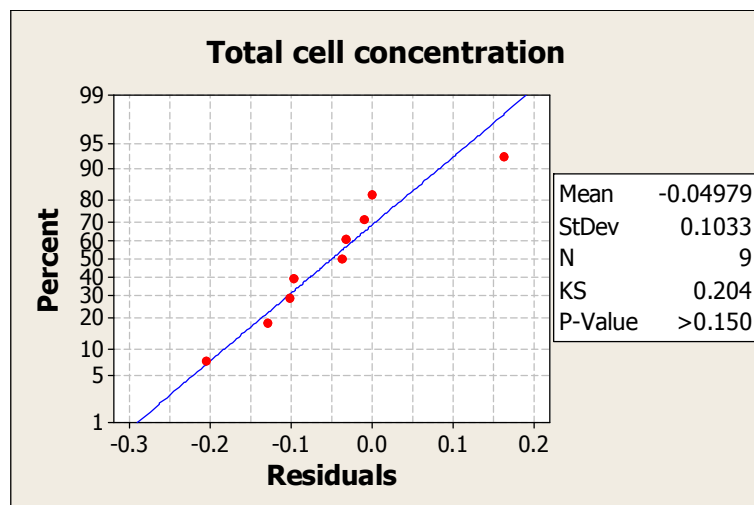


Figure B.5 – Probability plots of residuals for the mixture of 50% glucose and 50% xylose.

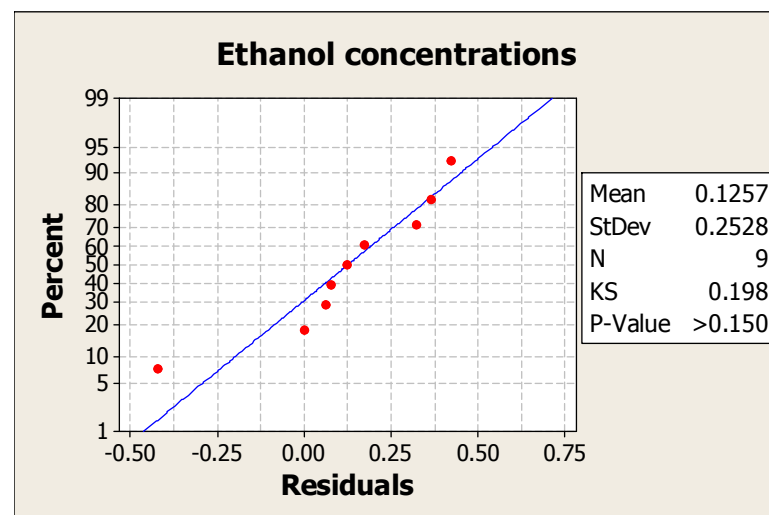
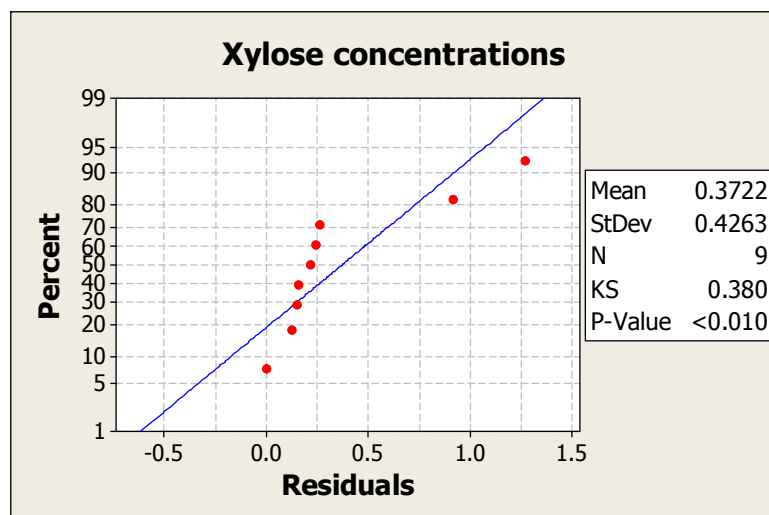
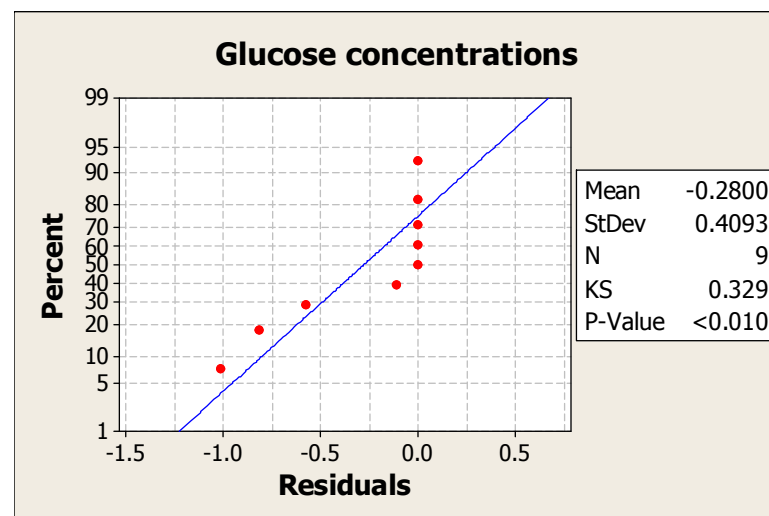
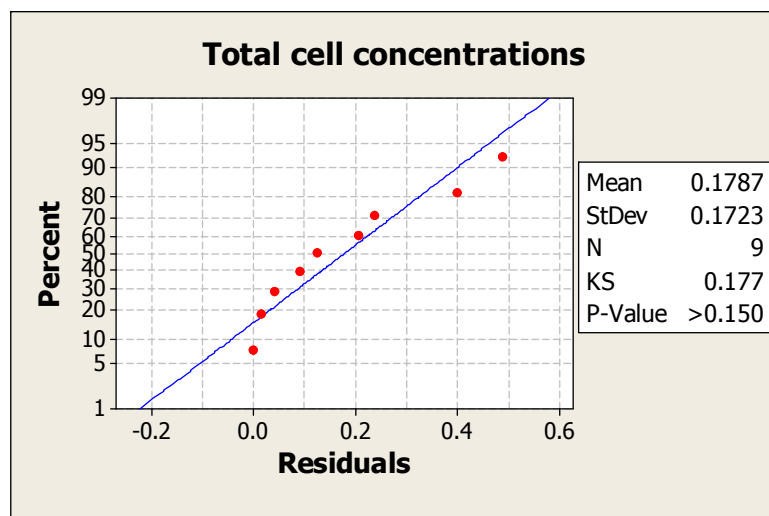


Figure B.6 – Probability plots of residuals for the mixture of 25% glucose and 75% xylose.